Comparative Safety Evaluation of Thorium Fuel to Natural Uranium Fuel in a CANDU 6 Reactor

COMPARATIVE SAFETY EVALUATION OF THORIUM FUEL TO NATURAL URANIUM FUEL IN A CANDU 6 REACTOR

BY

ZACHARY DEMERS, B.Sc.

A THESIS

SUBMITTED TO THE DEPARTMENT OF ENGINEERING PHYSICS

AND THE SCHOOL OF GRADUATE STUDIES

OF MCMASTER UNIVERSITY

IN PARTIAL FULFILMENT OF THE REQUIREMENTS

FOR THE DEGREE OF

MASTER OF APPLIED SCIENCE

Master of Applied Science (2017) McMaster University

(Engineering Physics) Hamilton, Ontario, Canada

TITLE:	Comparative Safety Evaluation of Thorium Fuel to Natural Uranium Fuel in a CANDU 6 Reactor
AUTHOR:	Zachary Demers B.Sc. (Physics) Western University, London, Ontario, Canada
SUPERVISOR:	Dr. John Luxat
NUMBER OF PAGES:	xiv, 104

Abstract

Fuel comprised of thorium has been explored since the early development of nuclear energy in the 1960s. In the last decade, there has been a renewed interest in thorium fuel and it has now become a primary focus in studies and proposed in next-generation nuclear reactors. This has been prompted by a limited supply of uranium in the foreseeable future and an abundance of thorium resources. Additionally, when compared to natural uranium (NU), thoria (ThO_2) produces substantially less long-lived radioactive waste and the fissile content can be reprocessed for additional fuel cycles. The CANDU 6 reactor has a unique ability to harvest thorium fuels because of its superior neutron economy. Thorium requires a driving isotope to sustain neutron fission until the long absorption chain produces viable amounts of U-233. Previous studies have investigated many different practical fissile isotopes and core modeling techniques that would make thorium feasible in a CANDU 6 reactor. This thesis focuses on a safety evaluation of thorium fuel compared to NU fuel in a lattice cell and full core configuration.

DRAGON 3.06 and SERPENT 2 are used to examine the infinite lattice cell containing NU and homogeneous thorium fuel enriched with 2.0% U-235, emphasizing the relationship between multiple nuclear libraries. This configuration is used to determine the enrichment concentration, temperature coefficient, coolant void reactivity, and the power relationship. Thorium fuel exhibits a higher negative temperature coefficient, a lower coolant void reactivity, and a greater reactivity change when simulated at different powers. If the lattice cell is simulated at 75% nominal power there is an 11 mk adjustment for thorium fuel, whereas the adjustment is only three mk for NU fuel. This is related to the extensive cross section of Th-232 and the long fertile absorption chain results in a sizeable inventory of the intermediate isotope Pa-233. The fissile content of the fuel bundle after exiting the reactor will continue to accumulate U-233 and should be monitored and properly stored.

A full core evaluation in a CANDU 6 reactor is performed in DONJON 4. Thorium fuel has an inferior reactivity worth for the control mechanism than does NU fuel in an operating CANDU 6 reactor. The reactivity worth of leakage and absorption in the reactor is estimated to be slightly lower for the thorium fuel.

This thesis presents a new computational model for analyzing full core power transients built upon previous results. The approximation model utilizes many assumptions to develop an expeditious code for analyzing the infinite square lattice retaining the isotopic densities. This model has demonstrated the ability to accurately emulate the reactivity of a lattice cell at different powers and power transients formed in DRAGON. The model is coupled with a point kinetic code to perform power transients in a CANDU 6 reactor.

Load following operations are performed in cycles of 24 hours examined at 80%, 60%, and 40% full power. Power adjustments are performed in increments of 10 minutes, two hour, or four hour periods with a constant reactivity input. The power adjustment time has minimal effect on the reactivity perturbations and only influences the rate of reactivity. Thorium fuel has enhanced load following capabilities compared to conventional NU fuel.

The long-lasting effects of Pa-233 introduces safety concern when reducing power or reactor shutdown scenarios. Reactivity transformation within the first two days of immediate power reduction will yield similar results for both fuels. Excess reactivity in the thorium fuel will continue to accumulate and eventually double the reactivity peak of NU fuel in the following 90 to 120 days. A shutdown simulation is performed in incremental power reduction steps of 20% for a range of different days. It is found that NU fuel can adequately control the additional reactivity in this simulation. Thorium fuel maintains a disconcerting amount of excess reactivity that will need to be addressed accordingly. The protactinium transient highlights the need to adequately monitor the buildup of Pa-233 for thorium-based fuels in a reactor.

Acknowledgements

I would like to express my sincere gratitude to the people that have influenced my graduate studies and time at McMaster University.

I would like to thank my supervisor, Dr. John Luxat, for the opportunity to pursue my graduate studies in the field of nuclear engineering. His many insightful comments and suggestions provided me with an abundance of knowledge in this field and helped guide me throughout the completion of this project. I would like to thank my defence committee, Dr Adriaan Buijs and Dr. Shinya Nagasaki, for reading my thesis and providing valuable feedback.

I have a wonderful family that has always provided a foundation of love and support in my life. I greatly appreciate the continuous encouragement and support I have received from my parents, Richard Demers and Dr. Dorothy Todd, throughout my time in academia. Special thanks to Rosemary Todd for taking the time to read and provide helpful comments and suggestions to this thesis.

My experience was greatly influenced by the people I have met at McMaster University. This includes the memorable times spent with graduate students in and out of the office and with other students while participating in intramural sports. I particularly enjoyed the early mornings endured on the water with my fellow varsity rowers. I am grateful for the people I have met and the unforgettable experiences I've had during this chapter of my life.

Contents

Abstract iii

Acknowledgements v

1 Introduction 1

1.1 Uranium Fuel 1

1.2 Thorium Fuel 2

1.3 CANDU 6 Reactor 2

1.4 Power Transient 3

1.5 Literature Review 5

1.5.1 Thorium Fuel 5

1.5.2 Reactor Kinetics 6

1.5.3 Power Transients 7

1.5.4 Full Core Simulations 8

1.5.5 Approximation Code 8

1.6 Objective 9

1.7 Outline 9

2 Basic Nuclear Concepts **11**

2.1 Power and Burnup 11

2.2 Neutron Flux 12

2.3 Neutron Cross Section 12

2.4 Multiplication Factor 13

2.5 Fermi's Four-Factor Formula 14

2.6 Xenon-135 Behaviour 15

2.7 Samarium-149 Behaviour 18

3 Methodology **19**

3.1 CANDU 6 Lattice Cell 19

3.2 Neutron Transport Equation 20

3.3 DRAGON Nuclear Code 22

3.4 SERPENT Nuclear Code 22

3.5 Approximation Model 23

3.6 Prompt and Delayed Neutrons 28

3.7 Effects of Delayed Neutrons 30

3.8 Point Kinetic Equation 31

3.9 Full Core Nuclear Code: DONJON 34

3.10 Temperature Coefficient 35

4 Lattice Cell Calculation **39**

4.1 Natural Uranium Lattice Cell Simulation 39

4.2 Isotopic Concentrations of Natural Uranium 42

4.3 Thorium Enrichment Concentration 43
4.4 Thorium Lattice Cell Simulation 44
4.5 Accuracy of the Nuclear Libraries 46
4.6 Isotopic Densities of Thorium 47
4.7 Simulating Various Bundle Powers 48
4.8 Temperature Coefficient 51
4.9 Coolant Void Reactivity 57
4.10 Transient Effects of Pa-233 and Np-239 58
4.11 Delayed Neutrons 60
4.12 Bundle Simulations of Power Transients 61
4.13 Summary 63

5 Full Core Analysis **64**

5.1 Reactivity Worth of Control Mechanisms 65
5.2 External Leakage 67
5.3 Reactor Age Map 69
5.4 Flux Distribution 69
5.5 Full Core Model 70
5.6 Fuel and Bundle Properties 72
5.7 Supercriticality and Prompt Criticality 73
5.8 Load Following 76
5.9 Continuous Load Following 80
5.10 Sustained Low Power 81
5.11 Shutdown Simulation 83

5.12 Summary 85

6 Summary and Conclusion **86**

7 Future Work **92**

A Pseudocode Examples **101**

List of Figures

1.1 CANDU 6 reactor assembly [7] 3

1.2 Advanced fuel cycle for the Generation III CANDU reactor [14] . . . 6

2.1 Xenon-135 concentration when power deviates 20% from full power. This is modelled in a CANDU 6 lattice simulated in DRAGON. . . . 17

2.2 Reactivity changes with deviating power modelled in a CANDU 6 lattice cell simulated in DRAGON. 17

2.3 Concentration of Samarium-149 as the bundle power simulates startup and shutdown scenarios. This is modelled in a CANDU 6 lattice cell simulated in DRAGON 18

3.1 2D lattice cell [34] 20

3.2 The four-factor formula for natural uranium generated in DRAGON . 24

3.3 The four-factor formula for thorium fuel enriched with 2.0% U-235 . . 25

3.4 The decay of ^{86}Br delayed neutron precursor groups [17] 29

3.5 Cross Sections for ^{233}U, ^{235}U, and ^{239}Pu 36

3.6 The temperature influence on neutron generation (η) and absorption ratio 37

4.1 Lattice cell simulation of natural uranium in DRAGON and SERPENT at a bundle power of 615 kW 41
4.2 DRAGON IAEA comparison to the approximation model at a bundle fission power of 615 kW 41
4.3 The evolution of isotopic concentrations in a lattice cell obtained using the approximation model for natural uranium fuel 42
4.4 DRAGON lattice cell simulation of thorium with different enrichment of U-235 using the WIMS-SD IAEA library. The black dots represent the bundle exit burnup assuming a reactivity loss of 48 mk accounting for leakage and control mechanisms in a CANDU 6 reactor. 44
4.5 Lattice cell simulation of thorium enriched with 2.0% U-235 in DRAGON and SERPENT at a bundle fission power of 578 kW 45
4.6 Comparison between the approximation model and DRAGON simulation using IAEA library 46
4.7 Library comparison of U-233, Pa-233 and Th-232 47
4.8 Evolution of isotopic densities obtained using the approximation model for thorium fuel 48
4.9 Fission powers at 10%, 25%, 50%, 100%, 125% and 150% of full power at 615 kW are presented comparing the results from the DRAGON simulation to the approximation model for NU fuel 50
4.10 Fission powers at 10%, 25%, 50%, 100%, 125% and 150% of full power at 615 kW are presented comparing the results from the DRAGON simulation to the approximation model for thorium fuel 50

4.11 The fissile isotope density for natural uranium fuel as a function of the power generated using DRAGON. It is assumed that full power for a bundle is 615 kW. 51
4.12 The fissile isotope density for thorium fuel as a function of power generated using DRAGON. It is assumed that full power for a bundle is 615 kW. 51
4.13 The relationship between reactivity and temperature of the fuel pellets simulated in DRAGON. The coolant and moderator are at a constant operating temperatures for this lattice cell simulation. 54
4.14 The relationship between reactivity and temperature for the coolant simulated in DRAGON. The fuel and moderator are at constant operating temperatures for this lattice cell simulation. 55
4.15 Coolant void reactivity in a lattice cell simulated using DRAGON . . 57
4.16 Reactivity change after a bundle is removed from the reactor at 30, 120, and 300 days corresponding to a burnup of 976, 3854, and 9609 MWd/Mg 59
4.17 Delayed neutron characteristics represented in the approximation model 60
4.18 Lattice cell load following to 80% full power simulation with NU fuel comparing the approximation model with DRAGON 61
4.19 Lattice cell load following to 80% full power simulation with thorium fuel, comparing the approximation model to DRAGON 62
4.20 A power dive from full power to 10% full power for NU fuel (left) and thorium fuel (right), comparing the approximation model to DRAGON 63

5.1 Reactivity worth of the control mechanisms for CANDU 6 reactor using natural uranium fuel [8] 65
5.2 Reactivity worth of the liquid zone controllers in a CANDU 6 reactor 67
5.3 Reactivity worth of the adjuster rods in a CANDU 6 reactor 67
5.4 Randomized reactor age map [9] 69
5.5 Reactor flux diagram 70
5.6 Flowchart describing the full core model at constant power 71
5.7 Flowchart of the full core model with changes in reactor power 72
5.8 Exponential power increase with reactivity insertion based on the point kinetic equation for the NU reactor 75
5.9 Exponential power increase with reactivity insertion based on the point kinetic equation for the thorium reactor 76
5.10 Load following at 80% full power for the NU reactor (left) and the thorium reactor (right) 78
5.11 The change in reactivity per second for the NU reactor (left) and the thorium reactor (right) 78
5.12 Load following at 60% full power for the NU reactor (left) and the thorium reactor (right) 79
5.13 Load following at 40% full power for the NU reactor (left) and the thorium reactor (right) 79
5.14 The average reactivity transition as load following is completed for 35 cycles in the NU reactor (left) and the thorium reactor (right) 80

5.15 The fissile isotopes in the NU reactor as load following completes 35 cycles 81
5.16 The fissile isotopes in the thorium reactor as load following completes 35 cycles 81
5.17 Power is reduced from full power and held constant to demonstrate the excess reactivity in the uranium reactor (left) and thorium reactor (right) 82
5.18 Excess reactivity in a NU reactor as power is decreased in increments of 20% to a power of 10% full power at different durations of time . . 84
5.19 Excess reactivity in a thorium reactor as power is decreased in increments of 20% to a power of 10% full power at different durations of time 84

Chapter 1

Introduction

Nuclear fission to create electrical power is considered one of the finest achievements of the latter half of the twentieth century. A major benefit of nuclear energy is that it produces a constant baseline power without toxic gas emissions. Given the significant increase in global temperature [1], exacerbated by the production of greenhouse gases, choosing electricity produced with limited carbon emissions is critical to the long term health of our environment. Nuclear power has proven that it can create substantial electrical power in a safe, reliable, and environmentally conscious manner [2].

1.1 Uranium Fuel

The nuclear industry has been utilizing uranium as its primary fuel for most of the worlds reactors. Uranium is the heaviest element found naturally on the earth's surface. The composition of natural uranium is divided into two categories, the majority consisting of the non-fissile isotope uranium-238 (U-238) and 0.72% consisting of the fissile isotope known as uranium-235 (U-235). Although U-238 is not fissile, it is considered to be fertile, meaning it can absorb a neutron then eventually create the fissile isotope plutonium-239 (Pu-239), as seen in Equation 1.1.

$$^{238}_{92}U + ^{1}_{0}n \longrightarrow ^{239}_{92}U \xrightarrow[23.5\ \text{min}]{\beta^-} ^{239}_{93}Np \xrightarrow[2.36\ \text{days}]{\beta^-} ^{239}_{94}Pu \tag{1.1}$$

As uranium is the primary resource used by the worlds nuclear industry, researchers have predicted that the global demand and the finite supply will create an inevitable barrier to acquiring uranium [3]. Using thorium as fuel has been suggested as a viable alternative to the foreseeable decline in obtainable natural uranium [4, 5].

1.2 Thorium Fuel

Thorium is also found naturally on the earth's surface. It is estimated to be three to four times more abundant than uranium [6]. Thorium is composed mainly of Th-232 that, similar to U-238, is considered a fertile isotope. The thorium absorption chain presented in Equation 1.2 requires more time to produce a fissile isotope, U-233, than the U-238 absorption chain. In addition, thorium does not contain a fissile isotope to assist in maintaining the initial chain reaction. To initially ensure a stable neutron economy, it is necessary to add a fissile element to thorium, such as plutonium extract from weapons or spent fuel, or enriched uranium.

$$^{232}_{90}Th + ^{1}_{0}n \longrightarrow ^{233}_{90}Th \xrightarrow[21.8\ \text{min}]{\beta^-} ^{233}_{91}Pa \xrightarrow[27\ \text{days}]{\beta^-} ^{233}_{92}U \tag{1.2}$$

1.3 CANDU 6 Reactor

The CANada Deuterium Uranium (CANDU) reactor ranks as one of Canada's top 10 engineering achievements. The CANDU reactor is unique in comparison to other reactors because it is fueled by reprocessed natural uranium dioxide and does not require enrichment of U-235. This is made possible by having a separate coolant and moderator comprised of heavy water (D_2O). The heavy water absorbs less neutrons, allowing for an enhanced neutron economy. As the lifetime of the fuel bundle is much lower than its reactor counterpart, online refuelling is used to replenish old bundles and maintain the chain reaction. This allows for a longer continuous operating time as the reactor is not shutdown while refuelling. This method avoids substantial financial costs for uranium enrichment but requires a higher upfront building cost due to the use of heavy water.

A typical CANDU 6 reactor produces a constant 600 - 700 MW of electrical power and can be found in Canada in Ontario and New Brunswick. Internationally, CANDU 6 reactors are located in South Korea, Argentina, Romania, and China. It consists of 380 fuel channels, each containing 12 fuel bundles. The core is surrounded in a calandria tube in a light water filled tank that shields the radiation from the surroundings. The basic day-to-day control mechanisms include the mechanical absorbers, moderator poison, adjuster rods and liquid zone controllers. For emergency conditions, there are 28 emergency shutdown units and six poison injection nozzles. A full core model is illustrated in Figure 1.1.

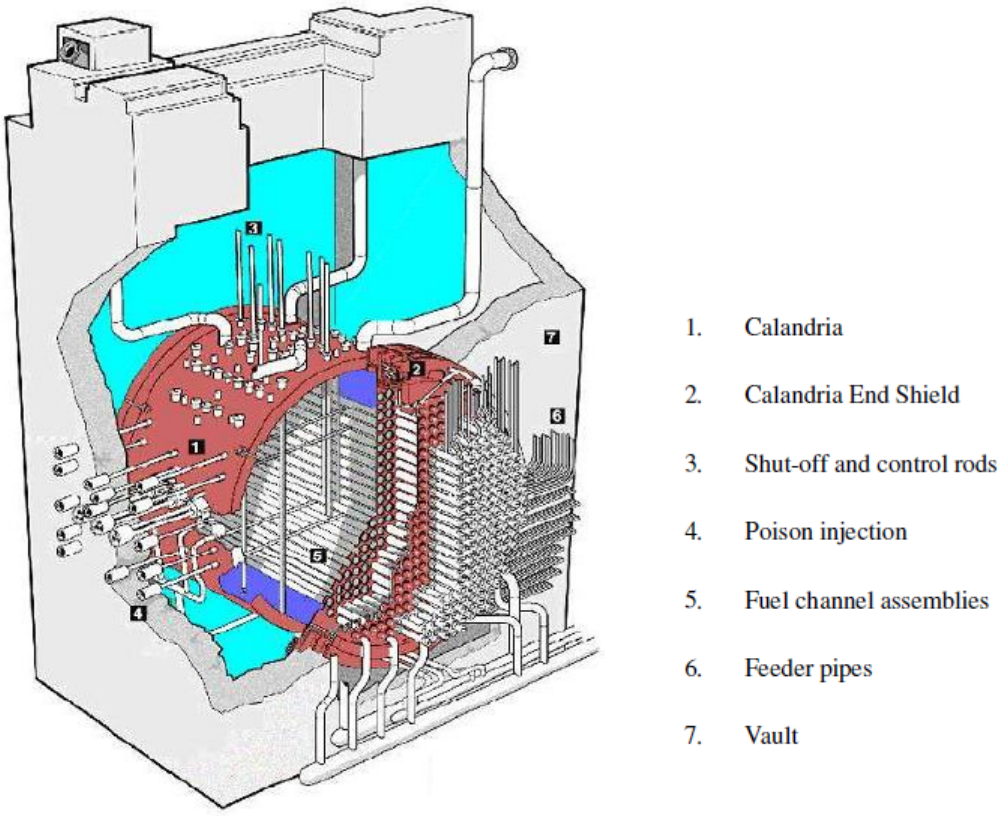

Figure 1.1: CANDU 6 reactor assembly [7]

1.4 Power Transient

If a reactor is to operate at constant power, the rate of neutron loss must be equal to the neutron production. The control mechanisms in a reactor detect the flux or neutron population and adjust accordingly to ensure a constant neutron generation. If there is a variation in this condition, it will result in a time-dependent change in neutron population causing a "power transient" to occur in the reactor. This can be caused by many different factors, such as: the operator adjusting the power to meet electrical needs; refuelling operations; adjusting control mechanisms for fuel depletion; and unexpected accident scenarios. These conditions make it important to predict time-dependent behaviour of neutron populations.

Load following is a well-known power transient that is performed by adjusting the reactor power to meet grid demands. Reactors are often operated at the maximum base load capabilities to provide the most energy to the grid. The grid demands follow a rhythmic 12-hour pattern where peak hours occur during the day and less demand is necessary at night. Thus, it is beneficial for the reactor to operate at lower powers during the off-hours to save fuel and operate at maximum load capacities during peak hours.

To maintain a stable reaction in a CANDU reactor the irradiated fuel is replaced with fresh fuel. It is standard practice to refuel eight bundles in a CANDU 6 channel at one time, however, the axial refuelling scheme allows for any number of bundles to be inserted into a channel at a time [8]. On average, 6 - 10 bundles reach their exit burnup in a reactor each day [9]. Refueling does not always occur every day; some stations prefer bulk refuelling two or three days a week. The act of removing irradiated fuel and replacing it with fresh fuel causes local flux disturbances and must be monitored to ensure reactor stability.

A change in isotope concentrations is caused naturally by irradiation, or it can be altered by power deviations and refuelling. Isotope concentrations tend to reach equilibrium in the fuel with constant power. If the power is changed, the isotope concentration may take several hours to days to reach the same equilibrium, resulting in disturbances in the neutron population and causing power transients.

As known in nuclear reactors, unforeseen accident scenarios can occur and the results may be disastrous. An accident scenario can include a failure in any of the reactor operations, such as a cracked coolant tube, turbine failure, or a pump malfunction. External factors such as severe ice storms and earthquakes can cause internal issues that need to be considered during all phases of the reactors design, construction, and operation. It is important to study and understand these power transients so that safety features can be implemented and proper operation procedures are put in place.

1.5 Literature Review

1.5.1 Thorium Fuel

The concept of utilizing thorium as fuel in reactors was explored in the 1960s and 1970s, but uranium was the preferred choice. In the past few years, there has been renewed interest and study in thorium prompted by the limited supply of uranium [3] and inherent advantages in using thorium. Thorium is naturally three to four times more abundant than uranium [6] and currently is not in demand. Thoria (ThO_2) produces substantially less long-lived radioactive waste than urania (UO_2) [10]. Moreover, it has been suggested that the exit bundle can be reprocessed as additional fuel.

The CANDU reactor has a unique benefit for harvesting fissile material from thorium fuel because of its superior neutron economy. This is partly due to the fact that thorium itself is not fissile but is fertile; it needs a driving isotope for thorium to eventually contribute to the nuclear reaction. There have been studies focused on using weapon grade plutonium fuel in CANDU 6 reactors to dispose of nuclear weapons [10, 11, 12]. Another approach is to use enriched uranium to maintain the initial reaction [5]. The advantage of this is that most countries with nuclear power have an enrichment facility and uranium at their disposal. The long half-life of Pa-232 continues to produce U-233 after a thorium bundle is removed from the reactor. After the initial once-through cycle, the remaining U-233 can be extracted and recycled into another thorium load, thus remaining self-sufficient. Studies have shown that using thorium for a once-through cycle [5] or fissile extraction for fuel reprocessing are both feasible [13]. Although thorium has not yet been implemented, it is one of the future Generation III goals for CANDU reactors as illustrated in Figure 1.2.

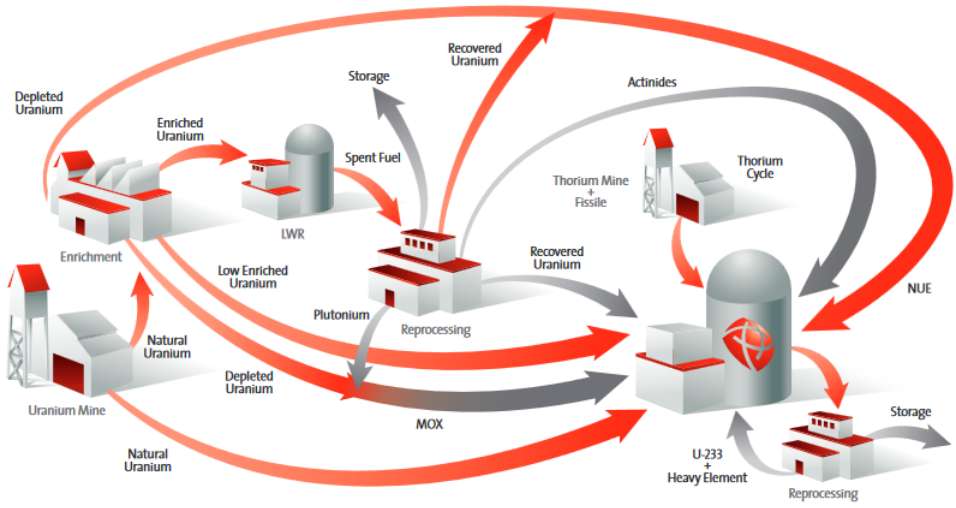

Figure 1.2: Advanced fuel cycle for the Generation III CANDU reactor [14]

There is a significant amount of research on how to properly exploit thorium fuel in a reactor, either as a homogeneous or heterogeneous mixture. Shaun Yee [15] explored both these mixtures in a CANDU 6 using the reactor codes DRAGON and DONJON. The heterogeneous mixture places thorium bundles in channels surrounded by slightly enriched uranium. The purpose of this is to extract U-233 from the thorium cycles and use it in a heterogeneous reactor. Thorium bundles placed closer to channels at the center of the core produce the double peak in the flux distribution that is achieved in a NU reactor. It operates within the current standards and licensing of CANDU 6 reactor, including the ability to refuel using an 8 bundle shift. Heterogeneous mixtures simulated in a lattice cell have been proven to operate with proper reactivity using U-233, U-235, and Pu-239 as fissile isotopes [15, 11, 13]. Although sufficient reactivity has been concluded, there is a lack of safety analysis using thorium fuel in the CANDU system. It is expected that there will be less neutron absorption for the control mechanisms using thorium fuel [16]. Thus, a further evaluation on the safety analysis using point kinetic codes has been suggested [11].

1.5.2 Reactor Kinetics

The point kinetic equation is a well known coupled bi-linear differential equation that is ubiquitous in the study of reactor kinetics [17]. An important and known issue with reactor kinetics is the "stiffness" in the system, resulting from orders of magnitude

difference in time between prompt and delayed neutrons. This often restricts the time step to very small increments in the numerical calculation of the point kinetic equation. There have been multiple suggestions to deal with this issue, Y. Chao [18] suggests a stiffness confinement method based on the fact that time response is present in the delayed neutrons but not in the delayed neutron precursors. The calculation allows for a larger time step and less simulation time. J. Sánchez [19] uses a generalization of the Runge-Kutta method to avoid the stiffness and calculates the truncation of error. Another method developed is an inversion of polynomials to solve the point kinetic equation [20]. This allows for a faster calculation with the same order of magnitude of accuracy. The method for solving the point kinetic equation that will be used in this study is M. Kinard's [21] piecewise constant approximation. This method takes advantage of the fact that reactivity and neutron source vary slowly with respect to time. This allows an exact numerical solution to the point kinetic equation resolving the stiffness problem. It has the feature of being simple yet proven accurate.

1.5.3 Power Transients

Control theory was first introduced in the 1960s by R. Kalman [22] as a branch of study that dealt with the mathematical behavior and theory of control systems. B. Frogner added to this by describing the problems, trends, and perspectives on controlling a nuclear power plant [23]. In the 1970s, D. Cherchas [24] began researching CANDU reactor controls of optimal performance, including the use of the point kinetic equation. Load following was suggested to minimize cost during load cycling intervals.

Load following simulations is a power transient that has been studied and performed in CANDU reactors. QB. Chou [25] has explored the concept of short term load following on Pickering Unit A and concluded it is possible to reduce power down to 50% within safety margins on a daily load following cycle. This however, requires that override devices be implemented to overcome the xenon transient. J. Veneze [26] and A. Lopez [27] examined load following capabilities of CANDU nuclear plants at Embalse in Argentina and Bruce B in Kincardine, Canada. They concluded that weekly operations down to 50% full power can be performed to save fuel based on previous maneuvers. D. Trudell [28] explored the concept of load following using TRUMOX fuel made of higher transuranic actinides, 60% of which is Pu-239 and Pu-241. This was performed using the nuclear code RFSP in a CANDU 9 reactor. It was determined that both fuels could achieve load following to 85% within safety

margins using only the liquid zone controllers. The TRUMOX fuel proved to be superior in load following capabilities to the traditional NU fuel.

1.5.4 Full Core Simulations

A full core simulation requires a two-level computational scheme. A lattice code is used to provide characteristics of a fuel bundle at a nominal power corresponding to the average fission power in a full-core simulation. The average fission power is estimated to be 615 kW in a full CANDU 6 reactor. This data is then used in a diffusion code that solves the full core simulation. The full core simulation is dependent on the power used and the lattice steps taken. This method, known as the time-instantaneous calculation, cannot accurately reflect deviations in power. This is illustrated by M. Guyot, [29] who compares a lattice cell calculation from DRAGON to a time-instananeous calculation performed by DONJON a low power. The difference between DRAGON and DONJON operating at 10% nominal power is greater than 10 mk. This result includes the xenon module in DONJON that adjusts reactivity based on xenon effects. The results are consistent in both methods for nominal power depletion.

The time-instantaneous method is inaccurate when trying to interpolate the lattice cell properties at low power. The incongruity is a result of the isotopic density and continuous depletion at a specific power. Individual bundles in a full core will operate at different power based on the location. For example, a bundle located at the periphery will operate at lower power than at the center of the core.

The micro-depletion method is developed to consider the isotopic density of specific isotopes in a full core calculation. This method is modelled in a CANDU 6 reactor using natural uranium fuel operating at full power. The results were similar to the time-instantaneous method since most of the bundles operate at nominal power. The change from the bundles operating at lower powers is adjusted by the near equal number of bundles operating at higher powers [29].

1.5.5 Approximation Code

The approximation code is formulated by the simple approach taken by S. Tashakor [30] using a point kinetic equation with fuel burnup and temperature feedback. This method was developed only to display the change in isotopic concentration with fuel

burnup using one-group of delayed neutrons. It has been enhanced to include four-factor formula to calculate reactivity, as well as a more reliable point kinetic equation with additional delayed neutron groups.

This method retains the isotope concentration for individual bundles, similar to the micro-depletion method in full core simulations. The benefit of the approximation method is the rapid calculation of individual depletions for the 4,560 bundles in a CANDU 6 reactor.

1.6 Objective

Fuel comprised of thorium has been explored since the development of nuclear energy. Although thorium-based fuel has been a topic of research for many years, there is an expressed need for a safety analysis that incorporates a point kinetic model to examine a thorium-fueled CANDU reactor [11]. The focus of this thesis will be a safety evaluation comparing thorium-based fuel to the conventional natural uranium fuel in a CANDU 6 reactor.

As explained earlier, the time-instantaneous method cannot accurately reflect power transients in a full core model. The lattice code is calculated at nominal power and used as input for the reactor code. Instead of using a two-level computational scheme, a computer simulation is developed in this thesis that will couple the lattice code and reactor code to accurately represent power transients. The computer simulation developed will include the point kinetic model to consider the effects of delayed neutrons.

This thesis will emphasize some of the safety advantages and disadvantages of using thorium-based fuel. In addition, a major safety concern known as the "protactinium transient" for thorium-based fuels is introduced and examined. Additional control features may be required to adequately control this transient in a full core reactor.

1.7 Outline

This thesis is organized into six chapters. The introduction chapter discusses fuel that will be examined, the CANDU 6 reactor layout, power transients, and a literature review of previous work. Chapter 2 involves basic reactor terms to be used in

the following chapters to explain concepts and results. Chapter 3 labeled methodology will include the methods used to obtain the result. This includes development of the approximation model and other computer simulations that will be used in the following result sections.

Chapter 4 is the first section of the result that analyzes the CANDU 6 lattice cell. In this chapter we discuss the evolution of the isotopes using natural uranium fuel and thorium fuel. It will confirm the approximation model using computational codes such as DRAGON and SERPENT. The temperature, coolant void reactivity, transient effects on isotopes, and delayed neutrons are analyzed and compared in the two different fuels.

Chapter 5 is a full core analysis of the CANDU 6 reactor. The safety control systems will be analyzed in DONJON modelling a CANDU 6 reactor. The external leakage is estimated by comparing the lattice cell to the full core simulation when all bundles are at the same burnup. The approximation model is coupled with the point kinetic model for a full core evaluation. The exit burnup and average delayed neutron results are re-evaluated from the previous chapter. The reactivity change per day and increase from refuelling is provided. Load following is examined at cycles of 80%, 60% and 40% full power for NU fuel and thorium fuel. The change and preservation of fissile fuel that occurs with continuous load following cycles is examined. The transient effects from the decay of Pa-233 and Np-233 are observed at sustained low power. A shutdown simulation is simulated to further explore the long-lasting effects on reactivity occurring at lower powers.

Chapter 2

Basic Nuclear Concepts

This section discusses the nuclear physics concepts that will apply to the following chapters. This chapter elaborates on nuclear physics concepts such as: neutron cross sections, neutron flux, fission power, multiplication and reactivity, four-factor formula, and nuclear poison. Additional information on these concepts can be found in Duderstadt's textbook "Nuclear Reactor Analysis" [17].

2.1 Power and Burnup

Nuclear reactors extract power by fission reactions occurring in the fuel. There are two types of fission categorized as fast fission and thermal fission, based upon the energy of a neutron when it bombards a nucleus. In thermal fission the neutron energy is around 0.0025 eV and fast fission often occurs at an energy of 1 MeV or greater. The focus in a CANDU reactor is on the thermal region that produces the majority of the power. When a neutron bombards a nucleus and fission occurs, the heavy nucleus normally splits into two smaller fragments producing energy and additional neutrons.

$$Neutron + U_{235} \rightarrow fission\ products + more\ neutrons + energy \tag{2.1}$$

If the fuel continues to produce energy from nuclear fission, the chemistry of the fuel will change as the fissile isotopes are depleted and fission fragments are produced. It is difficult to measure the percent of the depleted heavy elements in a bundle, instead, the term burnup has been adopted. Burnup expresses the amount of energy that has been extracted from the original fuel. It is expressed as the fission

power of the bundle multiplied by the time of operation divided by the initial fuel mass (Mega Watt days / Mega grams).

2.2 Neutron Flux

The neutron population in a reactor determines the power production from the reactor. It is necessary to define the neutron population in a mathematical format. A single neutron in a reactor is defined by the following properties:

- The vector position coordinates: $\mathbf{r} = x\mathbf{i} + y\mathbf{j} + z\mathbf{k}$
- The velocity coordinates: the velocity module $V_n = |V_n|$, and the two direction components $\Omega = \frac{V_n}{|V_n|}$
- The time: t

Introducing a term called the neutron density $n(\mathbf{r}, V_n, \mathbf{\Omega}, t)$ such that $n(\mathbf{r}, V_n, \Omega, t)d^3rd^2\Omega dV_n$ is the total amount of neutrons per unit volume at an instance t. From this, angular flux can be expressed as:

$$\phi(\mathbf{r}, V_n, \mathbf{\Omega}, t) = V_n n(\mathbf{r}, V_n, \mathbf{\Omega}, t). \tag{2.2}$$

The angular dependence is not as important, therefore the flux distribution can be approximated as:

$$\phi(\mathbf{r}, V_n, t) = \int_{4\pi} \phi(\mathbf{r}, V_n, \mathbf{\Omega}, t). \tag{2.3}$$

The neutron flux is used to define the quantity of neutrons traveling through a unit of area per time and will be used to describe the local motion of neutrons in a reactor.

2.3 Neutron Cross Section

The probability that a neutron-nucleus reaction will occur is defined as the neutron cross section. The microscopic cross section represents a physical area that if a neutron was to enter, there would be a neutron-nucleus interaction. A larger area

would represent a greater probability of integration. This is measured in barns which equal 10^{-24}cm^2. The rate of interaction is defined as:

$$\text{Rate} = \sigma N_a \phi \tag{2.4}$$

where:

σ is the microscopic cross section (cm^2)

N_a is the atoms per unit area (cm^{-2})

ϕ is the flux ($\text{cm}^{-2}\ \text{s}^{-1}$)

It is also common to introduce the macroscopic cross section that groups the atoms per unit area and the microscopic cross section such that $\Sigma = N_a\sigma$ then the equation becomes:

$$\text{Rate} = \Sigma\phi. \tag{2.5}$$

There are three types of reactions that are significant: radiative capture, nuclear fission, and scattering. Radiative capture (σ_γ) occurs when a neutron is absorbed into the nucleus, increasing the atomic number by one (${}^{A+1}_{Z}X$). Nuclear fission (σ_f) absorbs the neutron but instabilities cause the nucleus to split into two smaller isotopes. A neutron experiences a scattering interaction (σ_s) when the speed or direction is changed by a nucleus, resulting in an exchange of energy. The absorption cross section (σ_a) is expressed as the addition of the radiative capture cross section and the nuclear fission cross section. The total cross section (σ_t) is the sum of each individual cross section.

$$\sigma_t = \sigma_a + \sigma_s = \sigma_\gamma + \sigma_f + \sigma_s \tag{2.6}$$

2.4 Multiplication Factor

The multiplication factor (k) is the ratio of number of neutrons between two successive fission neutron generations [17]. It is used to describe neutron population change at each generation of fission. The values of k are expressed as:

$k < 1$ This is known as subcriticality occurring when the chain reaction dies over time. There are fewer neutrons being introduced into the system than being absorbed.

$k = 1$ This is known as criticality and occurs when every fission leads to another fission. Reactors that produce constant power will maintain criticality.

$k > 1$ This is known as supercriticality as there is an increase in neutron creation compared to absorption. In this state, the number of fissions and the neutron population will increase exponentially.

There is a distinction between the infinite multiplication factor (k_{inf}) and the effective multiplication factor (k_{eff}). k_{inf} is mainly used in lattice cell calculations as it assumes an infinite square lattice. This means that no neutrons leak outside of the system. k_{eff} is normally used for full core simulations as it includes neutrons that leak outside of the system or reactor. Another useful term expressed in nuclear physics is reactivity (ρ), which normalizes the multiplication factor to zero.

$$\rho = \frac{k-1}{k} \tag{2.7}$$

2.5 Fermi's Four-Factor Formula

The four-factor formula separates the infinite multiplication factor into individual components that describe specific interactions with neutrons. This equation is described as:

$$k_{\text{inf}} = \eta f p \epsilon \tag{2.8}$$

Symbol	Name	Definition
η	Thermal Fission Factor	$\frac{\textbf{neutrons produced from fission in the thermal range}}{\textbf{absorbed in the fuel in thermal range}}$
f	Thermal Utilization Factor	$\frac{\textbf{neutrons absorbed in fuel}}{\textbf{total neutron absorption}}$
p	Resonance Escape Probability	$\frac{\textbf{neutrons thermalized without being absorbed in fuel}}{\textbf{total fission neutrons}}$
ϵ	The Fast Fission Factor	$\frac{\textbf{total fission neutrons}}{\textbf{neutrons produced from fission in the thermal range}}$

The thermal fission factor represents the number of neutrons created from fission in the thermal range compared to the total thermal neutron absorption by the fuel. The thermal utilization factor is the probability that neutron absorption is in the fuel and not the system. This includes absorption in the structural material and in the liquid of the moderator and coolant. The resonance escape factor describes the probability that a neutron will manage to be thermalized without being absorbed by the fuel. The fast fission factor represents the probability that fission occurs outside of the thermal range. This predominately happens in the fast fission energy range.

2.6 Xenon-135 Behaviour

A major factor in reactor control and maintaining an adequate neutron balance is the presence of fission products that are parasitic absorbers and considered neutron poison. The fission yield products are considered poison because they absorb neutrons and are not fissile, thus creating negative reactivity. The dominant fission product poison is xenon-135 (Xe-135), which has a thermal absorption cross section of 2.7 million barns [31], compared to U-235, which has an absorption cross section of 685 barns.

The production of Xe-135 is predominately created from the beta decay of iodine-135 (I-135) with a small amount created directly from fission. The decay production chain of I-135 is given in Equation 2.9, including their respective half-life. Since the parent isotopes of I-135 rapidly decay, their individual fission yield probabilities are normally added to I-135.

$$fission \rightarrow {}^{135}Sb^{1.6s} \rightarrow {}^{135}Te^{29s} \rightarrow {}^{135}I^{6.7h} \rightarrow {}^{135}Xe^{9.15h} \rightarrow {}^{135}Cs \tag{2.9}$$

The change in isotope concentration of I-135 and Xe-135 are described in Equation 2.10 and 2.11 [17]. I-135 is only produced directly from fission that is proportional to flux and power. Xe-135 is depleted by radiative capture creating Xe-136 or beta decay into Cs-135.

$$\frac{\partial I}{\partial t} = \overbrace{\bar{\nu}\Sigma_f\phi}^{fission\ yield} - \overbrace{\lambda I}^{iodine\ decay} \tag{2.10}$$

$$\frac{\partial Xe}{\partial t} = \overbrace{\nu\bar{\Sigma}_f\phi}^{fission\ yield} + \overbrace{\lambda I}^{iodine\ decay} - \overbrace{\lambda Xe}^{xenon\ decay} - \overbrace{\sigma_a\phi Xe}^{xenon\ absorption} \tag{2.11}$$

The concentration of Xe-135 has a major impact on the reactivity because there is a lag in saturation concentration if there is a change in flux. This is due to the fact the inventory of I-135 changes gradually when there is a deviation in flux. When flux immediately changes, Xe-135 is produced at a similar rate as I-135 adjusts to the new flux and there is an instant adjustment in Xe-135 absorption. If flux decreases there will be an initial increase in Xe-135 concentration. This is because the production of Xe-135 will initially remain at the higher previous flux as the inventory of I-135 gradually adjusts to the new power, and there is less absorption of Xe-135 at a lower flux. Similarly, an increase in flux will initially cause a lower concentration of Xe-135 as the production rate adjusts slowly to power changes and there is an increase in absorption. Xe-135 concentration and the change in reactivity caused by this power transient requires roughly 40 to 50 hours to reach saturation conditions [32]. This is illustrated in Figure 2.1 and 2.2 as power deviates to 80% and back to full power. If there is a reactor shutdown, xenon will naturally decay over time. Knowing the amount of Xe-135 concentration in the reactor is paramount to reactor safety as sudden changes in flux can cause major deviations to reactivity.

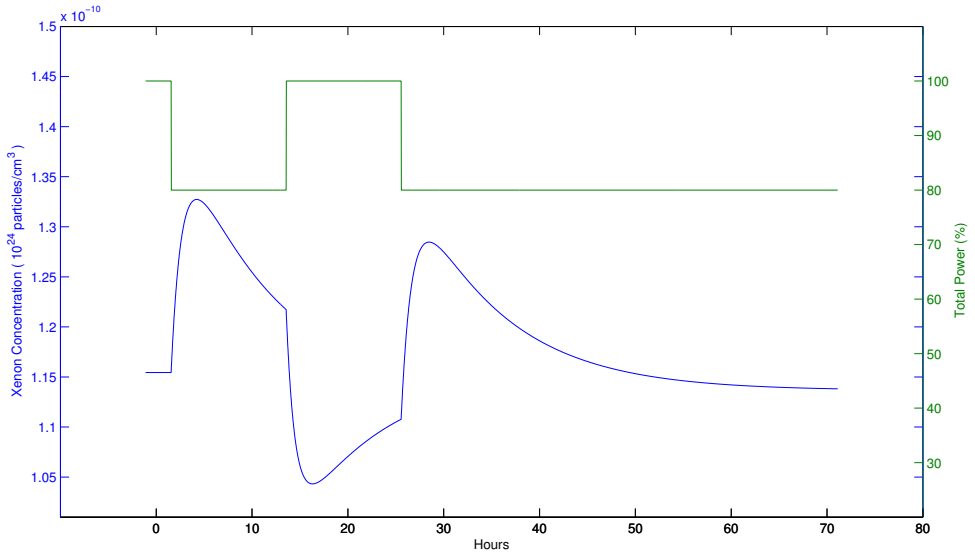

Figure 2.1: Xenon-135 concentration when power deviates 20% from full power. This is modelled in a CANDU 6 lattice simulated in DRAGON.

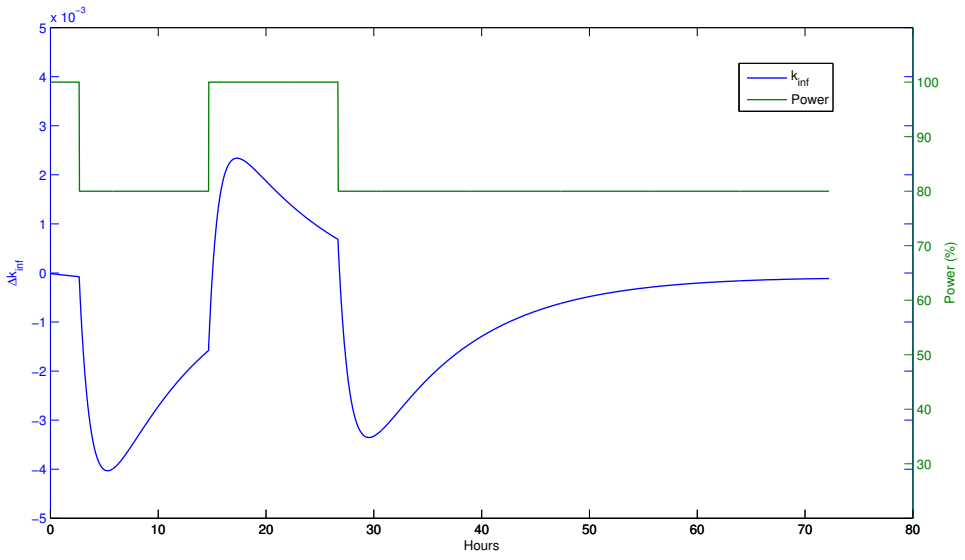

Figure 2.2: Reactivity changes with deviating power modelled in a CANDU 6 lattice cell simulated in DRAGON.

2.7 Samarium-149 Behaviour

The second largest neutron absorber produced by fission is samarium-149 (Sm-149), which is roughly two orders of magnitude lower than Xe-135 cross section. It is also mainly produced by the beta decay of promethium-149 (Pm-149) with a much greater half-life of 53 hours compared to I-135. Sm-149 behaves in a similar manner to Xe-135 except that it is a stable isotope and will not decay over time. This means that the concentration will continue to build after shutdown and remain at the same concentration until startup, as seen in Figure 2.3.

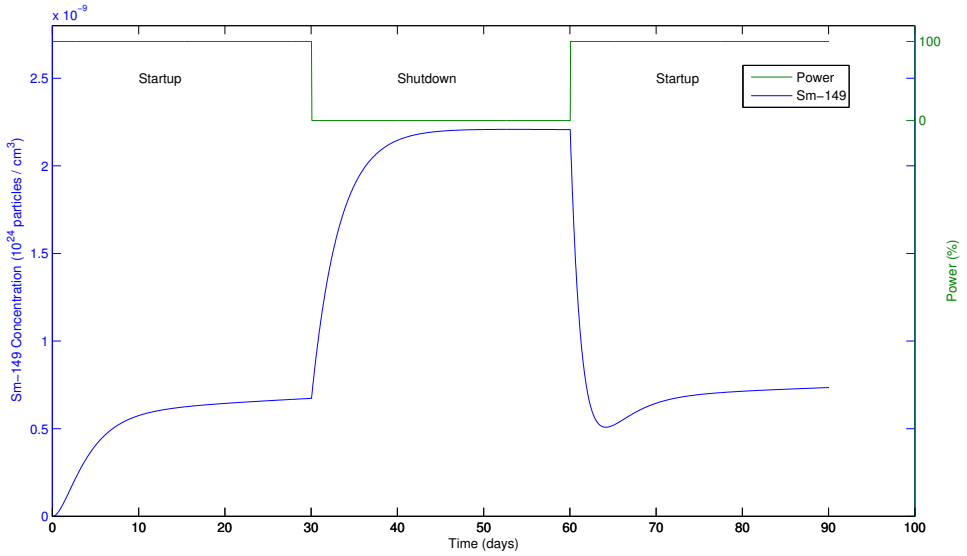

Figure 2.3: Concentration of Samarium-149 as the bundle power simulates startup and shutdown scenarios. This is modelled in a CANDU 6 lattice cell simulated in DRAGON

Chapter 3

Methodology

The scope of this chapter is to apply the nuclear reactor concepts to explain the theory and background of this thesis. The CANDU 6 reactor is examined in two different categories: the bundle will be analyzed to determine how it will interact in the reactor core and a full reactor core simulation. DRAGON and SERPENT will be used to examine the bundle and DONJON will analyze the full core reactor. A new method called the approximation model is proposed to rapidly accelerate the computational speed of the lattice cell calculation. The techniques and assumptions used in the approximation model are explained in this section.

3.1 CANDU 6 Lattice Cell

The lattice cell is a 2-D replica of a bundle in a CANDU 6 reactor with a square lattice pitch equal to 28.575 cm as seen in Figure 3.1 [33]. The pressure tube is composed mainly of zirconium-91 with small traces of natural boron located at a radius of 5.1689 to 5.6032 cm from the core. The annulus gap between the pressure tube and calandria tube is filled with carbon dioxide. The calandria tube, composed of zirconium with small traces of Ni-58, Cr-52, and natural boron, is located from 6.4478 to 6.5875 cm. The coolant is inside the pressure tube and the moderator is outside the calandria tube. The coolant and moderator both consist of heavy water (D_2O) with a purity of 92.222 % and 99.911 %, respectively. There are 37 fuel pins arranged in an annular ring formation with gaps that allow the coolant to flow between the pins. The uranium oxide pellets inside of the pins has a radius of 0.6122 cm surrounded in an 0.0418 cm zirconium alloyed sheath [33].

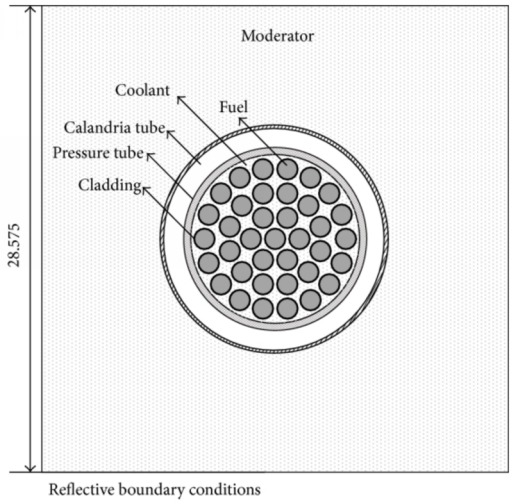

Figure 3.1: 2D lattice cell [34]

There have been improvements on the mass capacity of the CANDU 6 37-element bundle with time. The uranium mass was 18.8 kg in 1970 and changed to 19.3 kg in the late 1980s with dimensional refinements and higher density of uranium dioxide (UO_2). The density of uranium increased from 10.60 g/cm^3 to 10.73 g/cm^3 in the late 1980s [35]. These refinements allow the fuel bundle to operate in the reactor for a longer period of time.

3.2 Neutron Transport Equation

The neutron transport equation is a partial differential equation that is governed by the conservation of neutrons. This represents the gain and loss with energy and directional attributes in an arbitrary volume (V). The individual components of Equation 3.1 are expressed as [17]:

1. The rate of change of neutrons in the volume
2. Leakage term defined as neutrons leaving the volume
3. Neutron loss due to collisions, such as scattering or absorption
4. Inscattering term as neutrons change energy or direction into values of interest
5. Fission term defining neutrons creation

6. Neutrons source for neutrons entering the volume

$$\overbrace{\frac{1}{v}\frac{\partial\psi}{\partial t}}^{①}+\overbrace{\Omega\cdot\nabla\psi(x,\Omega,E,t)}^{②}+\overbrace{\Sigma_t(x,E,t)\psi}^{③}=$$
$$\overbrace{\int_0^\infty\int_{4\pi}\Sigma_s(x,\Omega'\to\Omega,E'\to E,t)\psi(x,\Omega',E',t)d\Omega' dE'}^{④}$$
$$+\overbrace{\frac{\chi(E)}{4\pi}\int_0^\infty\int_{4\pi}v\Sigma_f(x,E',t)\psi(x,\Omega',E',t)d\Omega dE'}^{⑤}+\overbrace{S(x,\Omega,E,t)}^{⑥} \tag{3.1}$$

The neutron transport equation is used primarily to simulate the neutron behavior for individual cells or fuel elements in a reactor. This is accomplished by using nuclear codes to solve the transport equation. The neutron transport equation cannot be computationally solved directly in this form but will need to be discretized and arranged into simplified equations to ease computational requirements. Nuclear codes are divided into two categories for solving this equation - deterministic simulations and the stochastic simulations.

The deterministic simulations are defined as models that do not use randomized methods to solve the transport equation. Although individual neutrons have a random nature in a reactor, there are an abundance of neutrons to produce an accurate distribution model. The definition of a deterministic code is that multiple runs with the same parameters will always yield the same result. The advantage of this method is that it requires less computing time and resources compared to the stochastic method. The disadvantage of the deterministic nuclear codes is that they must make assumptions and simplify the transport equation to make it numerically solvable [17].

The stochastic nuclear codes normally use a Monte Carlo simulation to produce a random sample model to analyze the neutron transportation equation. The problem is divided into interrelated probability trees where an individual neutron is recorded and its interactions produce a branch on the tree. The subsequent simulations will

build on the previous results, eventually producing an outcome. As the nuclear code increases in neutron sources or simulations, the results become more accurate and reliable.

3.3 DRAGON Nuclear Code

The computer code DRAGON is an open-source deterministic transport code developed by École Polytechnique de Montréal [36]. It was developed to unify and improve on different models and algorithms to rationalize the neutron transport equation. The code allows a detailed calculation of a two and three-dimensional model of the neutron behavior in a lattice cell or fuel assembly. It also allows users to choose from multiple nuclear libraries and several standard nuclear formats. DRAGON is a well-established nuclear code and has the ability to [37]:

- Provide resonance self-shielding calculations in multi-dimensional geometries
- Calculate the neutron flux in individual zones for two to three dimensional lattice cells that accounts for neutron leakage
- Calculate criticality of a lattice cell using k-eigenvalue method and 4-factor formula results
- Incorporate isotopic creation and depletion with time
- Provide many of the homogenized nuclear properties allowing for full core calculations

DRAGON 3.0.6 will be used in this thesis to model a 2D CANDU 6 cartesian lattice cell with burnup using multiple libraries available in WIMS-D4 [38]. It will also be used to calculate other characteristics of the CANDU 6 lattice cell, such as temperature coefficient and coolant void reactivity. The simulation will be mirrored on the stochastic nuclear code SERPENT for validation.

3.4 SERPENT Nuclear Code

SERPENT is a stochastic nuclear code using the Monte Carlo code to simulate random sampling developed by the VTT Technical Research Centre of Finland [39]. It uses a continuous-energy model that does not need to be discretized. The use of a combinatorial solid geometry (CSG) model allows for any two or three-dimensional lattice cell or small modular reactor. Additional capabilities of SERPENT are [40]:

- Spatial homogenization and group constant generation for deterministic reactor simulator calculations
- Fuel cycle studies that involve burnup calculations
- Validation of deterministic lattice transport codes
- Full-core modeling of smaller reactors and research reactors
- Coupled multi-physics applications

This study will use SERPENT 2 [41], an advanced beta version of SERPENT, to replicate the lattice cell used in DRAGON. Many different libraries and results will be compared to validate DRAGON as well as the approximation model.

3.5 Approximation Model

The approximation model will act as an accurate representation of the CANDU 6 lattice cell modeled by DRAGON and SERPENT without the significant computing time. A full core simulation that has 4,560 individual bundles would require enormous computational requirements for DRAGON or SERPENT. Most full-core simulations use data files generated by the lattice cell codes containing the bundle properties. The limitation of this technique is that it does not accurately model full-core transient behaviors. Thus, a rudimentary model is proposed as an alternative to solving the lattice cell simplified by many assumptions.

The model is built upon the four-factor formula results generated by the DRAGON lattice cell simulation. Figure 3.2 and 3.3 illustrate the individual four-factor formula results for simulations with different power density. The first assumption that will be made is that the only dependent variable for the calculation of the multiplication factor (k) is the thermal fission factor (η). As pointed out in the figures, the other factors remain constant as the thermal fission factor is the dominant variable that changes with burnup and power. Therefore, the other factor results will remain constant throughout the approximation model simulation. The constant four-factor formula is calculated as the average value between a fresh bundle and the estimated time of exit, as noted in Table 3.1.

Table 3.1: The average values of the four-factor formula generated in DRAGON

	η	f	p	ϵ
Uranium Fuel	1.1668	0.9527	0.9082	1.0250
Thorium Fuel	1.1987	0.9667	0.9021	1.0046

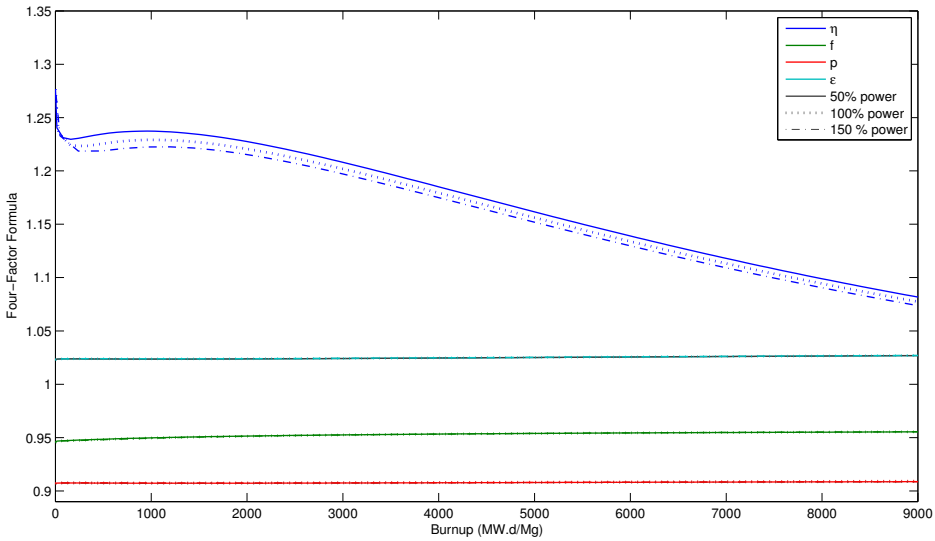

Figure 3.2: The four-factor formula for natural uranium generated in DRAGON

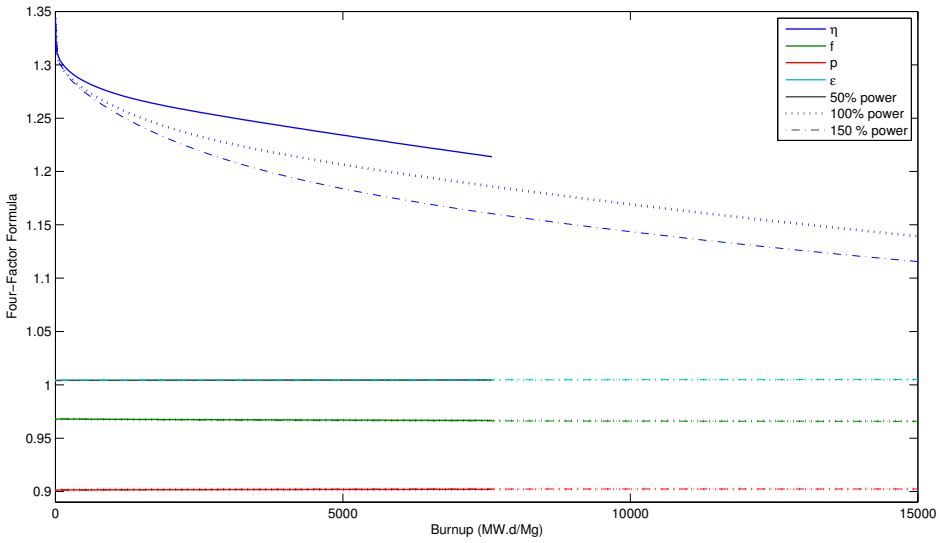

Figure 3.3: The four-factor formula for thorium fuel enriched with 2.0% U-235

It is necessary to establish a method to determine how the concentration changes with fission, absorption, and decay in a fuel bundle. DRAGON and SERPENT have a large inventory of the characteristics of important actinides and fission yield products.

In the approximation method, the focus will be on the main fissile and absorption chain actinide isotopes. In the case of NU fuel, this includes: U-235, U-238, U-239, Np-239, Pu-239, Pu-240, and Pu-241. For thorium fuel this includes: Th-232, Th-233, Pa-233, U-233, and U-235. The rate of change in the isotopic concentration in the thermal region can be represented as:

$$\frac{dn}{dt} = P - L \tag{3.2}$$

where n is the neutron density, P is the production rate, and L is the consumption rate. The consumption rate is the loss of the isotopes concentration by nuclear fission, nuclear absorption, or nuclear decay. Similarly, the production rate is the growth caused by the same methods. The interest in the production and consumption rate will only investigate in the thermal range. The absorption chain of U-238 to Pu-239

is summarized as:

$$\frac{dn_{238U}}{dt} = -\sigma_{\gamma_{238U}} n_{238U} \phi \tag{3.3}$$

$$\frac{dn_{239U}}{dt} = \sigma_{\gamma_{238U}} n_{238U} \phi - \sigma_{\gamma_{239U}} n_{239U} \phi - \lambda_{239U} n_{239U} \tag{3.4}$$

$$\frac{dn_{239Np}}{dt} = \lambda_{239U} n_{239U} - \sigma_{\gamma_{239Np}} n_{239Np} \phi - \lambda_{239Np} n_{239Np} \tag{3.5}$$

$$\frac{dn_{239Pu}}{dt} = \lambda_{239Np} n_{239Np} - (\sigma_{\gamma_{239Pu}} + \sigma_{f_{239Pu}}) n_{239Pu} \phi \tag{3.6}$$

where:

σ_γ is the microscopic cross section for radiative capture

σ_f is the microscopic fission cross section

n neutron number density

λ decay constant

ϕ neutron flux

These formulas describe the evolution of isotopic concentration and determine the amount of neutrons being absorbed and created from fission. The thermal cross sections are measured at a temperature of 293 K equivalent to an average neutron speed of 2,200 m/s or neutron kinetic energy of 0.025 eV. There is a temperature correction term for the thermal cross section because the fuel pellet is exposed to a much greater temperature. The thermal fission factor is a ratio of neutrons created by fission over neutron absorption in the thermal range, expressed as:

$$\eta = \frac{\Sigma \nu \sigma_f n}{\Sigma(\sigma_\gamma + \sigma_f) n} \tag{3.7}$$

where ν is the average number of neutrons produced by a specific nuclide. From this result, it is possible to determine the affects of the remaining three constant factors. The thermal utilization factor (f) does not directly affect the isotopic density and will remain a constant. The amount of neutrons absorbed in the resonance factor can be expressed as:

$$\text{neutron density absorbed before thermalization} = \Sigma\nu\sigma_f n(1-p). \tag{3.8}$$

For natural uranium fuel, the resonance absorption is primarily in U-238 which transmutes to U-239. For thorium fuel, Th-232 absorbs a neutron to become Th-233. Similarly, the majority of the fast fissions occur only in the isotopes U-238 and Th-232. Both are depleted at the rate of

$$\text{fast fission neutron density} = \Sigma\nu\sigma_f n(\epsilon-1). \tag{3.9}$$

It is now possible to calculate the multiplication term as:

$$k_\infty = \epsilon f p \eta. \tag{3.10}$$

To mimic the calculations performed in DRAGON and SERPENT, the flux adjusts to keep the fission power constant. The fission power calculation uses the WIMS-SD library for each individual fissile isotope [42]. This is the same library used in DRAGON.

Fission produces parasitic absorbers that are considered poison in the fuel. In the approximation method, the only poisons being modelled are the two largest parasitic absorbers, Xe-135 and Sm-149. The other parasitic absorbers in the fuel are considered constant with a small reactivity adjustment term based on power. There is less parasitic absorption at low powers than at high power. A small reactivity adjustment term with adjustment delay time is added to normalize the change in fuel poison based on power. The reactivity associated with these two parasitic absorbers can be expressed as:

$$\rho_{\text{poison}} = -\frac{\Sigma_{\text{poison}}}{\nu\Sigma_f} = -\frac{\sigma_{\text{poison}} n_{\text{poison}}}{\nu\sigma_f n_f} \tag{3.11}$$

where:

Σ_{poison} is the macroscopic parasitic absorption cross section

Σ_f is the macroscopic fission cross section

n_{poison} is the concentration of the poison

n_f is the concentration of the fission products

The fission yield data for I-135, Xe-135, Pm-149 and Sm-149 from the fissile isotopes is collected from the WIMS-SD library [42]. The multiplication factor is calculated using the four-factor formula including parasitic absorbers to replicate the bundle signatures produced by DRAGON using the WIMS-SD library. A pseudocode example of the approximation model is provided in Appendix A for a single lattice cell in Algorithm 1 and full core model in Algorithm 2 .

3.6 Prompt and Delayed Neutrons

Most of the neutrons that are produced by fission are "prompt neutrons" that appear within 10^{-14} seconds after a fission. The remaining neutrons are considered "delayed neutrons" and are produced on a time scale of milliseconds to minutes. This is caused by the residual fragments emitted during fission that remain neutron rich, meaning that there is a high ratio of neutrons to protons. This uneven ratio causes energetic daughter products that can undergo neutron emission instead of a beta or gamma emission. An example of this process is the fission fragment of Br-87, that has a half-life of 55 seconds, emitting a beta to decay to Kr-87 [17]. At this point, Kr-87 is considered neutron rich and will either decay further to produce Sr-87 or emit a neutron to become Kr-86, as seen in Figure 3.4. The process in which the daughter nucleus produced by a beta decay of a fission fragment undergoes neutron emission is known as the delayed neutron precursor.

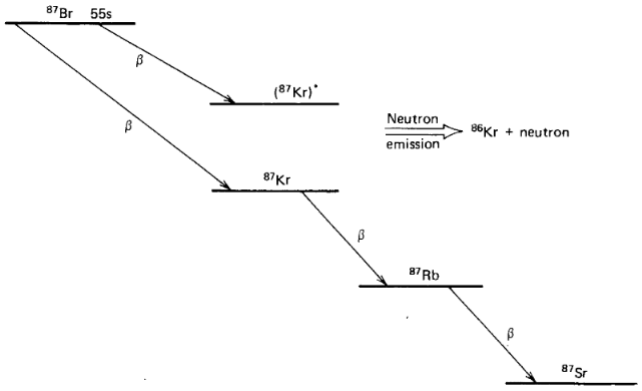

Figure 3.4: The decay of ^{86}Br delayed neutron precursor groups [17]

Neutron fission can yield multiple fission fragments that produce delayed neutron precursors with different half-life characteristics. It has become customary to separate these neutrons into six delayed neutron groups based on the Keepin's [43] result obtained from nonlinear least-square fit methods of experimental data. Instead of using the standard method of six delayed groups, this thesis will group the delayed neutrons into eight separate groups, as seen for U-235 on Table 3.2. The advantage in doing this is that each group contains the same decay constant for each fissile isotope, whereas the decay constant changes slightly for each fissile isotope using the six delayed neutron groups. The probability that a delayed neutron will be produced by fission in that specific precursor group is known as β_i. Another important variable is the total fraction of delay neutrons precursors (β), which is the sum of each β_i of all the precursor groups, representing the likelihood of a delayed neutron to be produced per fission.

Table 3.2: The eight precursor delayed neutron groups for ^{235}U using JEFF-3.1 nuclear library data [44]

Groups	$T_{1/2}$ (s)	λ (s^{-1})	Probability	β_i (%)
1	55.6	0.012467	0.0328	0.0218
2	24.5	0.028292	0.1539	0.1023
3	16.3	0.042524	0.0910	0.0605
4	5.21	0.133042	0.1970	0.1310
5	2.37	0.292467	0.3308	0.2200
6	1.04	0.666488	0.902	0.0600
7	0.424	1.634781	0.0812	0.0540
8	0.195	3.554600	0.0229	0.0152
Average	9.020	0.076849	1.00	0.665

3.7 Effects of Delayed Neutrons

Delayed neutrons play a crucial role in nuclear control and safety. The mean prompt neutron generation time (Λ) is considered the average time between the neutron birth and subsequent fission absorption producing another round of neutrons. The mean generation time can determine the rate at which the neutron population and reactivity can change. Without delayed neutrons, the neutron population, and subsequently power, would change at an exponential rate according to Equation 3.12.

$$N(t) = N(0)e^{(k_{\text{eff}}-1)t/\Lambda} \tag{3.12}$$

The typical value of the mean prompt generation time for a D_2O moderator in a CANDU reactor is 1 millisecond [33]. If the reactivity were to increase in a step change by 1 mk, then in three seconds the neutron population would increase to $N(0)^{20}$, an exponential growth that would be very difficult to control. Instead of using the mean generation time for prompt neutrons, the weighted average of mean generation time is used with delayed neutrons. Although delayed neutrons are roughly 0.5% of the neutron population, the generation time is predominately controlled by the delayed neutrons as illustrated in Equation 3.13. Because of the prompt neutrons short lifetime, it can be assumed the neutron generation time is

simply the delayed neutron fraction and the average delayed neutron lifetime.

$$\Lambda_{\text{total}} = \overbrace{\Lambda_{\text{moderator}}(1-\beta)}^{\text{Prompt Neutrons}} + \overbrace{\Lambda_{\text{delay time}}\beta}^{\text{Delayed Neutrons}} = 10^{-3}s \cdot 0.995 + 12.5s \cdot 0.005 = 0.0635s \tag{3.13}$$

If the same deviation in reactivity were to occur in the model that includes delayed neutrons, the neutron population would only change exponentially by $N(0)^{1.048}$ instead of $N(0)^{20}$, providing more time for control mechanisms to manage the nuclear population. This is assuming that the step change in reactivity is less than the average delayed neutron yield. If the reactivity change is greater than the average delayed neutron yield, the chain reaction is self-sustained on prompt neutrons alone, creating a prompt critically run-off effect. Although this method illustrates the importance of delayed neutrons in a reactor, it is a very elementary approach to neutron population and consequently power in a nuclear reactor. In a full core simulation, a common method to analyse these fluctuations is the point kinetic equation.

3.8 Point Kinetic Equation

A stable nuclear reactor operating at constant power will have reactivity equal to zero, meaning that neutron production is equal to neutron losses. A change in the power will result in a time-dependent change of the neutron population that may take some time to propagate back to equilibrium. A change in reactor power caused manually by the operators or naturally by the isotopes in the fuel is known as a power transient. It is important to know and predict the neutron population in the reactor to understand how to adjust control mechanisms to prepare for these transients. This time-dependent change in the reactor is referred to as nuclear reactor kinetics. The point kinetic equation has been widely adapted to analyse the nuclear reactor kinetics due to its simplicity, which complements the accuracy of this approach. The point kinetic equation for n delayed groups is given as [21]:

$$\frac{d}{dt}n(t) = \frac{\rho(t)-\beta}{\Lambda}n(t) + \sum_{i}^{8}\lambda_i C_i(t) + F(t) \tag{3.14}$$

$$\frac{d}{dt}C_i(t) = \frac{\beta_i}{\Lambda}n(t) - \lambda_i C_i(t) \tag{3.15}$$

where:

$n(t)$ is the neutron density

$\rho(t)$ is the time-dependent reactivity

β is the total delayed fraction

β_i is the delayed fraction for the i^{th} delayed fraction

$C_i(t)$ is the i^{th} precursor density

Λ is the neutron generation time

λ_i is the decay constant for the i^{th} group

$F(t)$ is the external neutron source

The point kinetic equation needs to be simplified and discretized to be solved numerically on a computer. The approach that will be used is the piecewise constant approximation model (PCA method) developed by M. Kinard et. al. [21]. The first step to this approach is to consider the equation in matrix form follows:

$$\frac{d\vec{\mathbf{x}}}{dt} = A\vec{\mathbf{x}} + B(t)\vec{\mathbf{x}} + \vec{\mathbf{F}}(t) \tag{3.16}$$

Where A is defined as a (n+1) x (n+1) matrix:

$$A = \begin{pmatrix} \frac{-\beta}{\Lambda} & \lambda_1 & \lambda_2 & \cdots & \lambda_n \\ \frac{\beta_1}{\Lambda} & -\lambda_1 & 0 & \cdots & 0 \\ \frac{\beta_2}{\Lambda} & 0 & -\lambda_2 & \cdots & 0 \\ \vdots & \vdots & \vdots & \ddots & \vdots \\ \frac{\beta_n}{\Lambda} & 0 & 0 & \cdots & -\lambda_n \end{pmatrix} \tag{3.17}$$

B(t) is defined as:

$$B = \begin{pmatrix} \frac{-\rho(t)}{\Lambda} & 0 & 0 & \cdots & 0 \\ 0 & 0 & 0 & \cdots & 0 \\ \vdots & \vdots & \vdots & \ddots & \vdots \\ 0 & 0 & 0 & \cdots & 0 \end{pmatrix} \tag{3.18}$$

And F(t) is:

$$\vec{\mathbf{F}}(t) = \begin{pmatrix} F(t) \\ 0 \\ 0 \\ \vdots \\ 0 \end{pmatrix} \tag{3.19}$$

The reactivity and source function are assumed to gradually change with respect to the time increments and are approximated as piecewise constant functions:

$$\rho(t) \approx \rho(\frac{t_i + t_{i+1}}{2}) = \rho_i \tag{3.20}$$

$$\vec{\mathbf{F}} \approx \vec{\mathbf{F}}(\frac{t_i + t_{i+1}}{2}) = \vec{\mathbf{F}}_i \tag{3.21}$$

Now the differential equation can be solved by using the integrating factor $e^{(A+B_i)t}$, where B_i is evaluated using the ρ_i from Equation 3.20 in matrix B from Equation 3.18. Evaluating the integral produces the following equation:

$$x_{i+1} = e^{(A+B_i)h_i} x_i + (e^{(A+B_i)h_i} - I)(A + B_i)F_i \tag{3.22}$$

where $h_i = t_{i+1} - t_i$ and I is an identity matrix. This is the proposed equation but it can be further decomposed and re-arranged for faster computing time. Assuming that $A + B = X_i D_i X_i^{-1}$, where X_i is the eigenvectors of $A + B_i$ and D_i, is a diagonal matrix of the eigenvalues are defined as: $\omega_1^{(i)}, \omega_2^{(i)} ... \omega_{n+1}^{(i)}$. The following equation becomes:

$$x_{i+1} = X_i e^{D_i h_i} X_i^{-1} [x_i + X_i D_i^{-1} X_i^{-1} F_i] - X_i D_i^{-1} X_i^{-1} F_i. \tag{3.23}$$

If there is no additional added source to the problem, the equation can be simplified as:

$$x_{i+1} = X_i e^{D_i h_i} X_i^{-1} x_i. \tag{3.24}$$

It is still necessary to solve the eigenvectors and the associated eigenvalues in a computationally effective manner. The eigenvalues of the point-kinetic matrix is the

solution for the roots of the inhour equation:

$$\rho_i = \beta + \Lambda\omega - \sum_{j=1}^{m} \frac{\beta_j \lambda_j}{\omega + \lambda_j} \tag{3.25}$$

that can be expressed in a polynomial form as:

$$P_i(\omega) = (\rho_i - \omega\Lambda) \prod_{l=1}^{n} (\lambda_l + \omega) - \omega \sum_{k=1}^{n} \beta_k \prod_{\substack{l=1 \\ l \neq k}}^{n} (\lambda_l + \omega) = 0. \tag{3.26}$$

The roots defined as ω_i of this equation will be real [45]. Kinard has suggested that this polynomial be solved by using Newton's method altered into Horner's method for accuracy and speed. Instead, the Jenkins-Traub algorithm is used because it that is the fastest globally convergent iteration and provides a higher magnitude of accuracy [46, 47]. The eigenvectors X_i and X_i^{-1} for the point-kinetic matrix are defined as:

$$X_i = U_i \qquad \text{where} \qquad u_k^i = \Big[1, \frac{\mu_1}{\lambda_1 + \omega_k^{(i)}}, \frac{\mu_2}{\lambda_2 + \omega_k^{(i)}}, \ \cdots, \frac{\mu_n}{\lambda_n + \omega_k^{(i)}}\Big]^T \tag{3.27}$$

and

$$X_i^{-1} = V_i^T \qquad \text{where} \qquad v_k^i = v_k^i \Big[1, \frac{\lambda_1}{\lambda_1 + \omega_k^{(i)}}, \frac{\lambda_2}{\lambda_2 + \omega_k^{(i)}}, \ \cdots, \frac{\lambda_n}{\lambda_n + \omega_k^{(i)}}\Big]^T \tag{3.28}$$

where $\mu_l = \frac{\beta_l}{\Lambda}$, u_k^i is the kth column of U_i and $\omega_k^{(i)}$ is the respectable eigenvalues. This is the piecewise constant method that will be used to solve the point-kinetic equation. It provides an accurate and effective numerical method for solving this equation each iteration.

3.9 Full Core Nuclear Code: DONJON

The tool that will be used to analyze a full-core configuration by solving the neutron diffusion equation is DONJON 4, developed by École Polytechnique de Montréal [48]. DONJON is designed to simulate multiple different reactor designs. The full-core calculation requires a two-level computational scheme, meaning that the lattice cell calculations are first performed in DRAGON and the results are stored in CPO files used as input for DONJON. The typical data that is generated and stored from

DRAGON for DONJON are:

- Cross-section database
- Burnup, irradiation, and neutron exposure
- Moderator, coolant, and fuel temperature and density
- Moderator and coolant purity
- Poison load
- Reflector properties
- Cross-section database in the presence of adjuster rods and liquid zone controllers

The CANDU 6 full-core evaluation in DONJON with the input files in DRAGON has been developed by M. Guyot [29]. This is a standard CANDU 6 core with 380 horizontal channels each containing 12 fuel bundles. It calculates the structural properties of the core, including the reflector and material configuration. It also calculates absorption caused by the control mechanisms, such as the control rods and liquid zone controllers.

3.10 Temperature Coefficient

Temperature in a reactor is caused by the pressure and fission energy in the fuel that radiates outwards through the constituent material to the coolant and moderator. Temperature and reactivity influence each others behaviour, known as a feedback mechanism. Reactivity influences the reaction rate that influences the temperature that again affects the reactivity. If there is positive feedback, temperature increase or decrease causes the same effect on reactivity. Likewise, negative feedback occurs if an increase or decrease in temperature causes an opposite effect on reactivity. The neutron energy spectrum, Doppler broadening, and thermal expansion mainly cause temperature influence on reactivity.

The neutron energy spectrum is described as a Maxwellian distribution of neutrons. The thermal absorption occurs around energy of 0.025 eV or a speed of 2200 m/s. A temperature change will cause a shift in the Maxwellian distribution. Most isotopes in the reactor have an absorption spectrum that is inversely proportional

to neutron speed before the resonance absorption. Thus, a positive increase in temperature shifts the Maxwellian distribution for all neutrons causing less absorption. However, if all isotopes in the reactor had the same behaviour with neutron speeds there would be no significant change in reactivity. Figure 3.5 demonstrates the change in absorption at different neutron energies for U-235, Pu-239 and U-233. There is a noticeable linear decrease for U-235 but Pu-239 and U-233 both have absorption peaks beyond the thermalized range.

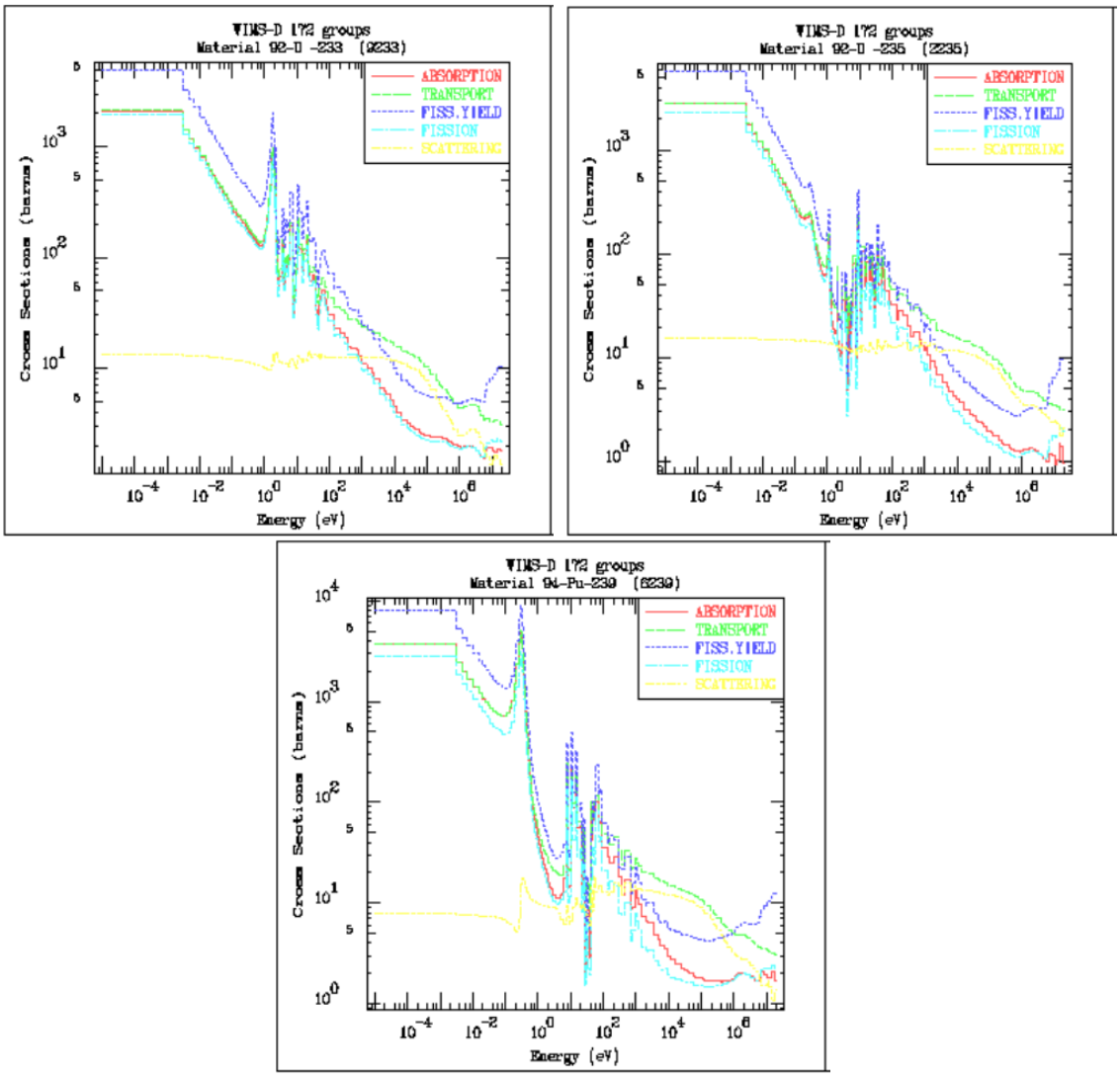

Figure 3.5: Cross Sections for ^{233}U, ^{235}U, and ^{239}Pu

In the case of NU fuel, the absorption cross sections with respect to temperature of U-235 and Pu-239 are normalized to U-238 in Figure 3.6. The absorption peak located outside of the thermal range causes the steady increase in Pu-239 absorption cross section. There is also a change in the number of neutrons created per absorption with temperature deviations. To understand how this affects reactivity, the thermal fission factor is divided into two variables: fissile absorption rate (Σ_f) and number of neutrons created per absorption (η).

$$\eta = \frac{\eta_{^{235}U}\Sigma_{f_{^{235}U}} + \eta_{^{239}Pu}\Sigma_{f_{^{239}Pu}}}{\Sigma_a(\text{Fuel})} \tag{3.29}$$

Figure 3.6 illustrates the change in the average neutrons created per fission (η) for U-235 and Pu-239 as a function of temperature in pure forms. Overall, there will be a negative temperature correlation result in U-235 but a positive temperature coefficient for Pu-239 for the thermal fission factor. Although there are fewer neutrons produced per fission, the rise in neutron fission absorption with temperature creates a positive temperature coefficient for Pu-239.

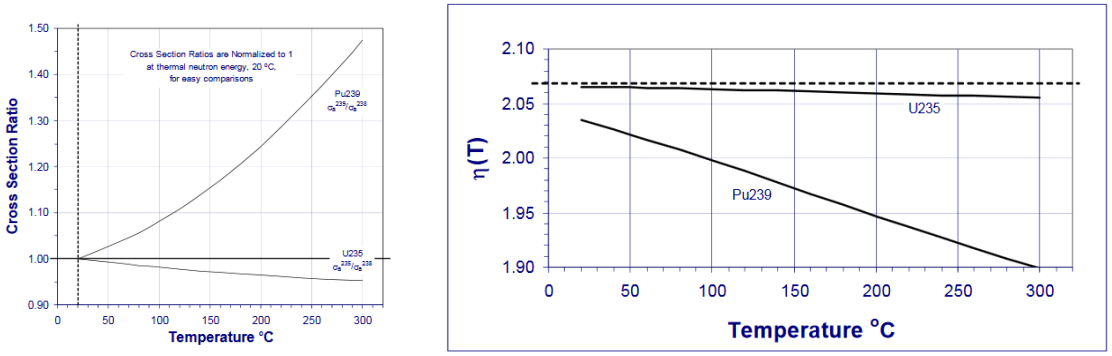

Figure 3.6: The temperature influence on neutron generation (η) and absorption ratio

The neutron energy spectrum can also affect the thermal utilization factor (f), fast fission factor (ϵ), resonance absorption (p), and the non-leakage probability (P). The structural material in the bundle is not strongly affected by temperature. If the neutron absorption in the fuel is altered by temperature but material absorption stays constant, a change will occur in the thermal utilization factor. The temperature also affects the mean free path of the neutron. More energetic neutrons will

have a longer mean free path traveling longer distances before being absorbed. This increases the likelihood of absorption in the coolant and moderator, or the possibility of leakage from the reactor. Higher temperature allows more neutrons to be pushed into greater energy ranges, allowing more resonance absorption and fast fission.

The Doppler broadening is caused by temperature changes directly in the fuel. As a neutron is being thermalized, it must go through an energy range known as the resonance energy range between 10 - 300 eV. Most actinides have a resonance capture that appears as sharp peaks in the absorption cross section profile (Figure 3.5). As the fuel temperature change, so does the vibration of nuclides in the fuel. The probability of absorption is considered the speed relative to the nucleus; if the nucleus is vibrating there is a change in the relative speed in the neutron-nucleus. The broadened resonance peak increases the neutron absorption range but decreases the absorption cross section at the specific peak energy. For the majority of actinides, the absorption peak regions are sizable, therefore peak broadening only amplifies neutron absorption in these regions.

Lastly, a temperature rise will cause thermal expansion of the fuel, moderator, and coolant, also affecting the reactivity. Thermal expansion will alter the volume and density of the fuel pellets but a bundle in a CANDU reactor is built to accommodate this modification. The thermal expansion of heavy water in the coolant and moderator will decrease the density. A lower density in the coolant reduces the likelihood of neutrons interacting with the coolant, allowing for more neutrons to be thermalized in the moderator. The decrease in density of the moderator provides neutrons with a longer mean free path, slowing down neutron thermalization. Lower density in the coolant and moderator will create a positive temperature coefficient.

Chapter 4

Lattice Cell Calculation

To analyze the intrinsic properties of fuel in a CANDU 6 reactor, it is necessary to understand how the fuel interacts in a single lattice cell configuration. This will be accomplished using the deterministic code DRAGON 3.0.6 and the Monte Carlo code SERPENT 2 to solve the neutron transportation code using multiple different nuclear libraries. The fuel that will be examined is natural uranium fuel and thorium fuel enriched with U-235. DRAGON will be used to investigate different power outputs for both fuels and the corresponding isotopic composition. The temperature coefficient, coolant void reactivity, and power transient effects will also be illustrated. The approximation model will be validated against DRAGON nuclear code to accurately predict reactivity transformations resulting from irradiation and power transients.

4.1 Natural Uranium Lattice Cell Simulation

The natural uranium lattice cell uses a constant power-to-weight ratio of 31.9713 kW/kg. A CANDU 6 bundle has a fuel weight of 19.236 kg and a density without porosity of 10.73 g/cm^3 [35], producing a bundle power of 615 kW. The average temperature of a fuel pin is suggested to be around 1000 K [49, 11] with a temperature gap of around 100 K at the pin-cladding interface [50]. The input for the calandra tube, pressure tube, and fuel cladding is illustrated on Table 4.1.

Table 4.1: CANDU 6 bundle properties used in DRAGON and SERPENT

	Calandria Tube	Pressure Tube	Fuel Cladding	Fuel Pin
Material	Zircaloy-2	Zr-Nb	Zircaloy-4	Natural UOX
Temperature (K)	345.66	560.66	560.66	1000
Density (g/cm^3)	6.44	6.57	6.44	10.73
External Radius (mm)	65.875	56.032	6.54	6.122
Internal Radius (mm)	64.478	51.689	6.12	-

Figure 4.1 represents the lattice cell results for DRAGON and SERPENT with multiple nuclear libraries. The approximation model uses data from the IAEA library and is compared to the DRAGON simulation using the same library in Figure 4.2. The DRAGON simulation is completed in increments of days starting at 1, 4, then 5 until reaching a burnup of 10,000 MWd/Mg. The SERPENT simulation uses incremental steps of burnup starting at 100 MWd/Mg until reaching 4,000 MWd/Mg then an increment of 500 MWd/Mg is used until reaching 9,000 MWd/Mg. The approximation model is calculated using increments of 100s.

The DRAGON and SERPENT results are similar and follow a general trend regardless of the nuclear library. The agreement between the nuclear libraries is related to the rigorous research that is done for uranium fuels. The initial drop shortly after the bundle is irradiated is caused by the build-up of parasitic absorption in the fuel. The peak that occurs at 1,400 MWd/Mg is caused by buildup and utilization of plutonium, known as the "plutonium peak." This also slows down the depletion of the initial fissile isotope U-235. Eventually, the regeneration of Pu-239 and Pu-241 plateaus and the depletion of U-235 reduces the amount of fissile isotopes in fuel, causing the multiplication factor to drop below one around 6,000 MWd/Mg. The bundle is removed shortly afterwards in a CANDU 6 reactor with an average exit burnup of 7,100 to 8,000 MWd/Mg [8, 51]. The approximation model follows a similar trend to the observed library except that the plutonium peak is less distinguished and there is a sharper reduction at 8,000 MWd/Mg. The poison buildup should reach equilibrium within the first couple of days, causing the initial dip. In the approximation model, only the parasitic absorbers Xe-135 and Sm-149 are considered to be variables, assuming other poisons are constant or do not fluctuate largely with power. This creates a less distinguishable dip in the initial reactivity signature for the approximation model.

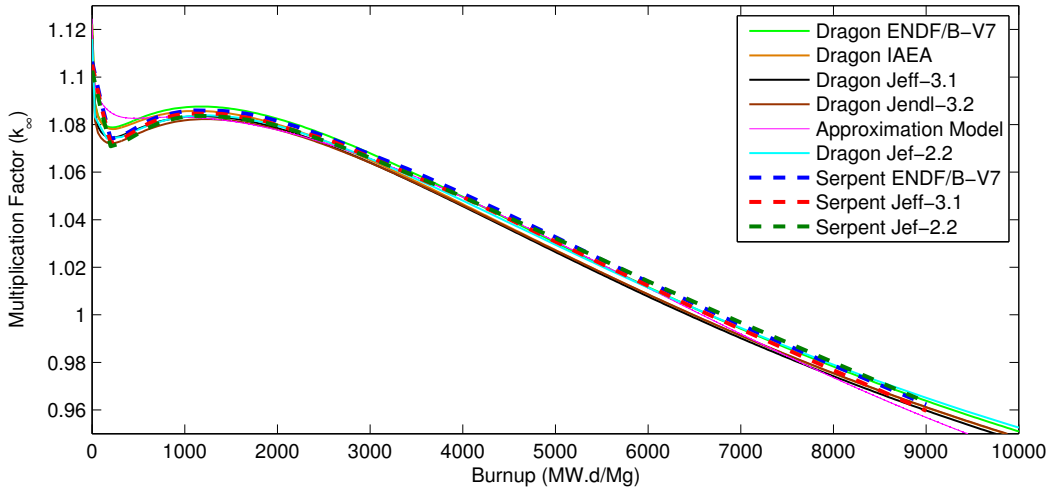

Figure 4.1: Lattice cell simulation of natural uranium in DRAGON and SERPENT at a bundle power of 615 kW

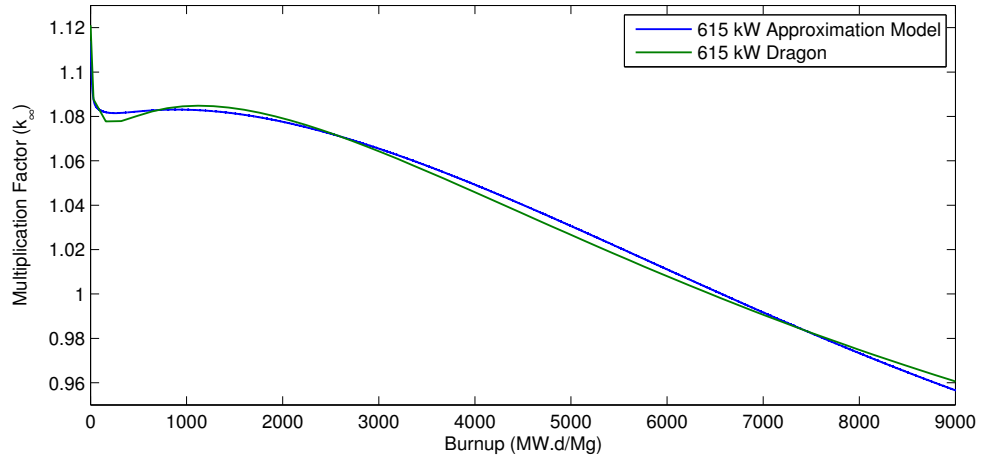

Figure 4.2: DRAGON IAEA comparison to the approximation model at a bundle fission power of 615 kW

4.2 Isotopic Concentrations of Natural Uranium

The power in the reactor is caused by the continuous fission in the fuel, primarily by the fissile isotopes. In a fresh bundle, the main source of power is derived from thermal fissions of U-235 with a small contribution to the fast fission of U-238. The fertile isotope U-238 will create Pu-239 by the resonance and thermal radiative capture of a neutron. Eventually, Pu-239 will become the dominant fissile isotope to drive the nuclear reaction, as illustrated in Figure 4.3. The cross-over between U-235 and Pu-239 occurs around 6,000 MWd/Mg, considerably early compared to other models that predict this should occur at 7,000 MWd/Mg [8]. The approximation model does not incorporate self-shielding calculations like other simulations. The absorption and depletion of isotopes in a fuel pellet change is based on the location in the bundle. The outer pellets are exposed to more neutrons and this causes greater absorption and depletion. The cross-over for the outer pellets is roughly 6,000 MWd/Mg, similar to the approximation model. The fraction of fission power generated by U-235, U-238, Pu-239, and Pu-241 to a burnup of 7,500 MWd/Mg is 57.9 %, 5.7 %, 34.6 %, and 1.8 %, respectively. It is expected that plutonium will contribute roughly half of the fission power in a CANDU 6 reactor [8].

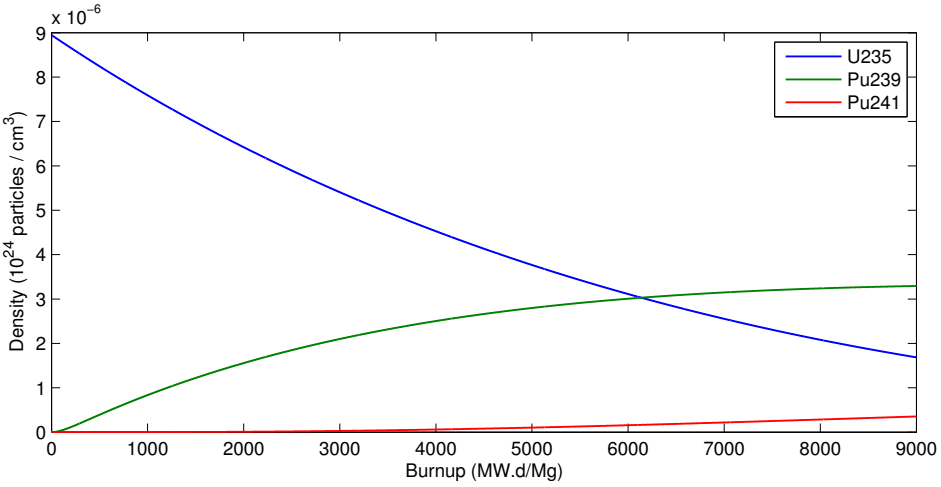

Figure 4.3: The evolution of isotopic concentrations in a lattice cell obtained using the approximation model for natural uranium fuel

4.3 Thorium Enrichment Concentration

Thorium is three times more abundant on earth than uranium but does not initially contain a fissile isotope. To maintain a stable neutron economy, thorium must undergo an enrichment process of adding a fissile element to the material. This study will investigate thorium enriched with U-235. The simulation will use the temperature and property characteristics for the calandra tube, pressure tube, and fuel cladding in Table 4.1. The fuel properties for thorium will need to be adjusted as they differ from NU fuel. The thermal conductivity of thorium dioxide (ThO_2) is much greater than uranium dioxide (UO_2), allowing for a higher transfer of heat between the fuel pellets and coolant fluid [52]. If the temperature of UO_2 is 1000 K, then recalculating the new average for ThO_2 results in a temperature of 900 K with a density of 9.85 g/cm^3 [11].

The calculation of the infinite multiplication factor in the lattice cell does not account for the reactivity losses in a typical CANDU reactor, such as the reactor core leakage and absorption by the control mechanisms. In order to evaluate the exit burnup of the bundle in the reactor, an estimated reactivity loss is assumed to relate k_{inf} to k_{eff}. Rouben suggests an average core leakage of -30 mk and an additional -18 mk based on the reactivity-device load in a CANDU 6 reactor [9, 33]. The reactivity losses will be different for thorium fuel and will change based on the enrichment rate. Instead of analyzing a full core with each enrichment, it is assumed that there is a total reactivity loss of 48 mk between k_{inf} to k_{eff}.

Figure 4.4 illustrates thorium with different enrichment percentage of U-235, simulated in DRAGON. For simplicity, each enrichment step uses a constant density of 9.85 g/cm^3 and a constant temperature of 900K. The change of temperature and density have minimal affect on the reactivity in a lattice cell calculation, as addressed in Section 4.8. The power-to-weight ratio is the same as NU fuel at 31.9713 kW/kg. The bundle is assumed to have a reactivity loss of 48 mk to account for leakage and control mechanisms in a CANDU 6 reactor. A CANDU 6 reactor features on-line refuelling, allowing new fuel to replenish older fuel that has negative reactivity. The exit burnup is evaluated when reactivity is equal to zero for the integrated burnup as seen in Equation 4.1. The black dots represent the exit burnup for each enrichment percent. A higher enrichment increases the longevity of the bundle allowing a greater utilization of the secondary fissile isotope U-233. The trade-off between greater burnup is the cost of enrichment as well as the initial burst of reactivity when refuelling the CANDU reactor. An enrichment of 2.0% was selected with an estimated exit

burnup of 13,700 MWd/Mg. This is about double the estimated exit burnup of NU fuel at 7,095 MWd/Mg, according to the approximation model.

$$0 = \int_0^{B_{exit}} \rho(B) - 0.048 \; dB \tag{4.1}$$

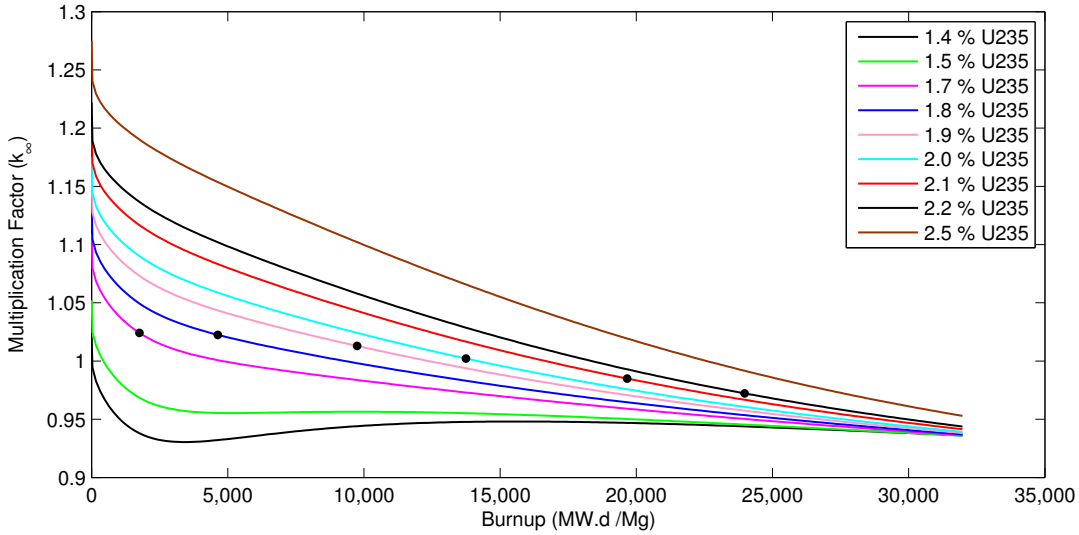

Figure 4.4: DRAGON lattice cell simulation of thorium with different enrichment of U-235 using the WIMS-SD IAEA library. The black dots represent the bundle exit burnup assuming a reactivity loss of 48 mk accounting for leakage and control mechanisms in a CANDU 6 reactor.

4.4 Thorium Lattice Cell Simulation

The approximation model is based on DRAGON using the IAEA library in Figure 4.5. The model is compared to DRAGON and SERPENT using different nuclear libraries in Figure 4.6. There is a noticeable discrepancy when comparing DRAGON and SERPENT using the same libraries. The initial drop is similar in both cases but there is a dramatic change after 4,000 MWd/Mg when the reactivity simulated in DRAGON decreases at a faster rate than SERPENT. It is difficult to determine this

discrepancy as both codes use different methods to solve the transport equation. It can be speculated that there is a greater build-up of U-233 in the SERPENT code, allowing for a higher reactivity near the end.

The simulation for thorium fuel uses the same power density as NU fuel, but both have different density, resulting in a change in bundle power. Thoria would have a bundle fuel weight of 18.11 kg producing an average power output of 578 kW, slightly lower than NU bundle power of 615 kW.

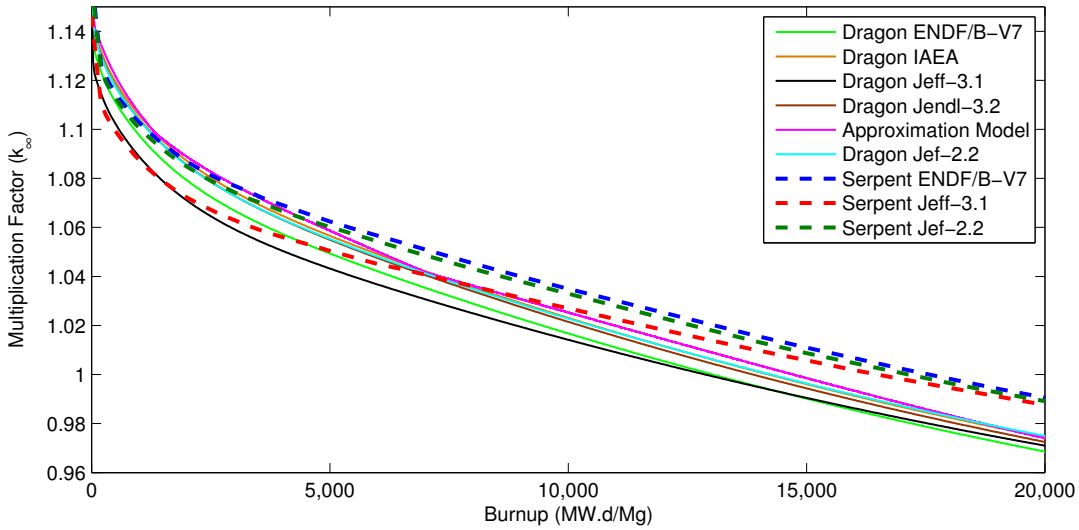

Figure 4.5: Lattice cell simulation of thorium enriched with 2.0% U-235 in DRAGON and SERPENT at a bundle fission power of 578 kW

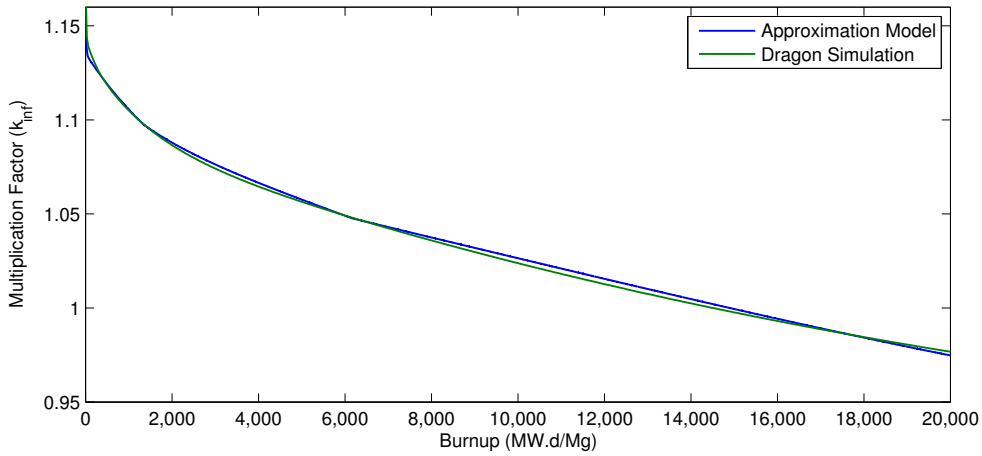

Figure 4.6: Comparison between the approximation model and DRAGON simulation using IAEA library

4.5 Accuracy of the Nuclear Libraries

In addition to the disagreement between DRAGON and SERPENT, there is a noticeable change when using different nuclear libraries. For NU fuel, as seen in Figure 4.1, the data from different libraries have a similar trend and are within reasonable agreement. The data libraries used for thorium fuel have a much larger deviation as seen in Figure 4.5. The nuclear libraries have studied uranium rigorously because it has been the main fuel for nuclear power plants around the world. Thorium has not been subject to the same degree of research, which will cause significant differences depending on the choice of libraries. As noted in Figure 4.7, there exists a large difference in cross section signatures based on the libraries. The IAEA library is a combination of other libraries that uses Jendl-3.2 for Pa-233 and Th-232 and Jef-2.2 for U-233. Jef-2.2 and ENDF/B-VI should have some similarities as both are based on ENDF/B-V. The absorption cross-section for Th-232 in the thermal region is well known, but the resonance and fast regions differ based on these libraries. Specifically, the inelastic, capture, and fission cross sections in the fast region require additional research [54]. More precision is necessary for U-233 on capture and inelastic cross-section, but overall the data from different libraries is more consistent. In addition, the cross-section data for protactinium (Pa-233) is not well known in these libraries. It should be mentioned that these libraries have been released years ago and have since been updated with more reliable information. The choice of libraries in this

study is limited to those available in DRAGON (ENDF/B-VII.0, Jeff-3.1, ENDF/B-VI rev. 8, Jendl-3.2, Jef-2.2, IAEA) and SERPENT (ENDF/B-VII.0, Jeff-3.1.1, Jeff-3.1, ENDF/B-VI rev. 8, and Jef-2.2).

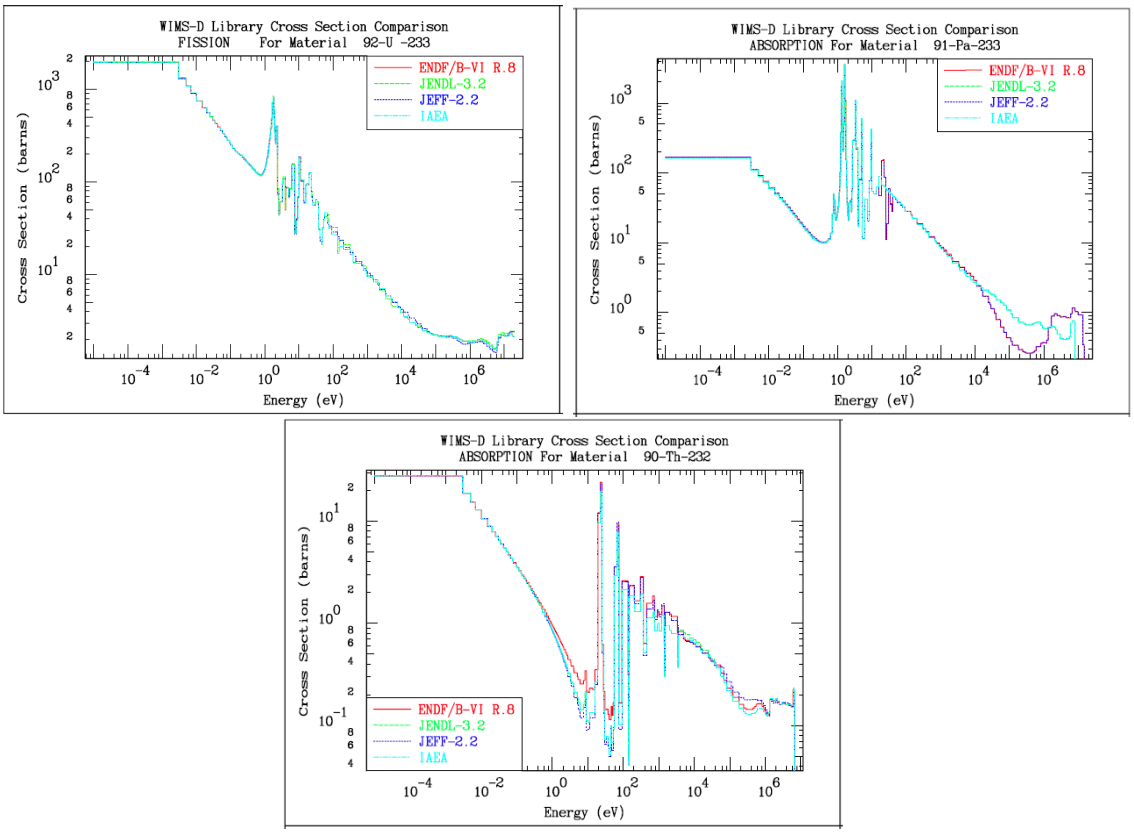

Figure 4.7: Library comparison of U-233, Pa-233 and Th-232

4.6 Isotopic Densities of Thorium

The dominant fissile isotope in thorium fuel is U-235 that is homogeneously combined with Th-232. Eventually, the thorium absorption cycle will create U-233, which will assist as a fissile isotope. Thorium fuel requires a higher ratio of fissile elements than NU fuel to sustain a constant neutron generation. This is partially caused by Th-232 having a much higher thermal absorption cross-section. It is roughly three times that of U-238, evidently requiring roughly three times more U-235 in the initial bundle.

Although there is more thorium absorption, the process to convert thorium into U-233 requires a month, whereas, NU absorption cycle takes only 2.35 days. Thus, the thorium bundle will require more time in the reactor for U-233 to become a dominant contributor compared to Pu-239 in the NU bundle. One of the benefits to the longer absorption cycle is that the increase of U-233 is gradual and does not produce a peak that is observed in the NU fuel. The fraction of fission power contributed by Th-232, U-233, and U-235 to a burnup of 15,000 MWd/Mg is 72 %, 26 %, and 1%, respectively. The contribution of thorium absorption cycle is much less than the U-238 absorption cycle responsible for roughly 40% of the fission power. The fission cross section for thorium in the fast energy range is significantly lower than U-238, representing a lower fast fission factor. To utilize more U-233, a higher enrichment may be necessary or a reduction in power to allow for a greater conversion of Th-232 to U-233.

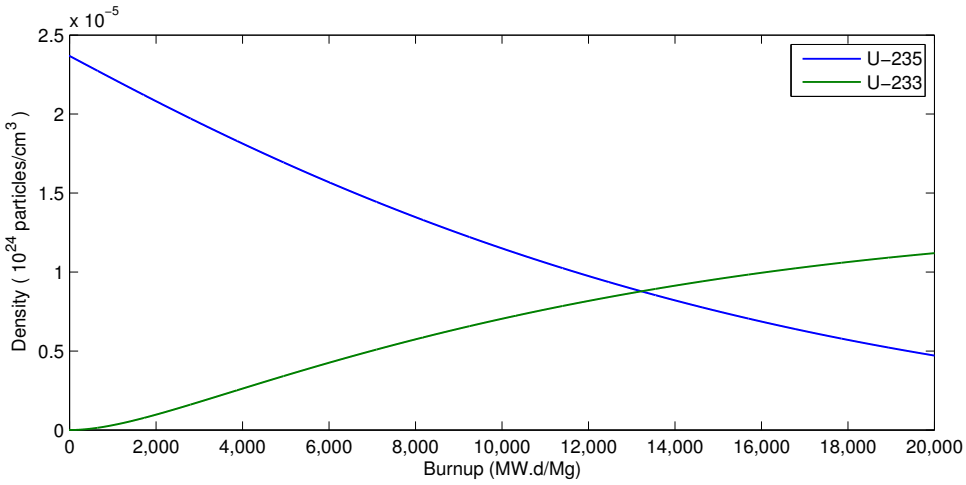

Figure 4.8: Evolution of isotopic densities obtained using the approximation model for thorium fuel

4.7 Simulating Various Bundle Powers

The lattice cell calculations thus far have been using a power density of 31.9713 kW/kg, creating bundle fission powers of 615 kW and 578 kW for NU and thorium fuel. Although this is the default setting for most lattice cell simulations, it is slightly higher than expected for the average bundle power. Estimating the power per bundle in a reactor can be difficult because the flux shape will determine the distribution of

power generated in the reactor core. If the flux in the reactor is equal everywhere, the average channel fission power from a CANDU 6 reactor is 5.67 MW, roughly equal to a fission power of 472 kW per bundle. This is not a realistic case. The flux is generally highest at the center of the core and lower in regions close to the periphery of the reactor. The operating licence for the upper limit of channel and bundle powers in a CANDU 6 reactor is 7.3 MW and 935 kW, respectively. This thesis will investigate a full core reactor in which bundles are exposed to a range of different powers. Thus, it is necessary to analyze the approximation model at different ranges of power and compare these results to DRAGON.

Figure 4.9 and 4.10 compare the DRAGON lattice cell simulation to the approximation model with bundle powers at 10%, 25%, 50%, 75%, 100%, 125%, and 150% of the nominal power of 615 kW. Each of these simulations is set for a maximum of 1,000 days or until they surpass the boundaries. In both cases, the reduced power results in a higher multiplication factor. A lower flux tends to generate less parasitic poison as illustrated by Xe-135, attributing to a particular change in the multiplication factor. If this were the only distinguishing change in the multiplication factor, then the NU and thorium fuel should roughly change equally with power. An incremental adjustment of power by 25% causes a reactivity change of 11 mk in the thorium fuel, much larger than the 3 mk change from NU fuel.

The absorption cycle in uranium fuel requires 2.36 days to produce Pu-239 (Equation 1.1). The absorption cycle for thorium is much longer and requires roughly a month to produce U-233 (Equation 1.2). The lower power provides thorium fuel with more time to convert the fertile isotope, Th-232, into a fissile isotope, U-233, preserving the initial fissile isotope, U-235. Figure 4.11 and 4.12 display the change in the fissile isotopes in NU and thorium fuel at different powers generated by DRAGON. There is a noticeable change in fissile isotopes in the thorium fuel and a less distinguished change in fissile isotopes in NU fuel, due to the longer absorption chain. The significant reactivity change with power for the thorium fuel is caused by the considerable change in the fissile isotope concentrations. In many full core simulations, the conditions of the fuel bundle are determined at nominal power and do not consider the relationship between power and isotopic densities and power, contributing to a significant change in reactivity.

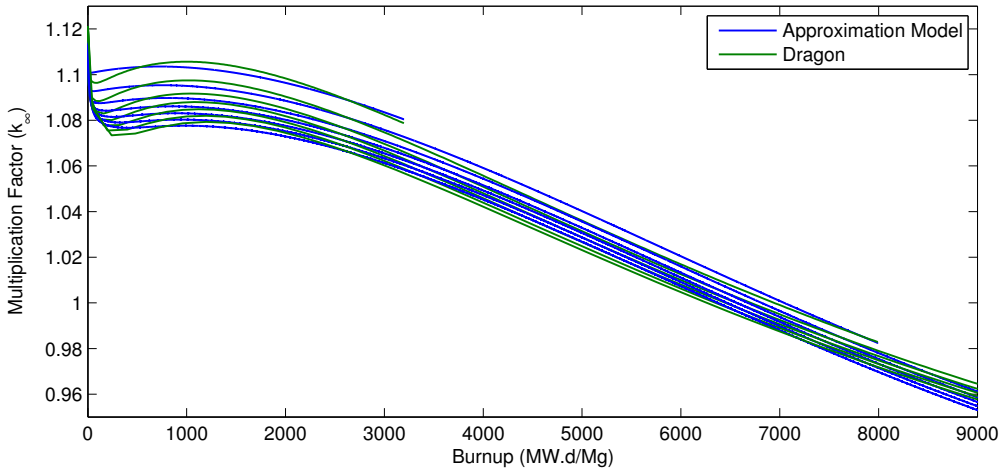

Figure 4.9: Fission powers at 10%, 25%, 50%, 100%, 125% and 150% of full power at 615 kW are presented comparing the results from the DRAGON simulation to the approximation model for NU fuel

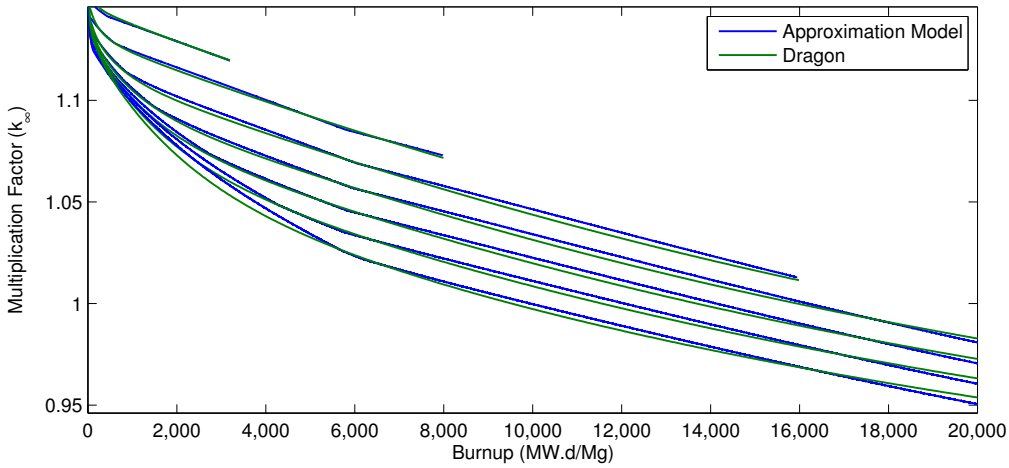

Figure 4.10: Fission powers at 10%, 25%, 50%, 100%, 125% and 150% of full power at 615 kW are presented comparing the results from the DRAGON simulation to the approximation model for thorium fuel

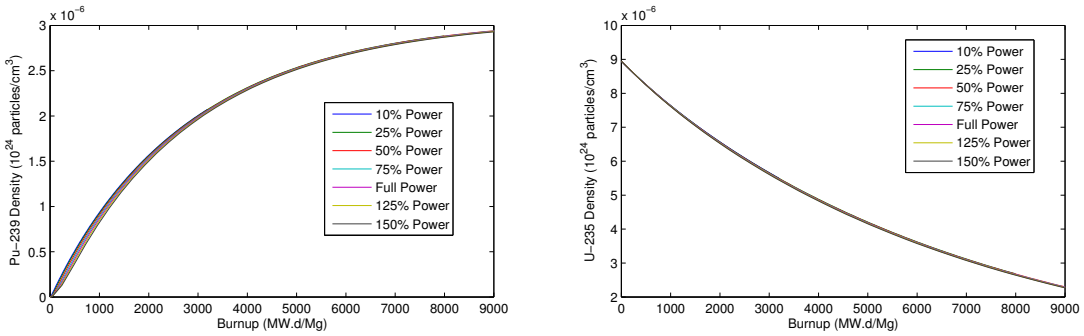

Figure 4.11: The fissile isotope density for natural uranium fuel as a function of the power generated using DRAGON. It is assumed that full power for a bundle is 615 kW.

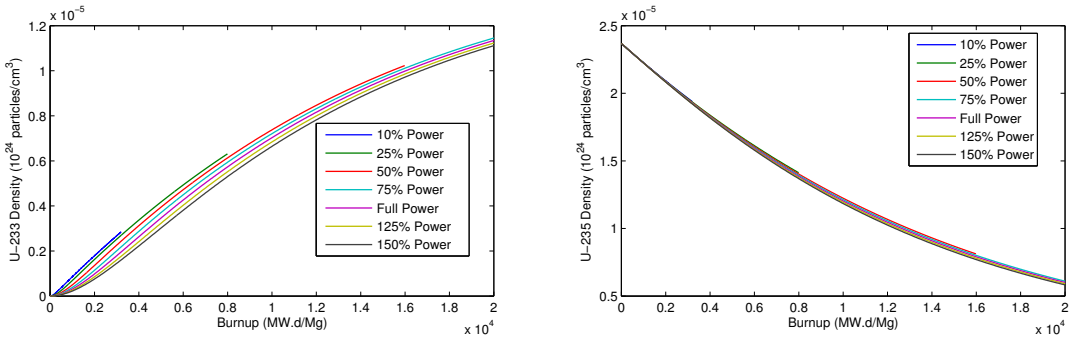

Figure 4.12: The fissile isotope density for thorium fuel as a function of power generated using DRAGON. It is assumed that full power for a bundle is 615 kW.

4.8 Temperature Coefficient

It should be mentioned that the previous simulations are run with the same temperature for all the components of the lattice calculation. As mentioned earlier, the temperature of the fuel, coolant, and moderator will have an effect on the individual four-factor formula of the multiplication factor. It is important to identify the temperature feedback to provide a proper understanding of the operations and control of the reactor. Typical temperature and states of a CANDU 6 reactor are cold shutdown, hot shutdown, and full power, as illustrated in Table 4.2 [49]. Hot shutdown

occurs minutes to hours after reactor shutdown. After reactor shutdown, the temperature of the moderator, coolant, and fuel will eventually reach equilibrium. This is known as a cold shutdown, which occurs months after a hot shutdown. This section will look at the effects of temperature: from hot shutdown to full power, then to exceeding full power to understand feedback in emergency conditions. The effects of temperature on the moderator will be ignored as changes often require long periods of time and can be controlled by the heat exchangers. The temperature coefficients are measured using the four-factor formula to address the property changes occurring in lattice cell.

$$\frac{1}{k}\frac{\partial k}{\partial T} = \frac{1}{\eta}\frac{\partial \eta}{\partial T} + \frac{1}{f}\frac{\partial f}{\partial T} + \frac{1}{p}\frac{\partial p}{\partial T} + \frac{1}{\epsilon}\frac{\partial \epsilon}{\partial T} \tag{4.2}$$

Table 4.2: Temperatures of Components in a CANDU 6 Reactor (°C) [49]

	Cold Shutdown	Hot Shutdown	Full Power
Fuel	25	290	790
Coolant	25	265	290
Moderator	25	66	69

The calculation is performed using DRAGON for the fuel and moderator. In the case of fuel, the composition of the fuel and density stayed constant at different temperatures. The density of the coolant will change with temperature due to thermal expansion. The moderator will be kept at the same composition and temperature throughout this section. The temperature of the fuel is adjusted from 290 °C to 1490 °C in increments of 100 °C as the coolant remains constant at 290 °C. Next, the coolant will be adjusted from 265 °C to 355 °C in increments of 10 °C as fuel temperature remains constant at operating temperature. The data for the material cross sections are adjusted for temperature using the IAEA 172 energy group library [38]. The four-factor formula is calculated as the accumulative average of NU fuel to 8,000 MW.d/Mg and thorium fuel to 14,000 MW.d/Mg with the simulation executed in increments of five days.

The fuel temperature has a negative feedback with reactivity as seen in Table 4.3. The two factors that have a primary effect on fuel temperature modification are Doppler broadening and a slight energetic shift in the neutron energy spectrum. Both fuels have a positive temperature coefficient in the thermal fission factor (η), meaning that the ratio of neutrons created from thermal fission has increased compared

to thermal neutron absorption. This shift in the NU fuel is caused by the increase in fission cross section of Pu-239. Pu-239 exhibits a cross section peak at 0.3 eV as seen in Figure 3.5. Doppler broadening will enlarge the peak widths and the shift in neutron spectrum will increase the ratio of neutron production in the fission range. This is also displayed in the thorium fuel as U-233 has an absorption peak around 1eV. Both U-238 and Th-232 have an absorption cross sections that is inversely proportional to neutron speed before the resonance absorption. Therefore, the thermal fission factor has a positive temperature coefficient with reactivity. The main contributor for a negative temperature coefficient in both fuels is the resonance escape probability (p). The Doppler broadening widens the range of radiative capture in the resonance energy region, allowing U-238 or Th-232 to absorb more neutrons before thermalization. The thermal utilization factor (f) represents the ratio of neutrons absorbed in the fuel compared to neutrons absorbed elsewhere, representing neutrons lost in the system. The shift in the neutron energy spectrum can create a longer mean free path for the neutrons, raising the likelihood of absorption in the heavy water or material. As most of the fuel isotopes have a neutron absorption spectrum inversely proportional to neutron speed, thermal neutron absorption is reduced, consequently decreasing the thermal utilization factor. The fast fission factor (ϵ) is defined as fission occurring outside of the thermal neutron range. This is mainly caused by fission in the fast energy ranges of U-238 and Th-232. There are two factors that affect the fast fission factor as temperature rises. Doppler broadening improves the fast fission absorption range and the shift in the neutron energy spectrum increases neutrons in the fast fission energy range. As temperature rises from hot shutdown to full power and beyond, the rate of change in reactivity begins to decelerate as seen in Figure 4.13.

Table 4.3: The four-factor temperature coefficient terms for fuel at equilibrium from 290 to 1490 °C (10^{-7} K^{-1})

	$\partial\eta/\partial T$	$\partial f/\partial T$	$\partial p/\partial T$	$\partial\epsilon/\partial T$	$\partial k/\partial T$
Natural Uranium	18.7	-0.674	-58.5	0.931	-50.8
Thorium	17.7	-2.70	-75.9	0.358	-75.1

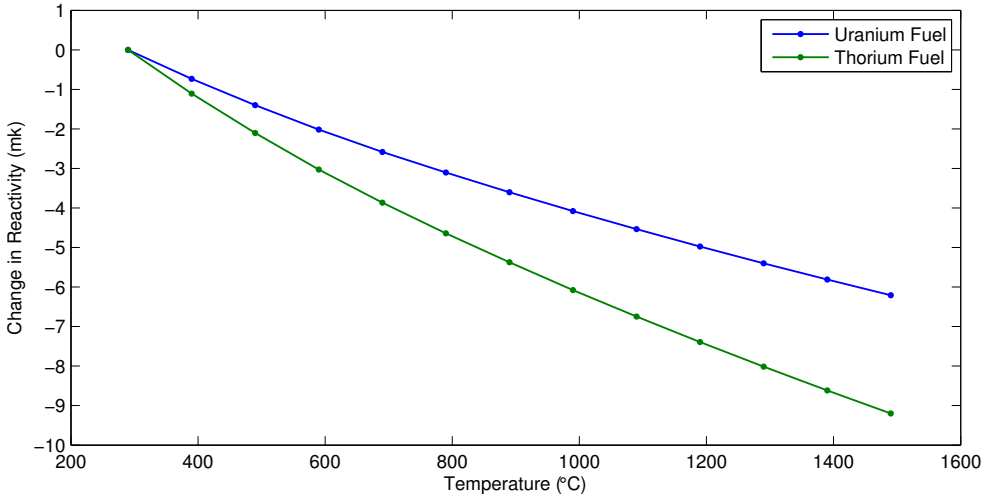

Figure 4.13: The relationship between reactivity and temperature of the fuel pellets simulated in DRAGON. The coolant and moderator are at a constant operating temperatures for this lattice cell simulation.

There is a positive temperature coefficient for the coolant as demonstrated in Table 4.4. The rise in temperature of the coolant causes a thermal expansion of D_2O, subsequently decreasing the density of the coolant. This influences neutrons in two primary ways: neutrons are less likely to interact with the coolant, and the system is more energetic, hardening the neutron energy spectrum. The major reason for a positive temperature coefficient is the adjustment in the resonance escape probability. With fewer neutrons interacting with the coolant, more neutrons are being thermalized in the moderator. Fewer neutrons will interact with the fuel in the resonance range, lowering the probability of resonance capture. The thermal fission factor is positive for NU fuel but negative for thorium fuel. Pu-239 has a peak fission ratio close to the thermal neutron energy range, whereas the peak for U-233 is closer to the resonance energy range. The shift in the energy spectrum, as well as more thermalized neutrons, causes a greater fission yield for Pu-239 but a dissimilar effect for U-233. The fission Westcott factor is below one for U-233 and U-235, meaning the hardening of the neutron energy spectrum will cause fewer fissions. There are fewer neutrons being absorbed by the coolant, increasing the thermal utilization factor. Fast fission typically occurs at high energy promptly after neutron birth. Less interaction with the coolant allows more prompt neutrons to

interact with the fuel pellet without being down scattered. Naturally, this is greater for NU fuel as U-238 exhibits a greater fast fission cross section.

Table 4.4: The average four-factor temperature coefficient terms for coolant as temperature ranges from 265 to 355 °C (10^{-7} K^{-1})

	$\partial\eta/\partial T$	$\partial f/\partial T$	$\partial p/\partial T$	$\partial\epsilon/\partial T$	$\partial k/\partial T$
Natural Uranium	24.2	88.3	177	59.3	382
Thorium	-49.3	76.1	219	12.2	307

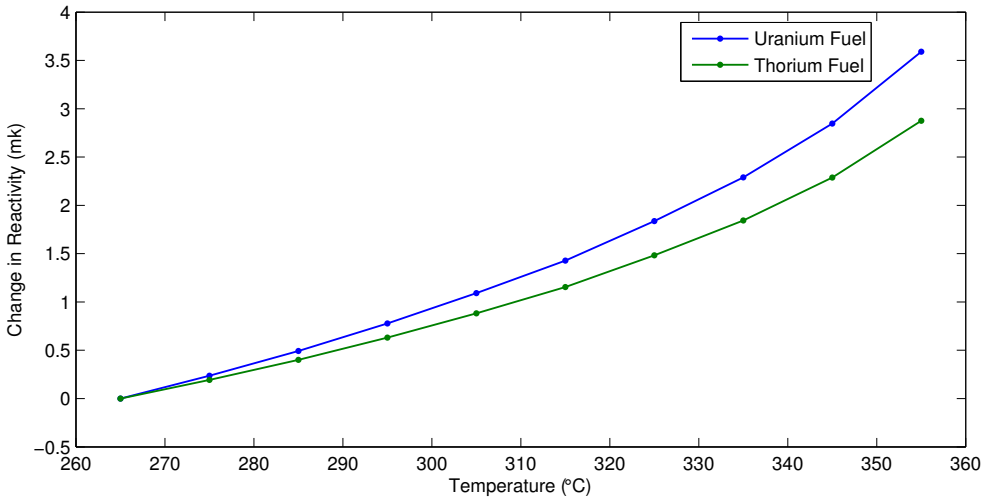

Figure 4.14: The relationship between reactivity and temperature for the coolant simulated in DRAGON. The fuel and moderator are at constant operating temperatures for this lattice cell simulation.

The average value for the temperature coefficient between hot shutdown and full power for NU fuel is -6.20 μk/°C. After full power, average value from 790 to 1490 °C is slightly lower at -4.34 μk/°C. This calculation is marginally lower than the estimate of -8.0 μk/°C for hot shutdown to full power and a slope of -4.0 μk/°C at full power for a CANDU 6 reactor [49]. The thorium fuel temperature coefficient is -9.26 μk/°C from hot shutdown to full power and -6.36 μk/°C after full power. The temperature coefficient of the NU coolant at normal operating power is 30 μk/°C, slightly lower than the estimate of 40 μk/°C [49]. The temperature coefficient between hot shutdown and full power is 25.9 μk/°C and after full power becomes 50.0

μk/°C. The temperature coefficient of the coolant for thorium fuel between hot shutdown and full power is 21.0 μk/°C and if 39.9 μk/°C after full power. The power coefficient is known as the reactivity change from a hot shutdown to full power. This value is typically around -2 to -4 mk in a CANDU 6 reactor, assuming the fuel is at equilibrium. The power coefficient from the results for NU fuel is roughly -2.46 mk, in agreement with the estimated value. Thorium fuel pellets operate at a lower fuel power due a higher thermal conductivity. The power coefficient for thorium is -3.35 mk for fuel pellets between 290 to 625 °C, assuming the same coolant temperature range.

A negative temperature coefficient is preferred for controllability of a reactor because it counteracts the change in reactivity, providing more time for control systems to regulate the neutron population. In emergency conditions, a negative temperature coefficient can slow down or compensate for increases in power. It should be mentioned that although thorium has an overall greater negative temperature coefficient, it also has a higher thermal conductivity, allowing for thorium fuel to more effectively transfer heat from the fuel pellets into the coolant. This prevents thorium fuel from reaching high temperatures transferring the heat into the coolant responsible for a positive feedback effect. Overall, thorium has a higher negative temperature coefficient in the fuel and a lower positive coefficient in the coolant, allowing for safe conditions in a reactor. Moreover, U-235 plays a significant role in lowering the power coefficient for the thorium fuel. The power coefficient would be higher if the thorium-based fuel is enriched with plutonium.

In this example, the power is constant as the temperature of the fuel and coolant independently changes. Of course, this is not realistic since the temperature change in the fuel is caused by the fission rate directly related to power. The coolant is also directly related to the fuel temperature by heat exchange and the thermal power stored in the coolant and moderator. It is very difficult to determine the change and rate of change of heat for the fuel and coolant. Thorium fuel will have a different relationship between fission power and temperature than NU fuel because of the differences in properties. There is also residual heat after a change in fission power for the fuel and coolant caused by the decay heat, pump heat, as well as ambient losses. When the fission power changes, the fission product inventory requires time to adjust to the new power. This creates a lag on the radioactive decay of the fission products that produce decay heat. The fluid friction creates heat and pressure in the coolant channels depends on the coolant flow rate that is independent of the fission power. This heat occurs as long as the pumps are operational. Lastly, ambient heat is caused

by the heat exchange from the coolant to moderator, dependent on the differential temperature. Although determining the association between temperature and power would require an in-depth study, the method presented provides understanding of the relationship. The temperature coefficient will be ignored in the full core calculation because of the noted complexity. However, this provides an assumption that the deviations in reactivity should be slightly less than the results in Chapter 5.

4.9 Coolant Void Reactivity

Another study associated with the safety of the reactor is the coolant void reactivity (CVR). This is defined as the change in reactivity if the coolant in the system is removed. It has been demonstrated that if the coolant density decreased there is a positive reactivity effect. If the coolant was voided, it produces a large positive reactivity insertion in a CANDU reactor. The CANDU reactor is designed to react to a CVR and the safety systems will prevent an uncontrollable disaster scenario. Other reactors, such as PWR, have a negative CVR as a result of using light water and combining the coolant and moderator. The simulation will be done using DRAGON by making the coolant density zero. This result will be compared to the normal lattice cell with coolant to analyze the change in reactivity, as seen in Figure 4.15. The coolant void reactivity is much lower in the thorium fuel than NU fuel throughout the fuel bundle lifetime.

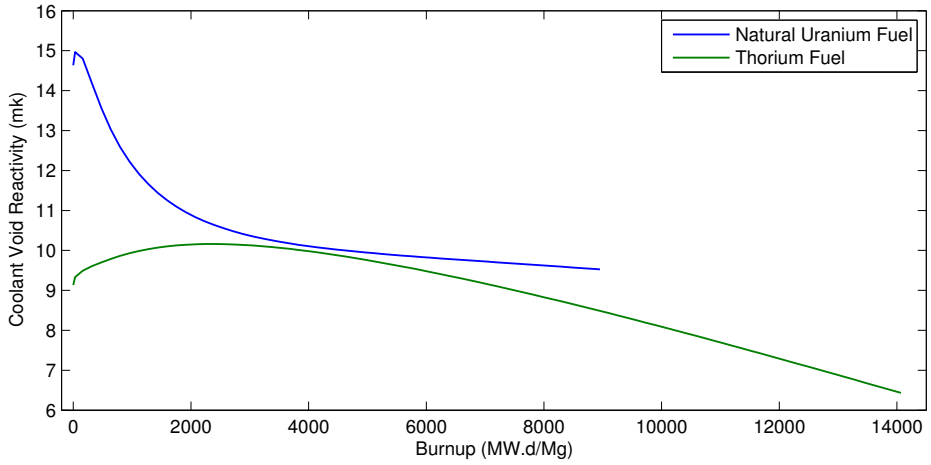

Figure 4.15: Coolant void reactivity in a lattice cell simulated using DRAGON

Table 4.5 displays the average change in each of the four-factors throughout the bundle's estimated lifetime as the coolant is voided. The four-factor effects are similar to the result achieved when the coolant temperature rises, subsequently lowering the coolant density. The coolant operates at a much higher temperature than the moderator. This can cause the coolant to excite or re-warm thermalized neutrons exiting the moderator. Without the coolant present, the neutrons will not need to be re-warmed thereby preserving thermalized neutrons. NU fuel has a large macroscopic thermal fission cross section for fresh fuel because of the low thermal absorption of U-238. This causes the thermal fission factor (η) to be much higher for fresh fuel, causing a peak in the coolant void reactivity. As parasitic absorbers are born from fission and fissile material is utilized, the thermal fission factor decreases as well as the coolant void reactivity. The presence of Th-232 reduces the initial peak in the thermal fission factor as a result of the large thermal cross section. The thermal fission factor begins to grow slightly in the thorium fuel until it naturally declines with the reduction in fissile material. Fewer neutrons will interact with the fuel in the resonance energy range, increasing the resonance absorption factor (p). There is less neutron absorption in the system as neutrons interact with heavy water at lower temperatures, increasing the thermal utilization factor (f). Neutrons are more likely to interact with a fuel pellet after birth without being down scattered, thereby increasing the fast fission factor (ϵ). Overall, the thorium fuel coolant void reactivity is lower than the NU fuel coolant void reactivity in a CANDU 6 reactor.

Table 4.5: The change in the four-factor formula averaged over the lifetime of the bundle as coolant is voided

	$\Delta\eta$	Δf	Δp	$\Delta\epsilon$
Natural Uranium Fuel	0.0011	0.0028	0.0047	0.0023
Thorium Fuel	-0.0002	0.0026	0.0059	0.0004

4.10 Transient Effects of Pa-233 and Np-239

When the reactor is shutdown there are transient effects with the parasitic absorbers that need to be considered. These poisons are created from the decay of isotopes and cause a lag in concentration when the flux deviates. Primarily Xe-135 creates a negative reactivity in a reactor shutdown scenario that can remain for 60 hours. If the operators are able to override instead of wait out the Xe-135 effects, it is necessary to withdraw the adjuster rods to produce additional reactivity. This effect also applies to fissile elements that are produced by the decay of fertile isotopes that will

increase the reactivity after shutdown.

Figure 4.16 shows the reactivity change in a lattice cell as the power density is set to zero to simulate a bundle removed from the reactor. Initially, the power is set to linearly decrease during the first day to create a gradual absorption from xenon. Both fuels display an initial absorption, then, as xenon decays, there is a rebound in the multiplication factor. In NU fuel, this effect occurs when Np-239 decays into Pu-239 with a half-life of 2.36 days and reaches saturation in 10 days after shutdown. In the case of thorium, Pa-233 decays into U-233 with a half-life of 26.97 days, requiring a much larger period of time for saturation conditions. The behaviour of both fuels is similar during the first 10 days when there is no power influencing the bundle. After 10 days, the reactivity for the thorium bundle will continue to grow for the next 90 days. This illustrates the excess reactivity in the thorium bundle that will continue to grow in a shutdown scenario or if the bundle is removed from the reactor. It has been suggested that this excess reactivity can be utilized for additional use in a reactor.

Table 4.6: Additional reactivity in a lattice cell after being irradiated for 120 days (3,854 MWd/Mg) is removed from the reactor

	10 days	30 days	60 days	90 days
NU Fuel	30 mk	30 mk	29 mk	29 mk
Thorium Fuel	32 mk	45 mk	55 mk	59 mk

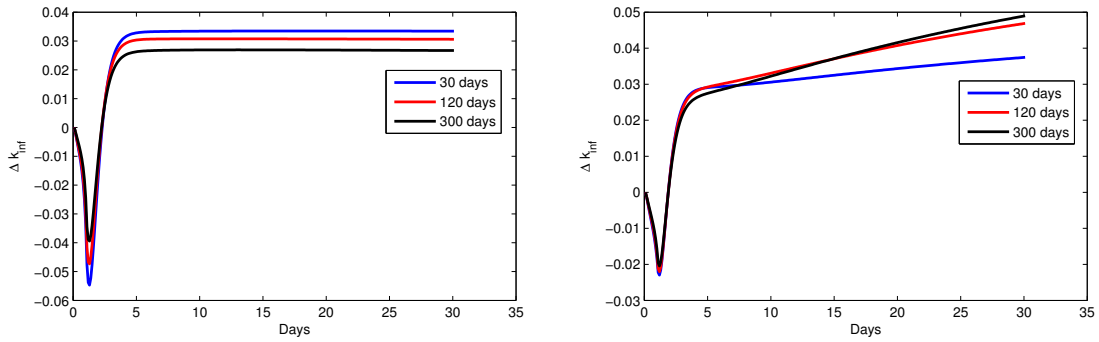

Figure 4.16: Reactivity change after a bundle is removed from the reactor at 30, 120, and 300 days corresponding to a burnup of 976, 3854, and 9609 MWd/Mg

4.11 Delayed Neutrons

Delayed neutrons play a crucial role in the ability to control the reactor. The average delayed neutron yield (β) is the average sum over the eight precursor groups. The mean generation time (Λ) is considered the average time between the neutron birth and subsequent fuel absorption undergoing fission. These values depend on the composition of the fuel bundle as illustrated in Figure 4.17. For the NU bundle, the dominant fissile isotope changes from U-235 to Pu-239 near the end of the cycle. Although the total delay time ($T_{1/2}$) of neutron production is slightly higher in Pu-239 than U-235, the probability that a delayed neutron will be created is much lower. Thus, the average delayed neutron yield and mean generation time both decrease with bundle burnup. Similarly, U-233 creates one third as many delayed neutrons as U-235 resulting in a similar change, albeit much slower for both variables than the NU bundle. A distinguishing feature in this comparison is that the fast neutrons produced by thorium have a higher delay neutron yield and delay time than U-238 but contribute significantly less because of the lower fast fission cross section. The delayed neutrons and mean generation time of U-233 is comparable to the contribution of both Pu-239 and Pu-241. The main reason that the thorium fuel is higher in both factors is that U-233 contributes much less overall due to the abundance of U-235. This raises the question of whether or not thorium enriched with plutonium would provide adequate delay time to safely operate a reactor.

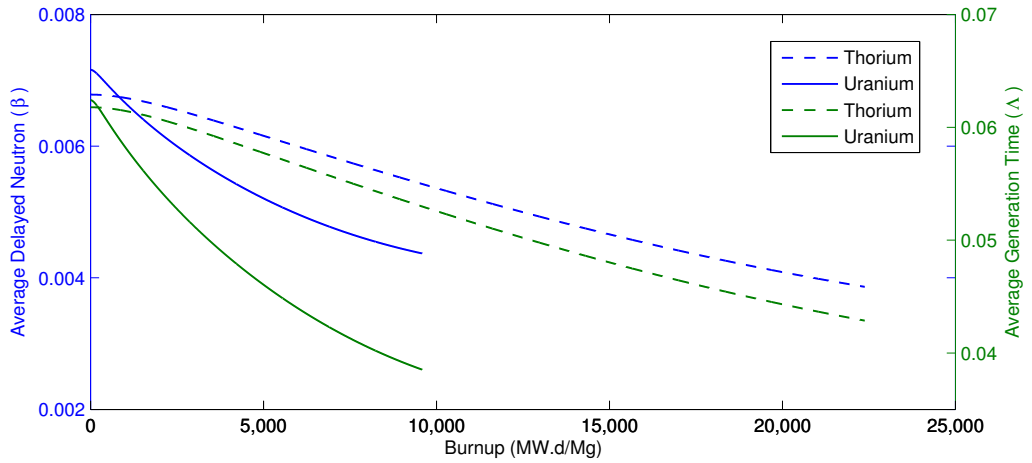

Figure 4.17: Delayed neutron characteristics represented in the approximation model

4.12 Bundle Simulations of Power Transients

To confirm that the approximation model will accurately represent the power transients in the full core simulation, it is necessary to compare power transients in a simplified one-bundle model to DRAGON simulations. The first transient that will be demonstrated will have power periodically diverging from full power at 615kW to a reduced power of 492 kW or 80% full power every 12 hours, which is commonly known as load following. The approximation model only considers two main poisons, those being Xe-135 and Sm-149, whereas the DRAGON calculation considers most of the prominent parasitic absorbers produced by the fission yield. Thus, in the approximation model, it is assumed that the only necessary poisons that will outline this change in reactivity is mainly Xe-135 and Sm-149 to a lesser extent. Figure 4.18 and4.19 display the changes of k_{inf} in hours as the power is cycled with both models. In both the thorium and NU bundle, the approximation model agrees within reasonable assumption with the DRAGON simulation.

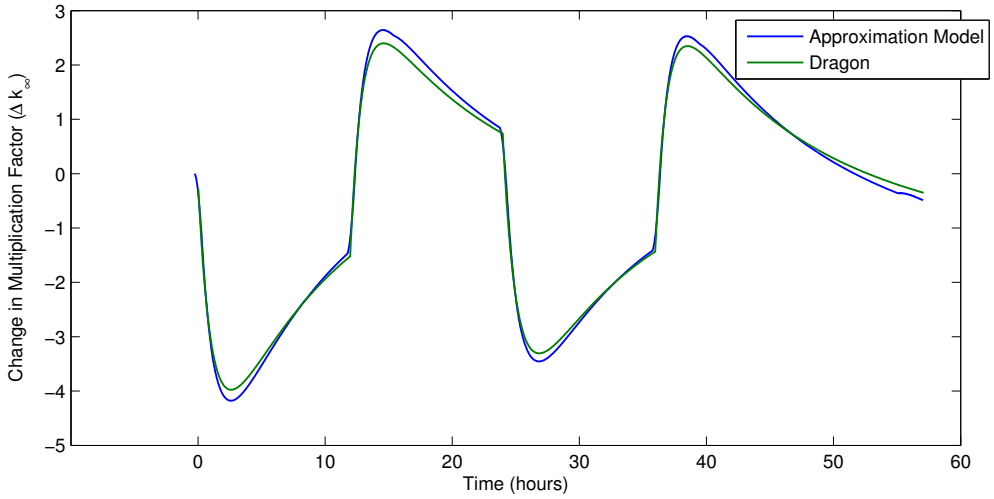

Figure 4.18: Lattice cell load following to 80% full power simulation with NU fuel comparing the approximation model with DRAGON

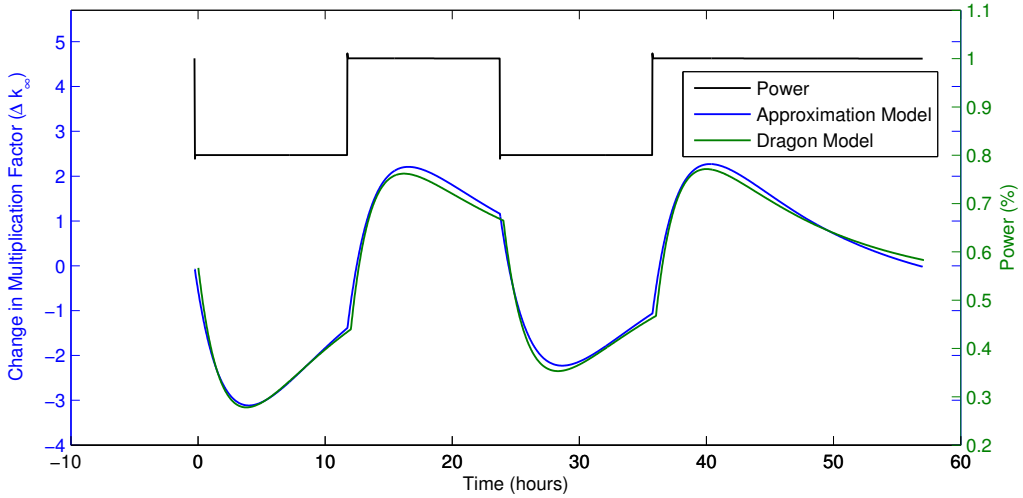

Figure 4.19: Lattice cell load following to 80% full power simulation with thorium fuel, comparing the approximation model to DRAGON

The second transient will highlight the effects of the protactinium transient that occurs in the thorium reactor. This will be performed with a power dive from full power to 10% full power. The dive will occur 200 days into the simulation and will remain at 10% power for the following 1,000 days. The time step on DRAGON will be in increments of five days until the power dive occurs, then adjusted to 1,000 second increments until 220 days, at which time will be returned to five day increments until 1,000 days is reached. The approximation model uses a time step of 100 s throughout the simulation. This power deviation is not a realistic change in a reactor because power cannot drop to 10% full power instantaneously. Delayed neutrons, photo neutrons, and residual decay heat would stabilize such a drastic change in power. The cause of the initial dip is mainly from the Xe-135 transient as it adjusts to the drastic change in power. This rapid decrease is approximately 50 mk for NU and 30 mk for the thorium fuel. As NU adjusts to the new power, there is a change of approximately 15 mk from the original reactivity. The thorium fuel produces large rebound in reactivity caused by the sizeable inventory of protactinium. As noted in Figure 4.20, the change to the new equilibrium in the case of NU is almost instantaneous, whereas it is more gradual in the case of thorium fuel. As pointed out in the case of varying power levels, thorium has a larger transformation in reactivity than NU at different powers. In both cases, the approximation model provides a

reliable representation compared to the DRAGON code in the power dive transients.

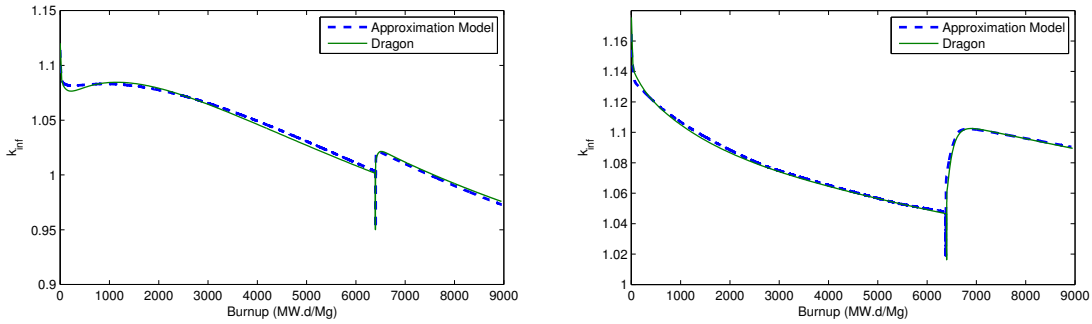

Figure 4.20: A power dive from full power to 10% full power for NU fuel (left) and thorium fuel (right), comparing the approximation model to DRAGON

4.13 Summary

Although the approximation model uses a wide range of assumptions, it has been shown to accurately represent the burnup features in DRAGON and SERPENT. Moreover, it has accurately reflected reactivity at different powers, as well as power transients occurring in the DRAGON bundle.

The thorium fuel provides safety features such as: negative temperature coefficient; a lower positive coolant void reactivity than NU fuel; and adequate delay neutron yield. These safety features will prevent rapid fluctuations in reactivity and allow adequate time to perform reactor control and safety actions, similar to NU fuel currently being used in CANDU 6 reactors. It is necessary to investigate thorium in a full core simulation to properly determine its safety features and controllability. This will be addressed in the following chapter.

Chapter 5

Full Core Analysis

After evaluating the lattice cell, it is necessary to model thorium fuel enriched with U-235 and natural uranium fuel in a full core configuration. DONJON 4 will examine the reactivity worth of the control mechanisms and the external leakage. DONJON uses a two-level scheme, the lattice cell results from DRAGON 3.0.6 are used as input in the full core DONJON model. The files that will be simulated are:

CELNAT : Burnup dependent two group cell averaged properties

REFL : Burnup independent two group reflector properties

ROB : Burnup independent two group adjuster properties

ZCPO : Burnup independent two group liquid zone controller properties

GTUBE : Burnup independent two group guide tube properties

MATSTR : Burnup independent two group other material properties including mechanical absorbers and shutoff rods

The lattice cell simulation uses a power density of 31.9713 kW/kg to generate these DRAGON files. A limitation of this approach is that power deviations affect the isotopic densities in a bundle. This has a direct relationship with the reactivity and other bundle properties that are not addressed in the time-instantaneous full core simulation. Instead, the approximation code has been created for rapid calculations of individual bundles retaining the isotopic densities. The approximation code will be coupled with the point kinetic model to accurately reflect power transients in a CANDU 6 reactor.

5.1 Reactivity Worth of Control Mechanisms

To properly evaluate the full core model, it is necessary to know the reactivity worth of the control devices. The control mechanisms are either part of the protective system or the regulating system. The protective system is both manual and automatic and used only in emergency reactor shutdown situations. There are 28 shutdown units and six poison-injection nozzles that can be invoked rapidly to greatly reduce reactivity. The regulating system is used daily to automatically adjust the reactivity to maintain constant power. These mechanisms include 14 liquid zone controllers, 21 adjuster rods, four mechanical control absorbers and moderator poison. The adjuster rods are responsible for flattening the flux and providing added protection against transients such as the xenon transient. Liquid zone controllers are responsible for keeping the reactivity normalized in each region of the reactor and change with daily operations such as refuelling and fuel burnup. The total reactivity worth of each of the devices in a CANDU 6 reactor using natural uranium is given in Figure 5.1.

Function	Device	Total Reactivity Worth (mk)	Maximum Reactivity Rate (mk/s)
Control	14 Zone Controllers	7	±0.14
Control	21 Adjusters	15	±0.10
Control	4 Mechanical Control Absorbers	10	±0.075(driving) - 3.5 (dropping)
Control	Moderator Poison	—	-0.01 (extracting)
Safety	28 Shutoff Units	-80	-50
Safety	6 Poison-Injection Nozzles	>-300	-50

Figure 5.1: Reactivity worth of the control mechanisms for CANDU 6 reactor using natural uranium fuel [8]

The adjuster rod reactivity is obtained by simulating a 2D lattice cell at mid-burnup when the control rods are at different increments. The same mid-burnup results are used to calculate liquid zone controllers worth at different insertions and

locations. This is used in the full core snapshot in DONJON and the reactivity worth of the devices can be calculated as the perturbation of reactivity given as:

$$\rho = \frac{1}{k} - \frac{1}{k_{per}} \tag{5.1}$$

It is expected that the reactivity worth of the control devices will be less when using MOX or thorium-based fuels [28, 16]. The reactivity of the liquid zone controllers and adjuster rods is given in Figure 5.2 and 5.3 for thorium and NU fuel. The results for the NU fuel agree with the predicted values given in Figure 5.1. Thorium reactivity worth is roughly 20% less for adjuster rods and 15% less for liquid zone controllers.

Table 5.1: Reactivity worth (mk) of the liquid zone controller at different insertions based on a CANDU 6 reactor

	0.0	0.1	0.2	0.3	0.4	0.5	0.6	0.7	0.8	0.9	1
NU reactor	0	0.789	1.55	2.31	3.08	3.84	4.58	5.25	5.87	6.41	6.88
Thorium reactor	0	0.669	1.32	1.96	2.62	3.26	3.89	4.47	5.01	5.48	5.90

Table 5.2: Reactivity worth (mk) of the control rods at different insertions based on a CANDU 6 reactor

	0.0	0.1	0.2	0.3	0.4	0.5	0.6	0.7	0.8	0.9	1
NU reactor	0	1.12	2.24	3.64	5.30	7.04	9.03	11.05	12.8	14.3	15.5
Thorium reactor	0	0.867	1.75	2.87	4.19	5.58	7.14	8.74	10.1	11.3	12.2

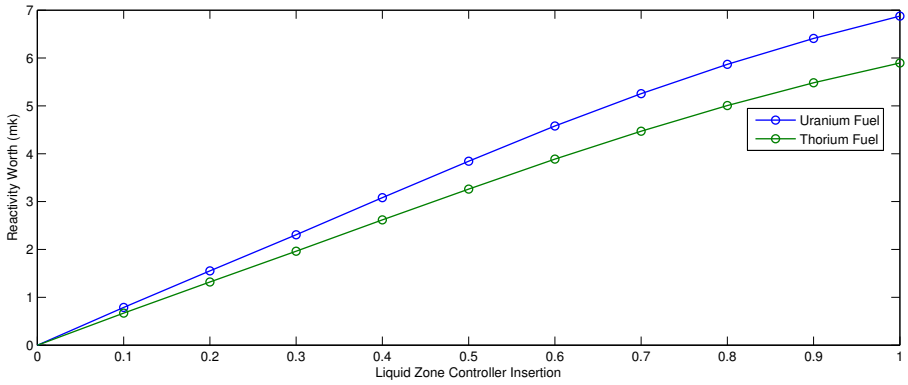

Figure 5.2: Reactivity worth of the liquid zone controllers in a CANDU 6 reactor

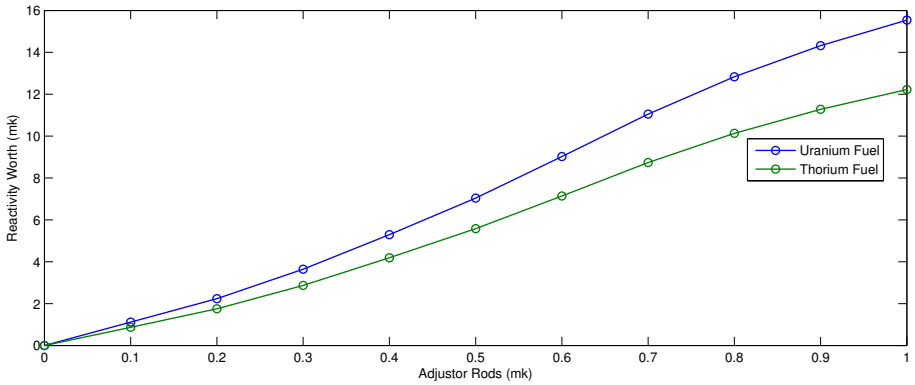

Figure 5.3: Reactivity worth of the adjuster rods in a CANDU 6 reactor

5.2 External Leakage

In the lattice cell simulations, a reactivity loss of 48 mk for the infinite multiplication factor is assumed. This accounts for the loss of reactivity when the lattice cell is used in a CANDU 6 reactor. This represents the leakage caused when neutrons escape the reactor and the loss of reactivity by the control mechanisms. The full core simulation will examine these factors and provide an estimated representation of the cut-off between the infinite and effective multiplication factor.

The CANDU 6 reactor has a reflector to reduce neutron leakage and assist in flattening the flux. The external leakage worth is calculated by instantaneous snapshots of the core with all of the bundles at the same burnup in the core. This result is compared to the infinite multiplication factor that is used as the input for the full core simulation. There is additional absorption caused by material in the core, such as brackets and locators, coupling nuts, guide tubs, etc. Table 5.3 and 5.4 compare the lattice cell and full core multiplication factor. The lower leakage and absorption in thorium is a result of lower overall flux and more fissile isotopes in the core. It is assumed that the adjuster rods are fully inserted and the liquid zone controllers are at 50% full capacity, the reactivity loss both fuels are given in Equation 5.2.

Table 5.3: External leakage with and without core material in a natural uranium reactor. Core material is the essential material that holds the safety mechanisms in place including: brackets and locators, coupling nuts, guide tubs, etc.

Burnup (MWd/Mg)	Lattice Cell	Full Core	Full Core with Core Material	Core Leakage
0	1.111	1.090	1.087	0.0246
4,476	1.034	1.012	1.009	0.0252
10,390	0.946	0.9207	0.9179	0.0286

Table 5.4: External leakage in thorium reactor

Burnup (MWd/Mg)	Lattice Cell	Full Core	Full Core with Core Material	Core Leakage
0	1.165	1.149	1.146	0.0185
4,476	1.060	1.041	1.038	0.0213
10,390	1.024	1.005	1.002	0.0221

$$\begin{aligned} \text{Reactivity Loss}_{\text{NU}} &= \overbrace{0.0252}^{\textit{Core Leakage}} + \overbrace{0.0155}^{\textit{Control Rods}} + \overbrace{0.0038}^{\textit{LZC}} = 0.0445 \\ \text{Reactivity Loss}_{\text{Th}} &= 0.0221 + 0.0122 + 0.0032 = 0.0375. \end{aligned} \tag{5.2}$$

Assuming that flux flattening by the control rods requires the same amount of reactivity in each core, an additional 0.0033 of reactivity is added to the thorium cut-off. The difference between the infinite and effective multiplication factor is 44.5 mk and 40.8 mk for the uranium and thorium reactor.

5.3 Reactor Age Map

The reactor is assumed to be operating in a well-mixed state with a multiplication factor close to one. The randomly generated age pattern that will be used consists of numbers between 1 and 380 without duplications. The pattern will determine the burnup distribution for the bundles in a channel. For example, the channel that contains number one will represent a relatively new bundle, while the channel that contains number 380 will represent the exit burnup.

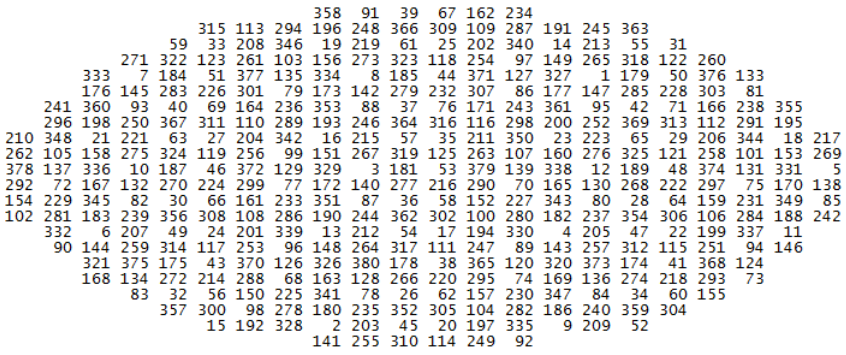

Figure 5.4: Randomized reactor age map [9]

5.4 Flux Distribution

A CANDU reactor must operate within the restriction that no individual bundle or channel will produce 935 kW and 7.3 MW of power, respectively. To maintain these limits, adjuster rods are responsible for stabilizing and flattening the flux in the core. The flux should be the same inside of the core and decline at the edges of the core as a result of neutron leakage. Bi-direction refuelling is added to reduce flux discrepancies in the axial direction. Selective channel refueling ensures that each region of the reactor has a similar flux shape.

The flux shape of the core is constantly fluctuating and determining the flux requires a nuclear reactor fuel management program. Instead of using such a program, a homogeneous flux is assumed. The point kinetic code will calculate the singular flux result that will be applied to the flux shape of the core. The flux in the reactor will be the same except in the boundaries of the core. In the radial direction, the bundles on the periphery will have a reduction of 50% power and the adjacent bundles will be reduced by 25% power. In the axial direction, the channels on the

periphery will decrease by 50% power and adjacent channel will be reduced by 25% power. If a bundle is located on the periphery in both the axial and radial directions, the overall power will be reduced by 75%. This method is a simple way to emulate the core flux in a CANDU 6 reactor.

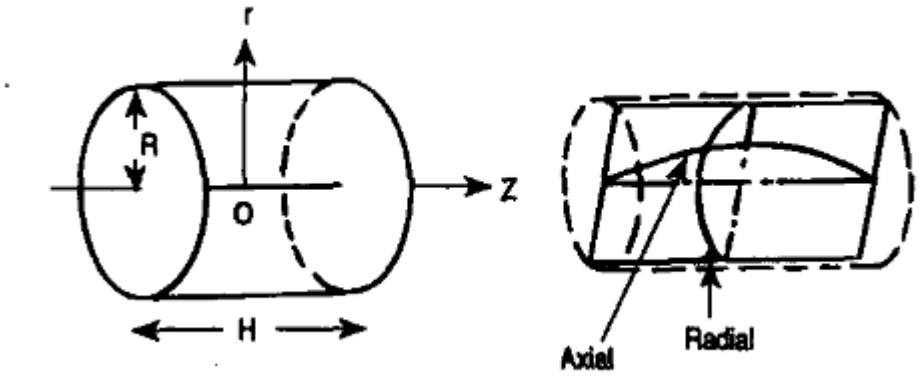

Figure 5.5: Reactor flux diagram

5.5 Full Core Model

The approximation model that is used to calculate the lattice cell is coupled with the point kinetic model that incorporates reactivity, flux, and delayed neutrons. The flowchart in Figure 5.6 illustrates the computer algorithm for constant reactor power. The starting input data uses the initial isotope concentrations of each bundle according to the reactor burnup map. The flux magnitude and initial delayed neutron concentration are also initialized. The flux magnitude is used to calculate the flux shape for each of the bundles. The focus of the approximation model is a fast computational method that will store and calculate the isotopic densities for 4,560 individual bundles using the flux map for an increment of time. The effective multiplication factor, delayed neutron fraction, concentration change, and fission power are all calculated in this step. The licensed limit of fission power in a CANDU 6 reactor is 2156 MW. The thermal power is 2061 MW and the gross electric power is between 680 and 720 MW [53]. If the power is within 0.0015% of the accepted fission power, the data collected for this increment in time would be saved and updated. This includes saving the multiplication factor, flux, delayed neutron concentration, and reactivity input, and updating the concentration, bundle irradiation, and time

increment. If the power is not within the selected limit, there is an adjustment in the input reactivity and the flux is recalculated using the point kinetic model. This occurs until the fission power is within a reasonable range, allowing the next time increment to occur until the target time is reached.

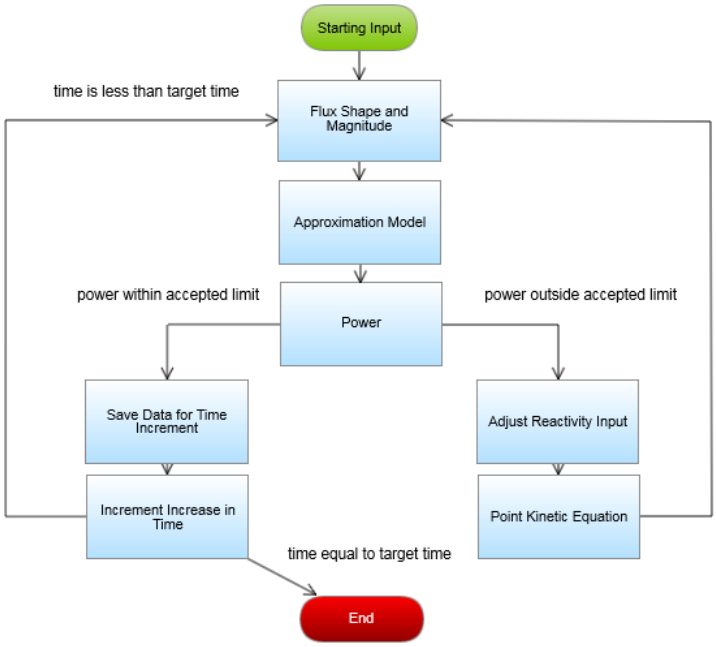

Figure 5.6: Flowchart describing the full core model at constant power

The flowchart in Figure 5.7 illustrates the computer algorithm when there are changes in reactor power. The point kinetic equation is first used with the change in reactivity calculating the resulting flux. The flux is used to calculate the flux shape of the reactor and the approximation model is executed. The information is saved and recalculated for the next increment of time unless the target time is reached.

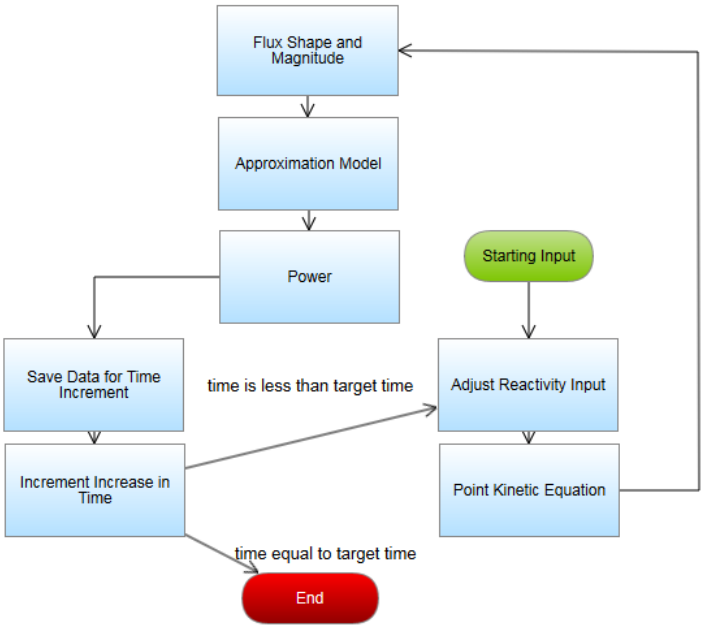

Figure 5.7: Flowchart of the full core model with changes in reactor power

In full core reactor computer simulations, the bundle properties are calculated at a specific power and these properties are fed into the simulation. As demonstrated in the previous chapter, the change in power will have a significant impact on reactivity and bundle properties. The change in bundle properties when modifying power is not reflected accurately in the time-instantaneous full core simulations. Moreover, most full core simulations are also limited in their ability to accurately simulate power transients. This method allows for rapid calculation and an accurate representation of power transients occurring in a reactor.

5.6 Fuel and Bundle Properties

In the previous chapter, most of the estimates were based on information collected from the lattice cell calculations. Now that a full core simulation can be performed, some of the properties will be re-evaluated. The simulation will run for 600 days in time increments of 100s for both thorium and natural uranium fuel. Refuelling will be completed instantaneously when reactivity is equal or drops below one. In normal operations, there are many criteria that must be considered when selecting a channel to refuel, such as operation restrictions and flux balance. Instead, since the

flux shape is static in this simulation, the channel that contains the highest burnup is selected for refuelling. This implies that the exit burnup will typically be higher than in an average operating reactor and there will be a lower refuelling rate.

The average loss of reactivity per day for uranium fuel is 0.4260 mk/day, slightly less than the loss each day of 0.4481 mk/day simulated in DONJON. The change in thorium reactivity per day is 0.1924 mk/day compared to 0.1940 mk/day generated by DONJON. Both are set to the same fission power but are using different reactor age schemes and flux maps, which can account for some of the difference. For the approximation model approach, the reactivity is more sensitive to changes in power, which can also be responsible for the reactivity discrepancies.

An eight-bundle shift for uranium fuel has an average exit burnup of 8,506 MWd/Mg. Although this result should be higher than expected, it is still within a reasonable range of the expected exit burnup [8, 51]. The average exit burnup for thorium using an eight-bundle shift is 2,307 MWd/Mg, much higher than previously estimated. This is due to the lower power experienced with many of the bundles and the change in the cut-off for the infinite multiplication factor. If thorium uses a four-bundle shift, the exit burnup is 2,572 MWd/Mg.

The average change in reactivity for a full core per refuelling is 0.2565 mk for uranium using an eight-bundle shift. The change for thorium using a four and eight-bundle shift is 0.2090 mk and 0.4396 mk, respectively. This means that refuelling occurs every 1.66 days for uranium and 0.920 and 0.438 times per day for thorium using four or eight-bundle shifts, respectively.

Since the average burnups are greater than expected, there is also an expected change in the average delayed neutron (β) results. For uranium and thorium, the average delayed neutrons for a mix core is 0.555 % and 0.517 %, repectively. Surprisingly, the average generation time (Λ) for a thorium reactor, which is 0.0503 s, is greater than the average generation time of 0.0479 s for a uranium reactor. Although the thorium reactor has less delayed neutrons, the parents of these delayed neutrons have a longer half-life, allowing for a greater average generation time.

5.7 Supercriticality and Prompt Criticality

Supercriticality is defined as the neutron growth in a system and takes place if the multiplication factor is greater than one or the reactivity is positive. The equation

for neutron or subsequent power growth without delayed neutrons is:

$$P(t) = P(0)e^{(k_{\text{eff}}-1)t/\Lambda} \tag{5.3}$$

Delayed neutrons play a crucial role in reactor safety. Even though delayed neutron yield consists of 0.5% of all neutron births, it is the dominant contributor to the mean generation time (Λ). The value of the mean generation time for prompt neutrons protracted by the heavy water moderator is 10^{-3} s. The mean generation time that includes the delayed neutrons is calculated in Equation 5.4. Equation 5.3 is a simplified model of the relationship between power and reactivity. The point kinetic model that incorporates eight-groups of delayed neutron precursors will be examined with both types of fuels. Table 5.5 and 5.6 compares the results from the point kinetic mode, delayed neutron model, and prompt neutron model when power multiplies by an exponential factor of three.

$$\Lambda_{\text{total}} = \overbrace{\Lambda_{\text{moderator}}(1-\beta)}^{\text{Prompt Neutrons}} + \overbrace{\Lambda_{\text{delay time}}\beta}^{\text{Delayed Neutrons}} \tag{5.4}$$

The behavior when lower reactivity is inserted into the system is similar to the estimate in the delayed neutron model. As the reactivity insertion rises, the delayed neutrons have a reduced effect on the rapid increase in power. Prompt criticality is defined as a reactivity insertion greater than one dollar, meaning reactivity insertion is greater than the sum of the delayed neutrons. In this case, the chain reaction is self-sustained on prompt neutrons for each generation of birth and subsequent fission. Prompt criticality neglects the effects that the delayed neutrons have on the reactor. This puts the reactor in a dangerous state, causing a rapid power excursion. Therefore, when the reactivity is close to or surpasses prompt criticality, the prompt neutron model is more accurate at describing the change in power.

Thorium fuel experiences a prolonged period of time between the reactivity insertion and the exponential increase in power. This is due to thorium having a higher neutron generation time than NU fuel. Since thorium has a lower delay neutron sum, it allows for an earlier self-sustained prompt criticality. Thus, for high reactivity insertions, there is an earlier run-off effect for the thorium reactor compared to the uranium reactor. When the reactivity change is much less than the prompt criticality, the power for the thorium reactor will change at a slower rate than the

NU reactor.

Table 5.5: The time change (s) required for power to multiply by an exponential factor of three with constant reactivity insertion in the NU reactor

Reactivity (mk)		Prompt Neutron Model (s)	Delayed Neutrons Model (s)	Point Kinetic Model (s)
0.555	10 cents	5.41	258	264
0.833	15 cents	3.60	172	147
1.11	20 cents	2.70	129	91.8
1.39	25 cents	2.16	103	61.4
2.78	50 cents	1.08	51.8	13.1
5.55	1 dollar	0.541	25.8	1.68
8.325	1.5 dollars	0.360	17.3	0.674
11.1	2 dollars	0.270	12.9	0.414
27.8	5 dollars	0.108	5.17	0.125
55.5	10 dollars	0.0541	2.59	0.0581

Table 5.6: The time change as the power multiplies by an exponential factor of three with constant reactivity insertion for thorium fuel

Reactivity (mk)		Prompt Neutron Model (s)	Delayed Neutrons Model (s)	Point Kinetic Model (s)
0.517	10 cents	5.803	298	301
0.776	15 cents	3.869	198	168
1.03	20 cents	2.901	149	106
1.29	25 cents	2.321	119	71.2
2.59	50 cents	1.160	59.5	15.3
5.17	1 dollar	0.580	29.8	1.86
7.76	1.5 dollars	0.387	19.8	0.727
10.3	2 dollars	0.290	14.9	0.446
25.9	5 dollars	0.116	5.95	0.135
51.7	10 dollars	0.058	2.98	0.062

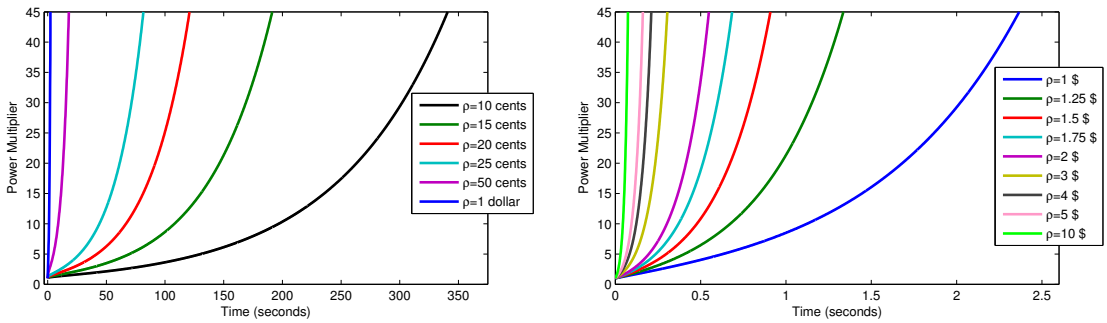

Figure 5.8: Exponential power increase with reactivity insertion based on the point kinetic equation for the NU reactor

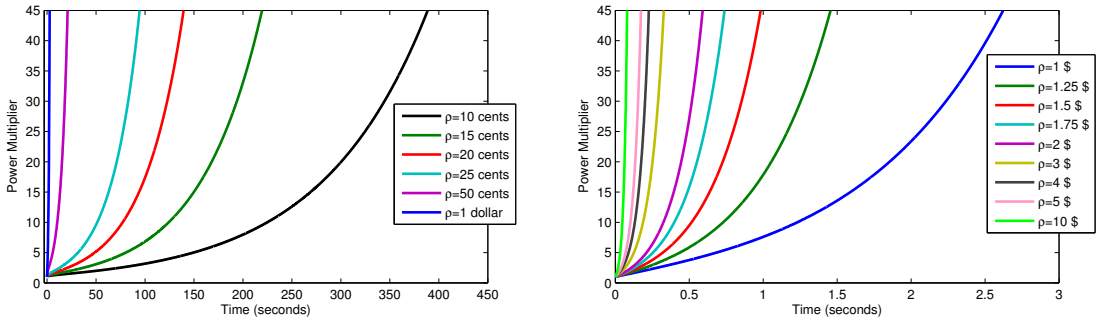

Figure 5.9: Exponential power increase with reactivity insertion based on the point kinetic equation for the thorium reactor

5.8 Load Following

The demand for electricity power fluctuates in cities throughout the day. The practice of power plant load following involves operating at full power when electrical needs are at the highest demand, and decrease power output a low demands to reserve fuel. In this simulation, load following will cycle between full power and reduced power every 12 hours. The power reductions that will be examined are 80%, 60% and 40% of full power. The point kinetic equation will alter the reactivity at a constant rate to the adjusted power in 10 minutes, two hours, and four hour increments. Table 5.7 and 5.8 displays the necessary reactivity to adjust the power in each load following case. Overall, the change in reactivity required to decrease the power is slightly greater than it is to return to full power. The thorium reactor requires a slightly greater change in reactivity to modify the power.

Table 5.7: Reactivity (mk) necessary to adjust to a new power in a NU reactor

Power Adjustment Time	FP to 80% (mk)	80% to FP	FP to 60%	60% to FP	FP to 40%	40% to FP
10 min	-0.0252	0.0244	-0.0586	0.0552	-0.107	0.0973
2 h	-0.00219	0.00216	-0.00502	0.00496	-0.00900	0.00890
4 h	-0.00109	0.00108	-0.00251	0.00249	-0.00451	0.00446

Table 5.8: Reactivity (mk) necessary to adjust to a new power in a thorium reactor

Power Adjustment Time	FP to 80% (mk)	80% to FP	FP to 60%	60% to FP	FP to 40%	40% to FP
10 min	-0.0259	0.0254	-0.0609	0.0574	-0.112	0.111
2 h	-0.00226	0.00226	-0.00523	0.00518	-0.0094	0.0092
4 h	-0.00113	0.00113	-0.00261	0.00260	-0.0047	0.0047

Figure 5.10 represents the change in reactivity for uranium and thorium reactors when the load following is reduced to 80% full power. There is not a significant change in reactivity when the reduction of power occurs over 10 minutes, two hours, or four hours. The xenon transient is mainly responsible for the change in reactivity in these transients, as discussed in section 2.6. It takes Xe-135 roughly 40 to 50 hours to adjust to a perturbation in power, and the power reduction time is not long enough to have a noteworthy effect on the xenon transient. The uranium reactor has an initial drop in reactivity of 3.5 mk to 3.7 mk, depending on the power adjustment time. When the reactor returns to full power, there is an additional positive reactivity spike of 2.2 mk to 2.3 mk. The initial drop for the thorium reactor is 2.55 to 2.65 mk and the rebound when returning to full power is 2.0 mk to 2.1 mk. Although the additional time contributes less to the change in reactivity, it influences the reactivity change per second. Figure 5.11 includes the reactivity change with respect to time. The maximum reactivity change occurs when the power deviates over 10 min as the reduced power returns to full power. This is $1 \cdot 10^{-3}$ mk/s for uranium and $5.5 \cdot 10^{-4}$ mk/s for thorium. If the liquid zone controllers are at 50% during the initial transient, the reactivity worth is 3.8 and 3.2 mk for the uranium and thorium reactor. Assuming control mechanisms allow the flux shape of the reactor to change uniformly with power, the liquid zone controllers can handle load following capabilities in the reduction to 80% full power. If power adjustment is completed for longer periods of time, the change of reactivity is lower, providing additional time for the control mechanisms to react.

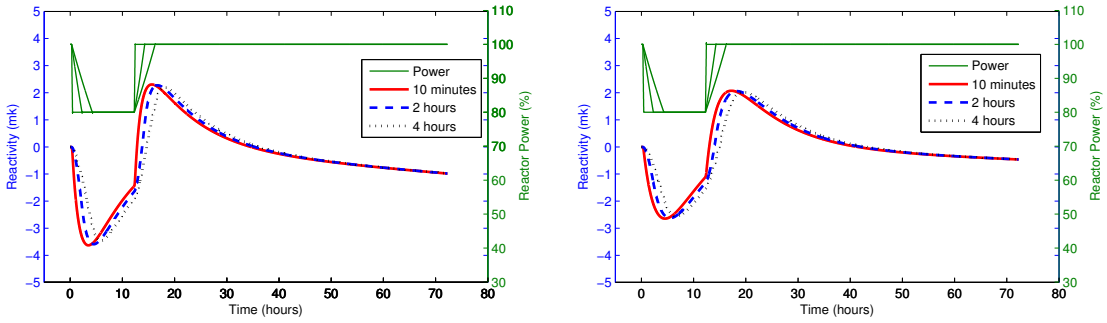

Figure 5.10: Load following at 80% full power for the NU reactor (left) and the thorium reactor (right)

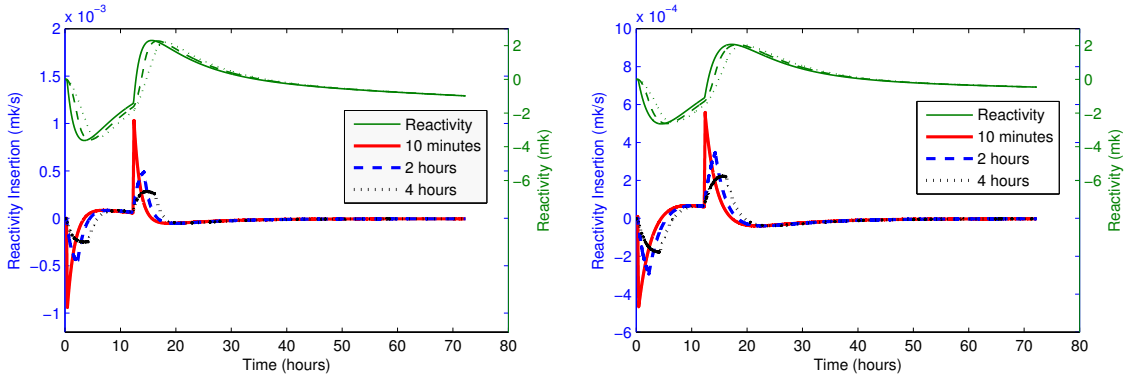

Figure 5.11: The change in reactivity per second for the NU reactor (left) and the thorium reactor (right)

Load following to 60% full power is examined and the results are provided in the figures below. The uranium reactor has an initial dip of 8.3 mk to 8.8 mk if the reduction of power occurs at four hours or 10 minutes, respectively. The dip that occurs in the thorium reactor is 6.1 mk to 5.9 mk, depending on the power adjustment time. When returning to full power, the additional reactivity change is 4.8 mk and 4.2 mk for the uranium and thorium reactors, respectively. The 10 min reduction in power has a maximum change in reactivity of $2.3 \cdot 10^{-3}$ mk/s or 0.0448 cents/s in a uranium reactor. The greatest change for a thorium reactor is $1.2 \cdot 10^{-3}$ mk or 0.0233 cents/s.

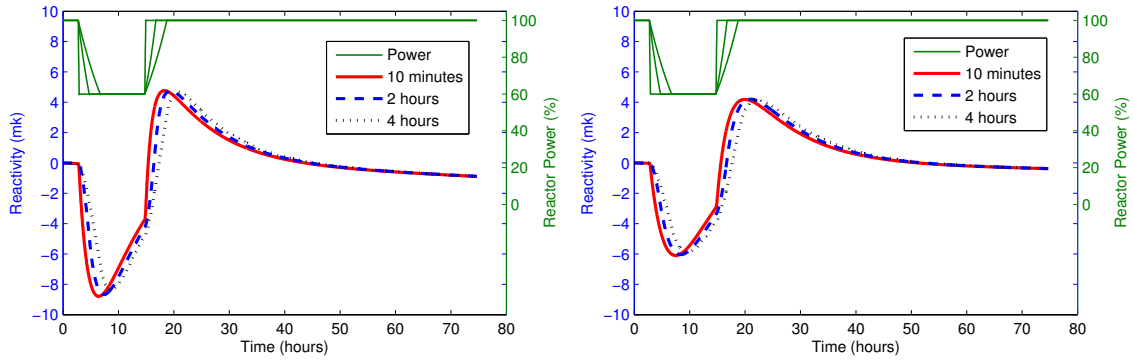

Figure 5.12: Load following at 60% full power for the NU reactor (left) and the thorium reactor (right)

When load following is reduced to 40% full power, there is a much greater change in reactivity. The reactivity dip as power is reduced is greater than 16 mk for the NU reactor and 10 mk for the thorium reactor. The rebound in reactivity when returning to full power is roughly 7 mk for the NU reactor and 6 mk for the thorium reactor. The maximum change in reactivity is $4 \cdot 10^{-3}$ mk/s and $2.1 \cdot 10^{-3}$ mk/s for the NU and thorium reactors, respectively. Load following at 40% or 60 % will require additional control mechanisms to address the reactivity fluctuations.

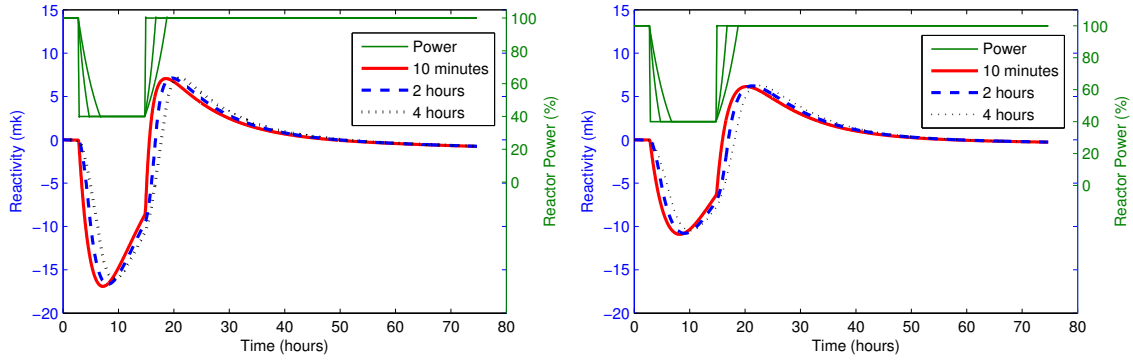

Figure 5.13: Load following at 40% full power for the NU reactor (left) and the thorium reactor (right)

5.9 Continuous Load Following

In the previous simulation, the isotopes in the reactor are assumed to be at a well mixed state before load following is performed. As power continues to oscillate as load following cycles for multiple days, there will be a change in the isotope concentration in the reactor. As previously discussed, the reduction of power will delay isotopes produced mainly due to beta decay of parent isotope. Xe-135 is produced by the beta decay of I-135, contributing to the reactivity change in the load following simulation. This also occurs with the fissile elements Pu-239 and U-233 in both uranium and thorium fuel. The absorption chain of Th-232 requires more time to produce fissile isotopes than the U-238 absorption chain. The change in reactivity as load following occurs for 35 cycles, assuming an initial homogeneous core, is illustrated in Figure 5.14. The change in isotopic concentration of the fissile elements in each fuel is shown in Figure 5.15 and 5.16. The initial dip in reactivity is caused by the xenon absorption, but eventually the reactivity by the fissile isotopes becomes prevalent. The rebound is less intense in the uranium reactor due to a greater xenon transient and greater reactivity decrease per day. The number density of Pu-239 displays an initial increase for load following operations before decreasing below the normal operating reactor at only full power. A similar pattern would be demonstrated for U-233 if the simulation were to run for a longer period of time. The lower operating powers produce less U-233 and Pu-239 but utilize these fissile elements more effectively overall. Operating at lower powers allow the production of fertile isotopes to be converted to fissile isotopes, limiting the depletion of the initial fissile isotope U-235.

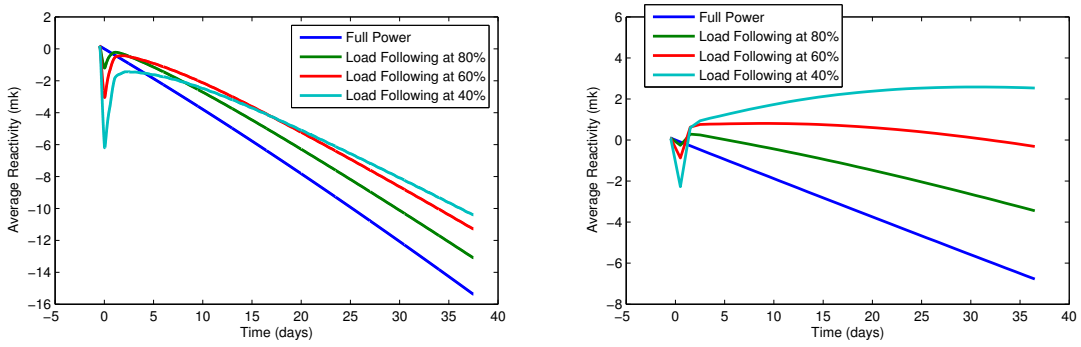

Figure 5.14: The average reactivity transition as load following is completed for 35 cycles in the NU reactor (left) and the thorium reactor (right)

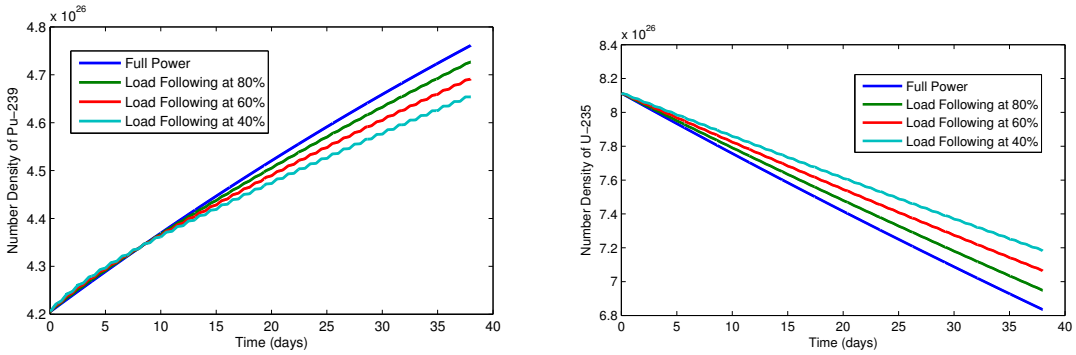

Figure 5.15: The fissile isotopes in the NU reactor as load following completes 35 cycles

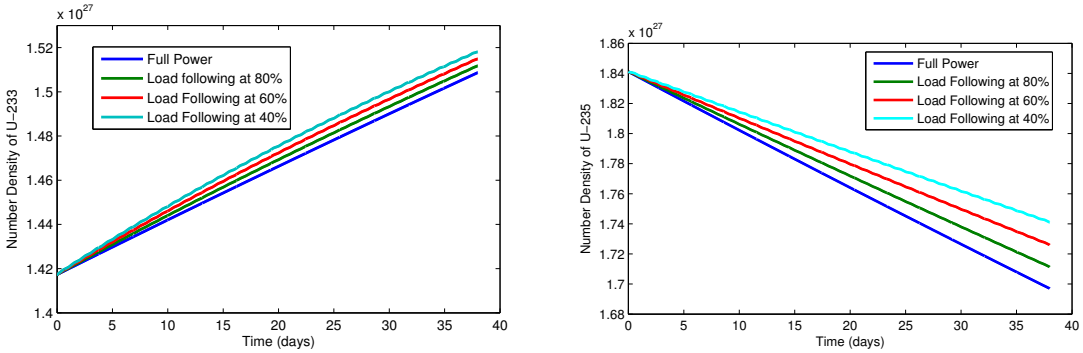

Figure 5.16: The fissile isotopes in the thorium reactor as load following completes 35 cycles

5.10 Sustained Low Power

The reduction of power creates additional fissile elements from the beta decay of the parent isotope. In the uranium absorption chain, U-238 absorbs a neutron and produces Np-239, which decays to Pu-239 in 2.3 days (Equation 1.1). In the thorium absorption chain, Th-232 absorbs a neutron to become Pa-233, which decays to U-233 with a half-life of 27 days (Equation 1.2). The longer decay time of protactinium will create a greater inventory of the isotope. This is concerning as it can produce additional reactivity in a reactor as power is being reduced, known as the

protactinium transient.

The differences between the reduction of power in uranium and thorium are compared in Figure 5.17. The power is reduced from full power to the selected power over two hours and held at that power afterwards. The effects of xenon are ignored and the primary focus is on the increase in reactivity. As expected, the thorium reactor produces more reactivity from the larger inventory of Pa-233 compared to Np-239. The immediate change of reactivity that occurs in the first two days of the simulation is similar but slightly greater in the thorium reactor. After two days, thorium continues to grow in reactivity as the uranium reactivity begins to decay. Eventually, the reactivity in the thorium reactor doubles the initial reactivity peak in the uranium reactors. This highlights the concern with an immediate shutoff of the thorium reactor, and demonstrates the need to properly monitor and understand the protactinium transient.

This also demonstrates the necessary requirements to safely store a thorium bundle after being removed from the reactor. The bundle will slowly increase in reactivity and should be stored in an safe environment that monitors reactivity. It has been suggested that this excess reactivity can be extracted and reused in advanced reactors.

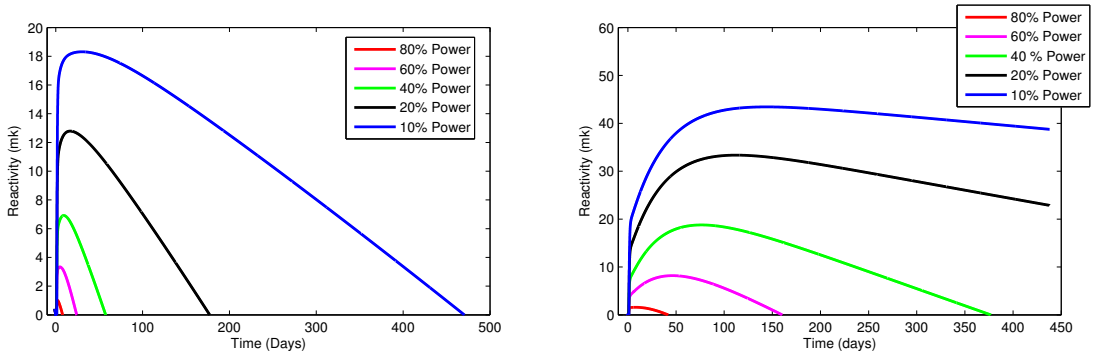

Figure 5.17: Power is reduced from full power and held constant to demonstrate the excess reactivity in the uranium reactor (left) and thorium reactor (right)

5.11 Shutdown Simulation

The excess reactivity produced by reducing the reactor power can be limited if the process is performed over an adequate amount of time, allowing the fissile isotopes to be used in this process. This is demonstrated by reducing the power to 10% of full power over a period of time. The power will be reduced in increments of 20% over two hours. Between the power reduction increments the power is kept constant, allowing isotopic saturation at the new power. The constant reactivity reduction is provided in Table 5.9. Naturally, as approaching lower power, a larger reactivity insertion is necessary.

Table 5.9: Sustained reactivity input to reduce power

Power Decrease	FP to 80%	80% to 60%	60% to 40%	40% to 20%	20% to 10%
Uranium Reactor	-2.19E-3 mk	-2.790E-3 mk	-3.934E-3 mk	-6.733E-3 mk	-6.732E-3 mk
Thorium Reactor	-2.25E-3 mk	-2.955E-3 mk	-4.132E-3 mk	-7.073E-3 mk	-7.07279E-3 mk

Figure 5.18 and 5.19 illustrate the reactivity at different shutdown durations using incremental power reduction steps. The result from the earlier section shows that a reactivity decrease to 10% full power in two hours has a positive reactivity of 18.3 mk for the NU reactor. There is a reduction of excess reactivity of 3.7 mk if the power decline is performed for 10 days. It is further reduced by 6.7 mk, 12.7 mk and 19.2 mk if power reduction is achieved in 30, 60, and 90 days. In the case of the thorium reactor, the excess reactivity is much larger and more difficult to reduce. If the power reduction occurs in two hours there is an excess reactivity of 43.4 mk. If the power reduction is performed over 10, 30, 90, or 180 days, the excess reactivity is reduced to 41.7, 40.1, 36.1, and 29.3 mk, respectively. This simulation highlights the excess reactivity that would exist in the thorium reactor during reactor shutdown scenarios.

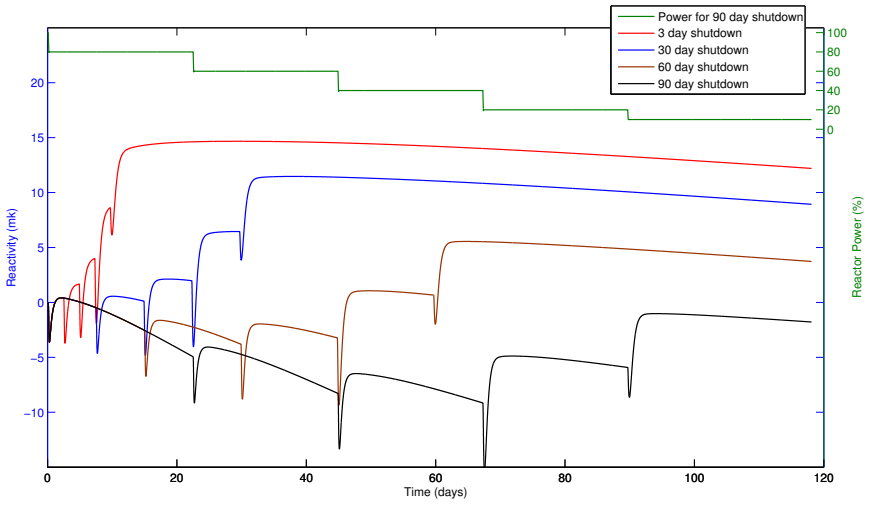

Figure 5.18: Excess reactivity in a NU reactor as power is decreased in increments of 20% to a power of 10% full power at different durations of time

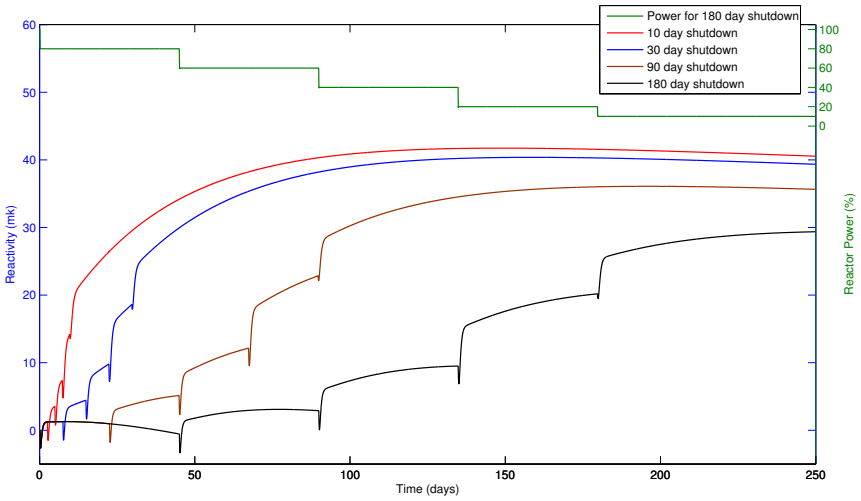

Figure 5.19: Excess reactivity in a thorium reactor as power is decreased in increments of 20% to a power of 10% full power at different durations of time

5.12 Summary

The full core is evaluated with the computer code DONJON using input files from DRAGON to understand the reactivity worth of the control mechanisms and to perform an estimate of external leakage. To properly model full core power transients, a computer simulation is created using the approximation model with the point kinetic code. The approximation model calculates the lattice cell while retaining the isotopic densities. The benefit to this model is the rapid calculation without demanding computational resources. The point kinetic model determines the flux and reactivity influenced by the delayed neutrons.

Five power transients are examined in a CANDU 6 reactor with natural uranium and thorium enriched with U-235. The rapid reactivity insertion demonstrates how the delayed neutrons influence the power. Load following is examined with a reduction from full power to 80%, 60% and 40% in a single cycle to determine the xenon effects. Continuous load following determines the change in reactivity and fissile isotopes with 35 cycles. An instantaneous and prolonged reactor shutdown occurs to monitor the effects with excess reactivity in the reactor.

Chapter 6

Summary and Conclusion

This thesis examines the characteristics of natural uranium and homogeneous thorium fuel enriched with 2.0% U-235 in a CANDU 6 reactor. The focus is a comparison of intrinsic fuel properties in a lattice cell and full core simulation. The lattice cell and full core simulation are examined using the nuclear codes DRAGON 3.0.6, SERPENT 2, and DONJON 4. A new computational model is established that utilizes many assumptions to develop an expeditious code for investigating full core power transients.

The preliminary infinite lattice cell calculation is performed in DRAGON and SERPENT using multiple different nuclear libraries for both fuels. The nuclear libraries for thorium are less established, causing a significant discrepancy in the results. A larger inconsistency exists between the lattice cell signature for DRAGON and SERPENT in the thorium bundle. It has not been established why this exists in the thorium bundle while both codes maintain agreeable results for the NU bundle.

The DRAGON simulation determines the enrichment concentration for thorium, as well as the temperature coefficient, coolant void reactivity, and the relationship between power and reactivity. The temperature coefficient for the fuel pellets between hot shutdown and full power for NU and thorium bundles are -6.36 μk/°C and -9.26 μk/°C, respectively. The coolant temperature coefficients are 30 μk/°C and 25.9 μk/°C for NU and thorium bundles, respectively. The estimated power coefficient for NU and thorium bundles are -2.46 mk and -3.35 mk, respectively. Although thorium has a greater negative power coefficient, it also has a higher thermal conductivity, allowing the fuel pellet to displace additional heat into the coolant and moderator.

The coolant is voided by setting the density of the coolant to zero in the infinite lattice cell in DRAGON. There is an average increase in reactivity of 11.5 mk for the NU bundle throughout its lifetime. The result for the thorium bundle is much lower at an average rate of 8.3 mk for the bundle's lifetime. Thorium fuel will perform within the existing safety features of a CANDU 6 reactor in the event of a CVR accident.

There is a relationship between bundle power and multiplication factor for the lattice cell signature. If the lattice cell is simulated at 75% nominal power there is an 11 mk adjustment for thorium, whereas the adjustment is only 3 mk for NU fuel. The extensive cross section and long fertile absorption chain of Th-232 results in a larger inventory of the intermediate isotope Pa-233. Power reduction allows the fertile absorption chain to produce more fissile isotopes, resulting in a higher multiplication factor. The sizeable inventory of Pa-233 will continue to produce U-233 for 90 to 120 days after the bundle is removed from the reactor. This introduces the possibility of extracting fissile isotopes or reusing the bundle after removal. The bundle should also be stored and monitored appropriately after removal.

The approximation model is developed based on the results from DRAGON using the IAEA library. The model utilizes many assumptions to develop an expeditious code for solving the infinite square lattice, retaining the isotopic densities. It has been shown to accurately reflect reactivity at different power inputs and can emulate transient effects simulated in DRAGON. The approximation model is coupled with the point kinetic equation to examine power transients in a full core simulation.

It is expected that there will be a change in reactivity worth of the control mechanisms when using different fuels. The reactivity worth of thorium fuel is measured in a DONJON simulation. It is determined that the reactivity worth for the liquid zone controllers is 5.9 mk and the adjuster rods are 12.2 mk for the thorium reactor. The change between k_{inf} and k_{eff} with reactor leakage, absorption, and control mechanisms is estimated to be 0.0408 for the thorium reactor and 0.0445 for the uranium reactor.

Delayed neutrons help stabilize power perturbations in the reactor so that the control mechanisms can adjust appropriately. The full core reactor at equilibrium will have the average delayed neutron (β) of 0.555% for NU reactor and 0.517 % for thorium reactor. The average generation time (Λ) is 0.0479 s for the NU reactor and

0.0503 s for the thorium reactor. For low reactivity insertions, the power change is less rapid for the thorium reactor due to the average generation time. At high reactivity insertions, the thorium reactor will become prompt critical earlier, meaning self-sustained prompt neutron generation, causing a more rapid power excursion.

Load following transient with 12-hour cycles are presented using the approximation model and the point kinetic equation. Power is adjusted in increments of 10 minutes, two hours, or four hours with constant reactivity input. Load following is examined at 80%, 60% and 40% full power. The necessary reactivity insertion to adjust power for the respective increments of time is given on Table 5.7. The power adjustment time has minimal effect on the reactivity perturbations, which are mainly produced by the xenon transients. However, it does influence the reactivity change per second providing additional time for the control mechanisms to react. The NU reactor has an initial reactivity reduction of 3.7 mk , 8.8 mk, and 16 mk when full power is reduced to 80%, 60%, and 40%, respectively. When returning to full power, there is a reactivity peak of 2.3 mk, 4.8 mk, and 7 mk for the respective powers. The thorium reactor has a reactivity reduction of 2.6 mk, 6.1 mk, and 10 mk, and a reactivity peak of 2.1 mk, 4.2 mk, and 6.0 mk for the power changes of 80%, 60%, and 40%, respectively. The deviation in reactivity is less for a thorium reactor due to a lower xenon density and higher fissile concentrations in the fuel. Continuous load following preserves fuel and offers additional time for fertile isotopes to produce fissile isotopes. Assuming control mechanisms allow the flux shape of the reactor to change uniformly with power, the liquid zone controllers alone can control load following capabilities at 80% full power.

The long lasting effect of Pa-233 introduces another safety concern that will need to be managed when the reactor power is reduced or initiating reactor shutdown. The reactivity transformation within the first two days of immediate power reduction is similar for both fuels. After the two days, the excess reactivity for NU fuel begins to diminish as the reactivity for thorium continues to climb for the next 90 to 120 days. The thorium reactor eventually doubles the initial reactivity in the uranium reactor during this time. A shutdown simulation is conducted using incremental power reduction steps. The excess reactivity in the NU reactor for a 30 day, 60 day, and 90 day shutdown is 11.6 mk, 5.6 mk, and -0.9 mk, respectively. The excess reactivity in the thorium reactor for a 30 day, 90 day, and 180 day is 40.1 mk, 36.1 mk, and 29.3 mk, respectively. The protactinium transient highlights the need to adequately monitor the reactor when reducing power or reactor shutdown scenarios. The buildup of U-233 will continue after the bundle is removed from the

reactor and should be stored and monitored appropriately.

The work in this thesis discusses a safety evaluation comparing thorium fuel enriched with U-235 to the conventional operating natural uranium CANDU 6 reactor. Thorium has many advantageous features that can enhance the safety of the CANDU reactor. Thorium fuel exhibits a higher negative temperature coefficient than NU fuel. A negative temperature coefficient is preferred as it is responsible for mitigating reactivity perturbation associated with a rise in reactor power. In the case of a coolant void accident, the thorium fuel will exhibit a lower raise in reactivity than NU fuel, allowing additional time for the emergency shutdown units to be engaged. Thorium fuel accumulates lower amounts of parasitic absorbers, specifically lower concentrations of Xe-135. This reduces the change in reactivity caused by the xenon transients. Additionally, the thorium reactor will have an enhanced load following capability due to the lesser xenon transient.

Even though there are some enhanced safety features for a thorium-fuelled reactor, there are safety concerns that will need to be properly addressed. Thorium fuel is less established than uranium based fuels. This causes inconsistency in the results when using different nuclear codes and libraries. The slightly lower delayed neutron yield can cause the thorium reactor to induce a state of prompt criticality at a lower reactivity insertion than the NU reactor. The thorium reactor has an additional safety concern known as the protactinium transients. The long absorption chain of Th-232 produces a sizable inventory of the intermediate isotope Pa-233. Pa-233 will continue to accumulate the fissile isotope, U-233, if the bundle is removed from the reactor or if the reactor power is reduced. The excess reactivity for power reduction can overwhelm the control systems in a CANDU 6 reactor and additional control systems or reactor poisons may be needed for the controllability of the protactinium transient.

The work in this thesis discusses a safety evaluation comparing thorium fuel enriched with U-235 to the conventional operating natural uranium CANDU 6 reactor. Thorium has many advantageous features that can enhance the safety of the CANDU reactor. Thorium fuel exhibits a higher negative temperature coefficient than NU fuel. A negative temperature coefficient is preferred as it is responsible for lowering reactivity when there is a rise in reactor power. In a run-off power excursion, the negative coolant void can help self-regulate this emergency condition by naturally reducing reactivity. In the case of a coolant void accident, the thorium fuel will exhibit a lower raise in reactivity than NU fuel, allowing additional time for the emergency

shutdown units to be activated. Thorium fuel accumulates lower amounts of parasitic absorbers, specifically lower concentrations of Xe-135. This mitigates the reactivity perturbations when reactor power is changed caused by the xenon transient. Additionally, the thorium reactor will have an enhanced load following capability due to the less significant xenon transient.

Even though there are some enhanced safety features for a thorium-fuelled reactor, there are safety concerns that will need to be properly addressed. Thorium fuel is less established than uranium based fuels. This causes inconsistency in the results when using different nuclear codes and libraries. The slightly lower delayed neutron yield can cause the thorium reactor to induce a state of prompt criticality at a lower reactivity insertion than the NU reactor. The thorium reactor has an additional safety concern known as the protactinium transients. The long absorption chain of Th-232 produces a sizable inventory of the intermediate isotope Pa-233. The inventory of Pa-233 will continue to accumulate the fissile isotope, U-233, if the bundle is removed from the reactor or if the reactor power is reduced. The excess reactivity for power reduction can overwhelm the control systems in a CANDU 6 reactor and additional control systems or reactor poisons may be needed for the controllability of the protactinium transient.

In summary, this thesis discusses the implementation of thorium bundles in a CANDU 6 reactor. The advantages and disadvantages of thorium enriched with 2.0% U-235 compared to NU fuel are recapitulated below:

Advantages:

- More abundant in nature
- Less long-lived radioactive waste
- Potential to reprocess and reuse
- Less parasitic absorption including less xenon
- Higher negative temperature coefficient
- A lower coolant void reactivity
- Enhanced load following capabilities

Disadvantages:

- Requires initial enrichment
- Nuclear libraries are less established
- Requires longer reactor lifetime to adequately utilize U-233
- Slightly lower average delayed neutron yield
- Less reactivity worth for control mechanisms
- The protactinium transient creates excess reactivity when power is reduced or the reactor is shutdown.
- The bundle will continue to create excess reactivity after being removed. It should be stored safely and monitored appropriately.

Chapter 7

Future Work

This thesis presents a new method for analyzing power transients in a full core simulation. The focus is an expeditious approach that uses many assumptions about the bundle properties and the full core of a CANDU 6 reactor. The approximation model only analyzes certain isotopes and considers the thermal fission factor as the only variable in the four-factor formula. The full core assumes a constant flux shape that uniformly changes with power. Although control mechanisms are in place to control the flux distribution, the shape will change with the type of fuel and fuel irradiation at different regions. Some of these assumptions can be eliminated if the bundle or core calculation was performed on existing nuclear codes. This would require more computational resources and longer execution times. It would also validate the results illustrated in this thesis.

Provided more time, the initial reactor startup with thorium could have been examined. Thorium fuel enriched with 2.0% U-235 has a much greater initial reactivity peak than NU fuel. The simulation would determine how much spent uranium fuel would be required to safely start the reactor, and the subsequent effects of the delayed neutrons.

Thorium has often been examined with weapon grade or recycled plutonium as the enrichment fuel. Pu-239 is responsible for a lower negative temperature coefficient and has a lower beta yield than U-235. Properly examining these values in a full core simulation is needed to determine if Pu-239 would yield the same safety features as U-235 enriched thorium. Moreover, examining different enrichment amounts for both fuels will produce variations in a full core simulation.

The reactor core can be altered in a heterogeneous bundle configuration using a mixture of pure thorium bundles and slightly enriched uranium bundles. The purpose is to reuse or extract the fissile isotopes from the thorium bundle. Thorium fuel has a greater reactivity change when simulated at different powers. Reactivity produced by thorium fuel will greatly depend on the magnitude of the flux interacting with the bundle, represented by its placement in the reactor. The fissile content of the bundle after being removed from the core is also dependent on the placement of the bundles. The computer simulation created in this thesis can help determine how thorium interacts at different regions in a heterogeneous core.

The micro-depletion method has been developed for DONJON to simulate a CANDU 6 reactor. This method retains certain isotope concentrations in a full core simulation. There is minimal change between the time-independent method and the micro-depletion method in a CANDU 6 reactor at full power for NU fuel [29]. The conclusion is that there are an equal number of bundles operating above the nominal power than below, adjusting reactivity accordingly. It has been proven in this thesis that thorium fuel is more responsive to changes in nominal power than NU fuel. It is suggested that evaluating thorium fuels using both micro-depletion method and a time-instantaneous method may yield a different result.

Bibliography

[1] Hansen, James, et al. "Global Temperature in 2015" (2016).

[2] Steed, Roger G. *Nuclear Power: In Canada and Beyond.* General Store Publishing House, 2006.

[3] Uranium Markets. "World Nuclear Association, and World Nuclear Association." June 2013. [Online]. Available on: http://www.world-nuclear.org/information-library/nuclear-fuel-cycle/uranium-resources/uranium-markets.aspx Accessed on: (September, 2016)

[4] Nuclear Power Technology Development Section, Thorium Fuel Utilization, Vienna: IAEA, 2002.

[5] Milgram, Michael. *Once-through thorium cycles in CANDU reactors.* Chalk River Nuclear Laboratories, 1982.

[6] Dekoussar, V., et al. *Thorium fuel cycle - Potential benefits and challenges. IAEA.* IAEA-TECDOC-1450, Vienna, 2005.

[7] Canadian Nuclear FAQ "The Canadian Nuclear FAQ - Section A: CANDU Technology." [Online]. Available on: http://www.nuclearfaq.ca/cnf_sectionA.htm Accessed on: (September, 2016)

[8] Rouben, Ben. "CANDU Fuel-Management Course." *Atomic Energy of Canada Limited, Montreal, Canada* (1999).

[9] Rouben, Ben. "Nuclear Fuel Management." Engineering Physics 784. McMaster University, Hamilton, ON. 1 Sept. 2015.

[10] Schaffer, M. B. "Abundant thorium as an alternative nuclear fuel: Important waste disposal and weapon proliferation advantages." *Energy policy 60* (2013): 4-12.

[11] Nuttin, A., et al. "Comparative analysis of high conversion achievable in thorium-fueled slightly modified CANDU and PWR reactors." *Annals of Nuclear Energy* 40.1 (2012): 171-189.

[12] Sahin, Sumer, et al. "Increased fuel burn up in a CANDU thorium reactor using weapon grade plutonium." *Nuclear Engineering and Design* 236.17 (2006): 1778-1788.

[13] Choi, Hangbok, and Chang Je Park. "A physics study on thorium fuel recycling in a CANDU reactor using dry process technology." *Nuclear technology 153.2* (2006): 132-145.

[14] AFCR "Advanced Fuel CANDU Reactor." July, 2013. [Online]. Available on: http://www.candu.com/site/media/Parent/CANDU%20brochure-AFCR-FINAL-HR%20SINGLES.pdf Accessed on: (September, 2016)

[15] Yee, Shaun Sia Ho. *Modelling Pure Thorium Bundle Implementation in the CANDU-6 Reactor.* MA thesis. McMaster University, 2015.

[16] Holmes, Bradford. *Automated Refueling Simulations of a CANDU for the Exploitation of Thorium Fuels.* MA thesis. École Polytechnique de Montréal, 2013.

[17] Duderstadt, James J., and Louis J. Hamilton. "Nuclear reactor analysis." (1976).

[18] Chao, Yung-An, and Anthony Attard. "A resolution of the stiffness problem of reactor kinetics." *Nuclear Science and Engineering* 90.1 (1985): 40-46.

[19] Sanchez, J. "On the numerical solution of the point reactor kinetics equations by generalized Runge-Kutta methods." *Nuclear Science and Engineering* 103.1(1989): 94-99.

[20] Aboanber, Ahmed Ebrahim, and Abdallah Alsayed Nahla. "Generalization of the analytical inversion method for the solution of the point kinetics equations." *Journal of Physics A: Mathematical and General* 35.14 (2002): 3245.

[21] Kinard, Matthew, and E. J. Allen. "Efficient numerical solution of the point kinetics equations in nuclear reactor dynamics." *Annals of Nuclear Energy* 31.9 (2004): 1039-1051.

[22] Kalman, Rudolf. "On the general theory of control systems." *IRE Transactions on Automatic Control 4.3* (1959): 110-110.

[23] Frogner, B., and H. S. Rao. "Control of nuclear power plants." *IEEE Transactions on Automatic Control 3* (1978): 405-417.

[24] Cherchas, Dale B., and Ron T. Lake. "An optimal control algorithm for nuclear reactor load cycling." *Automatica* 13.3 (1977): 279-285.

[25] Chou, Q. B. "Characteristics and maneuverability of CANDU nuclear power stations operated for base-load and load-following generation." *IEEE Transactions on Power Apparatus and Systems* 94.3 (1975): 792-801.

[26] Vinez, J. C., et al. "Load following in Central Nuclear en Embalse: Operating experience and analytical summary." *Annual Conference (Proc. 7th Ann CNS Conf. Toronto, 1986), Canadian Nuclear Society, Toronto.* 1986.

[27] Lopez, A. M., et al. "Ontario Hydro's load following requirements, issues, experience and strategy." *Proceedings of the 7th Annual Canadian Nuclear Society Conference.* 1988.

[28] Trudell, David A. "A Controllability Study of TRUMOX Fuel for Load Following Operation in a CANDU-900 Reactor." MA thesis. McMaster University, 2012 .

[29] Guyot, Maxime. *Development of the Micro-Depletion Method in the Chain of Codes DRAGON4/DONJON4.* MA thesis. École Polytechnique de Montréal, 2011.

[30] Tashakor, S., G. Jahanfarnia, and M. Hashemi-Tilehnoee. "Numerical solution of the point reactor kinetics equations with fuel burn-up and temperature feedback." *Annals of Nuclear Energy* 37.2 (2010): 265-269.

[31] Bernstein, S., et al. "Neutron Cross Section of Xenon-135 as a Function of Energy." *Physical Review 102.3 (1956):* 823.

[32] DOE Fundamentals Handbook: Nuclear Physics and Reactor Theory Volume 2. *U.S. Department of Energy. January 1993.*, pp. 3542.

[33] Rouben, Ben. "Introduction to reactor physics." *Atomic Energy of Canada Ltd* (2002).

[34] Yoo, Seung Yeol, Hyung Jin Shim, and Chang Hyo Kim. "Monte Carlo Few-Group Constant Generation for CANDU 6 Core Analysis." *Science and Technology of Nuclear Installations* 2015.

[35] Palleck, S. J., R. Sejnoha, and B. J. Wong. "Bundle Uranium Content and Performance of CANDU Fuel." *Proc. Fifth Int. Conf. CANDU Fuel.* 1997.

[36] Marleau, G., R. Roy, and A. Hébert. "DRAGON: a collision probability transport code for cell and supercell calculations." *Report IGE-157, Institut de genie nucleaire, École Polytechnique de Montréal, Montréal, Quebec* (1994).

[37] Marleau, G., A. Hébert, and R. Roy. "A user guide for DRAGON 3.06." *Report IGE-174 Rev 7* (2008).

[38] IAEA WIMS Library Update Project, and S. Ganesan. *Update of the WIMS-D4 Nuclear Data Library: Status Report of the IAEA WIMS Library Update Project.* IAEA Nuclear Data Section, 1994.

[39] Leppanen, Jaakko. "Serpenta continuous-energy Monte Carlo reactor physics burnup calculation code." VTT Technical Research Centre of Finland 4 (2013).

[40] Leppanen, Jaakko. "PSG2/Serpent-A Monte Carlo Reactor Physics Burnup Calculation Code, Users Manual (February 2, 2009)." (2008).

[41] Leppanen, Jaakko. "On-going Work and Future Plans: Serpent 2.", *VTT Technical Research Centre of Finland.* [Online]. Available on: http://montecarlo.vtt.fi/development.htm Accessed on: (September, 2016)

[42] "WIMS Library Update Project", *Main features of the WLUP libraries.* [Online]. Available on: https://www-nds.iaea.org/wimsd/libraries.htm Accessed on: (September, 2016)

[43] Keepin, George Robert, T. F. Wimett, and R. K. Zeigler. "Delayed neutrons from fissionable isotopes of uranium, plutonium and thorium." *Journal of Nuclear Energy (1954)* 6.1-2 (1957): IN21IN35-421.

[44] Forrest, Robin, et al. *The JEFF-3.1 nuclear data library.* Ed. Arjan Koning. OECD, 2006.

[45] Hetrick, David L., and R. G. Jarvis. "Dynamics of nuclear reactors." *Physics Today 25*(1972): 61.

[46] Jenkins, Michael A., and Joseph F. Traub. "A three-stage variable-shift iteration for polynomial zeros and its relation to generalized Rayleigh iteration." *Numerische Mathematik* 14.3 (1970): 252-263.

[47] Jenkins, Michael A. "Algorithms 493: Zeros of a real polynomial" *ACM Transaction on Mathematical Software (TOMS)* 1.2 (1975): 178-189.

[48] Sekki, D., A. Hébert, and R. Chambon. "A user guide for DONJON Version 4." *Institut de Génie Nucléaire, Tech. Rep. IGE-300* (2010).

[49] Canadian Nuclear Safety Commission: *Science and Reactor Fundamentals Reactor Physics.* CNSC, Ottawa, ON, Canada (2003).

[50] Capellan, Nicolas, et al. "3D coupling of Monte Carlo neutronics and thermal-hydraulics calculations as a simulation tool for innovative reactor concepts." *International Conference GLOBAL 2009" The Nuclear Fuel Cycle: Sustainable Options & Industrial Perspectives".* 2009.

[51] Yu, Stephen, Jerry Hopwood, and Dan Meneley. "Reacteurs a eau lourde." *Techniques de l'ingenieur. Genie nucleaire* BN3210 (2000): BN3210-1.

[52] Sobolev, Vitaly, and Sergei Lemehov. "Modelling heat capacity, thermal expansion, and thermal conductivity of dioxide components of inert matrix fuel." *Journal of nuclear materials* 352.1 (2006): 300-308.

[53] Rouben, Ben. "Control Programs & Process Systems." Engineering Physics 6P03. McMaster University, Hamilton, ON. Jan-April. 2008.

[54] Kuzminov, B. D., and V. N. Manokhin. "Status of nuclear data for the thorium fuel cycle." *Report No. INDC (CCP)-416* (1998).

[55] Aldama, D. Lopez, F. Leszczynski, and A. Trkov. "WIMS-D Library Update." Final Report of a Co-ordinate Research Project (2003).

Appendix A

Pseudocode Examples

Algorithm 1 Approximation Model for the Lattice Cell

Input
initial time=0, initial flux, initial isotopic densities, end time
N is the neutron number density of a single isotope

while initial time $\neq$ end time **do**

  Isotope Decay: N_λ=N-N $e^{-\lambda \Delta t}$
  Neutron Absorption: N_a=N-N $e^{-\sigma_a \phi \Delta t}$
  Neutron Fission: $N_f = \frac{\sigma_f}{\sigma_a} N_a$

  Four-Factor Formula

  $\eta = \frac{\nu N_f + ...}{N_a + ...}$
  total fission = $\epsilon(\nu N_f + ...)$
  Resonance Absorption = total fission $(1 - p)$
  $k = \eta p f \epsilon$
  Fission Power = $E_{fission}$ N_f + ... / Δt

  if Fission Power is within accepted range **then**
    Incremental increase in time
    initial time = initial time + Δt
    Isotopic Densities are update
    N $\leftarrow$ N_λ, N_a, N_f, Resonance Absorption, Fast Fission
  else
    Flux is Adjusted
  end if
end while

Algorithm 2 Approximation Model for the Full Core

Input
Isotopic Concentrations for 4560 bundles, Flux of 4560 Bundles (ϕ), Time Step (Δt)
Output
Adjusted Isotopic Concentrations of 4560 Bundles, Fission Power, Delayed Neutron Groups, Reactivity

Isotope Decay: N_λ=N-N $e^{-\lambda \Delta t}$
Neutron Absorption: N_a=N-N $e^{-\sigma_a \phi \Delta t}$
Neutron Fission: $N_f = \frac{\sigma_f}{\sigma_a} N_a$

Four-Factor Formula

$\eta = \frac{\nu \sum(N_f)+...}{\sum(N_a)+...}$
total fission = $\epsilon(\nu \sum(N_f) + ...)$
Resonance Absorption = total fission $(1-p)$
$k = \eta p f \epsilon$

Reactor Fission Power = ($E_{fission} \sum N_f + ...$) / Δ t
Beta Calculation
B_i = N_{U235} / total fission B_{U235_i} + N_{Pu239} / total fission B_{Pu239_i} + ...

Algorithm 3 Full Core Model at Constant Power

Starting Input
Mixed Isotopic Densities for 4560 Bundles, End Time, Time Increment (Δt), Initial Flux Magnitude, Initial Time = 0

while initial time $\neq$ end time **do**
  Flux Shape
  Input: Flux Magnitude
  Output: Flux Shape of Core

  Approximation Model
  Input: Isotopic Concentration for 4560 Bundles, Flux Shape of Core (ϕ)
  Output: Temporary File for Isotopic Concentration, Reactor Fission Power, Delayed Neutron Groups, Multiplication Factor

  if Fission Power is within accepted range **then**
    Save and Update Data
    Isotopic Concentration $\leftarrow$ Temporary File for Isotopic Concentration

    Incremental Increase in Time
    initial time = initial time + Δt

  else
    Reactivity is Change
    Input: Reactor Fission Power, Previous Adjusted Reactivity $\Delta\rho$
    Output: Adjusted Reactivity Change $\Delta\rho$

    Point Kinetic Model
    Input: Neutron Generation Time, Delayed Neutron Groups, Half-life Groups of Delayed Neutrons, Adjusted Reactivity Change ($\Delta\rho$), Flux Magnitude, Delayed Neutron Density Groups, Time Increment (Δt)
    Output: Flux Magnitude, Delayed Neutron Density Groups

  end if
end while